Suomen ja Ruotsin kallioperän lämmöntuoton vertailua

Veikkolainen, Toni Henri Kristian

2019

Veikkolainen , T H K , Kukkonen , I T & Näslund , J-O 2019 , Suomen ja Ruotsin kallioperän lämmöntuoton vertailua . julkaisussa XXIX Geofysiikan Päivät . Vuosikerta. 29 , Geofysiikan Päivät , Helsinki , Sivut 133-136 , XXIX Geofysiikan Päivät , Rovaniemi , Suomi , 21/03/2019 .

http://hdl.handle.net/10138/303477

GEOFYSIIKAN SEURA
GEOFYSISKA SÄLLSKAPET
GEOPHYSICAL SOCIETY OF FINLAND

XXIX GEOFYSIIKAN PÄIVÄT

Rovaniemellä 21.-22.5.2019

Toimittaneet

Toni Veikkolainen, Lauri Holappa, Sirpa Rasmus, Irene Suomi, Kalevi Mursula ja Toivo Korja

HELSINKI 2019

ISSN 1798-2200

Julkaisu vapaasti saatavilla Geofysiikan seuran sivustolta https://www.geofysiikanseura.fi

Alkusanat

Geofysiikan Päivät on perinteisesti järjestetty joka toinen vuosi toukokuussa. Tapahtuman paikkana on ollut vuorotellen Helsinki ja Oulu. Tällä kertaa XXIX Geofysiikan Päivät pidetään poikkeuksellisesti jo 21.-22. maaliskuuta ja ensimmäistä kertaa seuran historiassa kokoonnumme Rovaniemellä. Tiedekeskus Arktikum isännöi tapahtumaa, mistä olemme hyvin kiitollisia. Paikka on hyvin ajankohtainen, sillä arktinen tutkimus on ilmastonmuutoksen takia yhä enenevissä määrin keskeisessä roolissa geofysiikan alalla sekä kansainvälisesti että Suomessa. Arktinen tutkimus myös yhdistää eri alojen tutkijoita, sillä ilmastonmuutos ei koske vain ilmakehätutkimusta vaan sen vaikutukset ovat laaja-alaiset.

Geofysiikan Päivät on erinomainen esimerkki tutkimusalojen välisestä vuorovaikutuksesta. Olemme pyrkineet huomioimaan tämän kokouksen ohjelmaa laatiessamme. Meillä ei ole tutkimusalakohtaisia istuntoja, vaan kuhunkin istuntoon on pyritty kokoamaan laaja-alainen kattaus eri aiheita kiinteän maan, vesikehän, ilmakehän ja lähiavaruuden tutkimuksen aloilta. Lisäksi esitimme puhujille toiveen, että esitykset pidetään osittain yleisellä tasolla, jotta mahdollisimman suuri kuulijakunta saa käsityksen tutkimusaiheen laajemmasta merkityksestä. Näin pyrimme edistämään geofysiikan alan tutkijoiden verkottumista yli tutkimusalarajojen. Toivommekin, että kohtaamisissa syntyy paljon uusia ajatuksia ja ideoita miten kehittää tiedettä eteenpäin.

XXIX Geofysiikan Päiville on ilmoittautunut yhteensä 64 osallistujaa. Kaksipäiväisen tapahtuman aikana tulemme kuulemaan 33 suullista esitystä ja 16 posteriesitystä. Päivien pääpuhujia on kolme. Heistä Prof. John Moore (Lapin yliopisto, Arktinen keskus) pohtii esitelmässään ilmastonmuutoksen hillitsemiseen liittyviä kysymyksiä ilmastonmuokkauksen näkökulmasta. Prof. Timo Vihman (Ilmatieteen laitos) esitys puolestaan käsittelee arktista ilmastonmuutosta ja sen yhteyksiä keskileveysasteiden säähän ja ilmastoon. Kolmannen pääpuhujan, Prof. Martin Vermeerin (Aalto-yliopisto), aiheena on aika-avaruuden geometria. Lisäksi torstaina illalla saamme kuulla Prof. Jaan Praksin (Aalto-yliopisto) yleisöluennon piensatelliittien vallankumouksesta. Praksin luento on avoin kaikille Arktikumin kävijöille. Pääpuhujien lisäksi olemme kutsuneet seitsemän kutsupuhujaa, joiden joukkoon mahtuu sekä lupaavia nuoria tutkijoita että jo pidemmälle tutkijanurallaan edenneitä.

Geofysiikan Päivien järjestämisestä suuri kiitos kuuluu etenkin paikalliselle järjestelytoimikunnalle, puheenjohtaja Lauri Holapalle ja Kalevi Mursulalle Oulun yliopistosta sekä Sirpa Rasmukselle Lapin yliopiston Arktisesta keskuksesta. Myös seuran sihteerin Toni Veikkolaisen (Helsingin yliopisto) ja taloudenhoitaja Toivo Korjan (Luulajan teknillinen yliopisto) työpanokset Päivien järjestelyissä ovat olleet huomattavat. On ollut hienoa olla mukana tässä mahtavassa tiimissä, ja toivon että tämä hyvä meininki välittyy myös osallistujille Päivien aikana.

Helsingissä, 14.3.2019

Irene Suomi

Geofysiikan seuran puheenjohtaja

Sisältö

* pitää esitelmän / gives the presentation

XXIX Geofysiikan Päivät Rovaniemellä Arktikumissa 21.-22.3.2019
XXIX Geophysics Days in Rovaniemi, Arktikum, March 21-22, 2019

- Paikka: Tiedekeskus-museo Arktikum, Pohjoisranta 4, Rovaniemi
- Sivusto: https://www.geofysiikanseura.fi
- Osallistumismaksu: 90 € (eläkeläiset, opiskelijat ja työttömät 45 €)
- Maksuun sisältyy: kokousohjelma, lounas- ja kahvitarjoilut sekä kokousillallinen
- Esitelmät: Kokousjulkaisu on saatavissa sähköisessä muodossa päivien sivustolta kohdasta ”Kokousohjelma”

Kokousohjelma torstaina 21.3.2019 / Conference programme on Thursday, March 21, 2019

8.00-9.00	Ilmoittautuminen, postereiden kiinnitys Registration, setup of posters
9.00-9.10	Päivien avaus (Geofysiikan seuran puheenjohtaja *Irene Suomi*, järjestelytoimikunnan puheenjohtaja *Lauri Holappa*)
9.10-9.20	Arktikumin tervehdys (*Osmo Rätti*)
Istunto / Session 1	Puheenjohtaja / Chair: *Lauri Holappa*
9.20-9.50	***John Moore (pääpuhuja / keynote)*** What role for targeted geoengineering to mitigate climate change?
9.50-10.10	*Jarkko Jokinen* Interpretation and 3D-visualization of Electromagnetic Exploration Data
10.10-10.30	*Takayuki Shuku* Data-driven Modelling for Wind Fields over Lakes
10.30-11.00	**Kahvitauko / Coffee break**
Istunto / Session 2	Puheenjohtaja / Chair: *Toivo Korja*
11.00-11.20	*Kaisa Lakkala* Solar UV radiation in Arctic and Antarctic sites measured by ground instruments and satellites
11.20-11.40	*Jouni Nevalainen* INFACT (Innovative, Non-Invasive and Fully Acceptable Exploration Techniques) - Geophysical aspect of the project
11.40-12.00	***Antti Salminen (kutsupuhuja / solicited)*** Effects of energetic electron precipitation and quasi-biennial oscillation on the northern polar vortex

12.00-12.20	*Anna Kontu* Snow research in Sodankylä
12.20-12.40	*Heikki Juntti* Konenäön käyttö näkyvyyshavainnoinnissa
12.40-13.00	*Esa Turunen* The Scientific Payload of the Lappi satellite (LAPPISAT) and Data Visualisation in the Service Concept of the Satellite
13.00-14.00	**Lounas / Lunch**
Istunto / Session 3	Puheenjohtaja / Chair: *Kalevi Mursula*
14.00-14.20	***Andrés Muñoz-Jaramillo (kutsupuhuja / solicited)*** How Hemispheric Polar Field Reversal Sets the Timing and Shape of the Solar Cycle
14.20-14.40	*Raul Mollehuara-Canales* Hydrogeophysical approach for Characterization of Mining Wastes: Tailings Storage Facilities (TSFs)
14.40-15.00	*Leena Leppänen* Lumen mikrorakenteen mittauksiin ja mallinnuksiin perustuva tutkimus Sodankylässä
15.00-15.20	*Nikita Afonin* Development of events detector for monitoring cryoseisms in upper soils
15.20-15.40	*Lauri Pesonen* Geophysical methods in impact crater hunting – Case Summanen
15.40-16.00	***Samuli Helama (kutsupuhuja / solicited)*** Lapin puulustodata paleoklimatologisena arkistona
16.00-17.00	**Kahvitauko ja posterisessio / Coffee break and poster session**
17.00-18.00	***Jaan Praks (yleisöluento)*** Piensatelliittien vallankumous
19.00-	**Kokousillallinen / Conference dinner (Cafe Koti, Valtakatu 21, Rovaniemi)**

Posteriesitykset torstaina / Poster presentations on Thursday

P01. Hanna Silvennoinen: Northern Finland seismological network: status in early 2019

P02. Timo Huttula: Suihkuvirtausmallinnus jäteveden purun suunnittelussa

P03. E. Kozlovskaya (K. Moisio):* Geophysical research and teaching at Oulu Mining School: challenges and solutions

P04. Eija Tanskanen: Magnetic environment in polar and equatorial regions during space era

P05. Otto Kärhä: DigiMAG method and historical magnetic recordings for better magnetic environment understanding

P06. Marko Holma: Borehole muography – A new geophysical tool

P07. Seppo Leinonen: Green Minerals Project – Exploration Techniques for Flake Graphite

P08. Hiroaki Somura: Influence of climate change on water resource availability in a watershed

P09. Tomi Teppo: A new spectral riometer for ionosphere research

P10: Iina Jaakonaho (Eija Tanskanen):* Auroral substorm energetics from 1993 to 2016

* esittelee posterin / presents the poster

Kokousohjelma perjantaina 22.3.2019 / Conference programme on Thursday, March 21, 2019

Istunto / Session 4	Puheenjohtaja / Chair: *Irene Suomi*
8.15-8.35	*Toni Veikkolainen* Suomen ja Ruotsin kallioperän lämmöntuoton vertailua
8.35-8.55	***Pilvi Siljamo (kutsupuhuja / solicited)*** Hyönteiset ilmakehämallien vieminä
8.55-9.15	*Jyrki Manninen* Simultaneous Kannuslehto and ARASE satellite ELF-VLF observations
9.15-9.35	***Joula Siponen (kutsupuhuja / solicited)*** Comparing sea ice thickness in the Arctic from reanalysis and satellite altimetry
9.35-10.20	**Kahvitauko ja posterisessio / Coffee break and poster session**
Istunto / Session 5	Puheenjohtaja / Chair: *Toni Veikkolainen*
10.20-10.50	***Timo Vihma (pääpuhuja / keynote)*** Arctic climate change and its mid-latitude linkages

10.50-11.10	*Pyry Peitso* High-frequency geomagnetic fluctuations, comparison between northern and southern hemisphere
11.10-11.30	*Jia Jia* Mesospheric Monitoring of Ozone above the Polar Vortex (MeMO)
11.30-11.50	*Mauri Timonen* Ilmaston vaihtelut puulustojen valossa
11.50-12.10	***Abiyot Workayehu (kutsupuhuja / solicited)*** Ionospheric currents in the two hemispheres during low and high magnetic activity by the Swarm satellite
12.10-13.10	**Lounas / Lunch**
Istunto / Session 6	Puheenjohtaja / Chair: *Lauri Holappa*
13.10-13.40	***Martin Vermeer (pääpuhuja / keynote)*** Suhteellisen tarkka vaaitus: aika-avaruuden geometria maanmittareille
13.40-14.00	***Françoise Martz (kutsupuhuja / solicited)*** Winter climate change affects subnivean conditions and conifer seedling survival in boreal forest
14.00-14.20	*Edith Liliana Macotela* High frequency VLF banded emissions observed at Kannuslehto: Geomagnetic analysis
14.20-14.40	*Irene Suomi* Historical overview of wind gust measurement techniques – from traditional anemometry to new possibilities
14.40-15.00	*Timo Saari* Itäisen Suomenlahden GNSS-mittaukset
15.00-15.30	**Kahvitauko / Coffee break**
Istunto / Session 7	Puheenjohtaja / Chair: *Sirpa Rasmus*
15.30-15.50	*Sergej Zilitinkevich* Towards revision of current theory of turbulence in stratified sheared flows
15.50-16.10	*Ilkka Ratinen* Ilmastokasvatus – riittääkö geofysiikan näkökulma?
16.10-16.30	*Heikki Virtanen* Suprajohtavat gravimetrit Metsähovissa 1994-2019
16.30-16.50	*Tuija Luhta* New geophysics study programs at the University of Helsinki

	Nuoren tutkijan palkinnon jakaminen (palkintotoimikunnan puheenjohtaja) Kokouksen päättäminen (Geofysiikan seuran puheenjohtaja)
16.50-17.10	
	Awarding the Young Scientist's Award (chair of the award committee) Closure of the meeting (chair of the Geophysical Society of Finland)

Posteriesitykset perjantaina / Poster presentations on Friday

P01. Tuomas Naakka: Luotausverkoston alueellisen kattavuuden vaikutus numeerisessa säänennustamisessa arktisilla alueilla

P02. Juha Sorri: Observations of MeV electron precipitation to the upper atmosphere and differences in the electron energy spectrum between satellite and ground based measurements

P03. Niina Mäkinen: The effect of magnetograph saturation and resolution on the observations of the photospheric magnetic field

P04. Kalevi Mursula: Geomagnetic history of the Grand Modern Maximum: Centennial evolution of geomagnetic activity and geomagnetic storms

P05. Sirpa Rasmus: Lumiolosuhteiden moninaiset vaikutukset petojen aiheuttamiin porovahinkoihin Suomessa

P06. Tuija Luhta: Petrophysical properties of the Kylylahti Cu-Au-Zn sulphide mineralization and its host rocks

Development of events detector for monitoring cryoseisms in upper soils

N. Afonin[1] and E. Kozlovskaya[1, 2]

[1] Oulu Mining School, POB-3000, FIN-90014, University of Oulu, nikita.afonin@oulu.fi
[2] Geological Survey of Finland, P.O. Box 96, FI-02151, Espoo

Abstract

In this article, we describe the first results of the development of the seismic events detector with an artificial neural network (ANN) based identification. Such a detector is necessary for studying seismic events induced by soil freezing that can be hazardous for urban and mining infrastructures. We used the data of about 300 such seismic events recorded by seismic station OUL of Northern Finland Seismological Network for testing the detector and neural network learning. We processed about two months of continuous data and found out, that in some cases the number of detected and identified seismic events per day depends on air temperature variation.

1. INTRODUCTION

For the solution of some scientific and applied problems, analysis of huge amount of seismic data is necessary. One of such problems is investigation of an impact of extreme weather changes to water-saturated shallow layers of the subsurface. Weather extremes such as rapid temperature decrease can result in so-called “frost quakes” or cryoseisms resulting from cracking of soil and rock that occurs when water in rock has suddenly frozen and expanded. As cryoseisms can be hazardous for industrial and civil objects, their monitoring and analysis is necessary to increase the safety of these objects.

One of the important tasks in studying cryoseisms is development of efficient data processing routine capable to separate cryoseisms from other seismic events and noise. Nowadays artificial neural networks (ANNs) are used in earthquake seismology for development of procedures for classification of seismic events. Examples are classification of recorded events into regional, local, teleseismic earthquakes or industrial blasts (Scarpetta et al., 2005), detection of low-magnitude events (Kislov et al., 2012) etc. Nevertheless, there are several reasons why ANNs are still not widely used. They are: difficult and long learning process, the necessity of taking into account characteristics of each seismic station of the monitoring network, difficulties in evaluation of quality and reliability of probabilistic classification results (Kislov and Gravirov, 2017). Because cryoseisms are present in seismograms as strong impulses with high signal-to-noise ratio, we applied an “STA/LTA” algorithm for their detection and simple neural network for their classification using selected characteristics of the records (length, central frequencies, etc.).

2. DESCRIPTION OF THE DATA ANALYSIS

We used continuous data recorded by seismic station OUL since the end of November, 2015 to the end of February, 2016. This time interval was selected because of the strong

cryoseismic event in Talvikangas district of Oulu on 06.06.2016 that caused damage to road surface and basements of buildings. During this day, many seismic events with similar waveforms were recorded by the OUL station. Assuming that these events were also caused by soil freezing, we used them as a learning sample for the neural network.
Analysis of these events has shown that most of them have many similarities in selected records characteristics (central frequencies, duration etc.) with the major event and with each other. We applied these identification criteria to events detected during other time intervals and compare the number of events per day with air temperature (Figure 1)

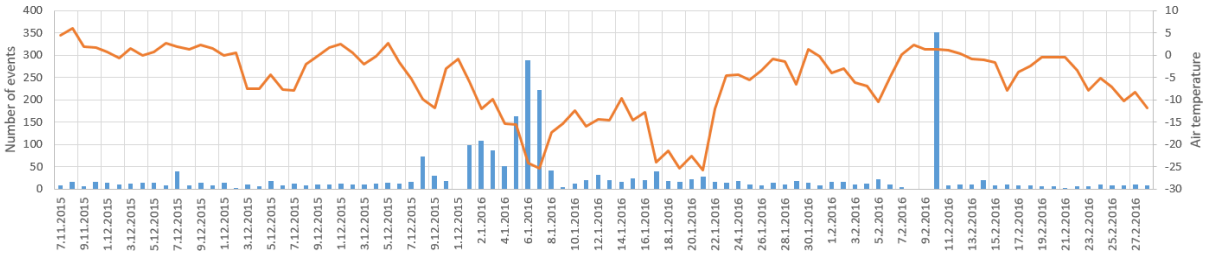

Figure 1: Dependence between air temperature and number of impulses per day.

As one can see in Figure 1, the number of events is highest since 1.01.2016 to 8.01.2016 and another peak in observed on 10.02.2016. In January, the increase in the number of events is most probably caused by the strong gradient of air temperature and hence fast soil freezing. Nevertheless, the huge number of impulses on 10.02.2016 is apparently not depended on the air temperature gradient. This may be caused by joint impact of atmosphere condition changes and hydrogeological processes in the subsurface, which requires further investigation.

3. CONCLUSION

We developed an efficient algorithm based on STA/LTA for detection and simple neural network for separation of cryoseisms from other seismic events. Comparison of results with air temperature variations partially confirms the detection results. Nevertheless, number of seismic events not always has correlation with air temperature, suggesting that cryoseisms can be caused by more complicated interaction between atmosphere and hydrological processes in the shallow subsurface.

ACKNOWLEDGEMENTS

This work is part of project "*Impact of extreme weather events in the Arctic on technological systems, critical facilities and urban environment*" funded by KVANTUM Institute of the University of Oulu.

REFERENCES

Scarpetta, S., F. Giudicepietro, E.C. Ezin, S. Petrosino, E. Del Pezzo, M. Martini and M. Marinaro, 2005. Automatic classification of seismic signals at Mt. Vesuvius Volcano, Italy, using neural networks. *Bull. Seismol. Soc. Am.*, **95**, 185-196.

Kislov, K.V., F.E. Vinberg, A.F. Kushnir and V.V. Gravirov, 2012. Early warning system and man-made noise. *Proceedings of the IV International Conference Problems of Cybernetics and Informatics*, Baku, Azerbaijan, 52-55.

Kislov, K.V. and V.V. Gravirov, 2017. Using of artificial neural networks for classification of noisy seismic signals. *Seismic instruments*, **52**, 46-64.

Lapin puulustodata paleoklimatologisena arkistona

S. Helama[1]

[1] Luonnonvarakeskus, Rovaniemi, samuli.helama@luke.fi

Abstract

Tree rings provide evidence of palaeoclimatic conditions and extend the record of climatic variability beyond the era of instrumental measurements. This is crucial for understanding how large and rapid natural climatic variations can be and which internal mechanisms drive them. Tree-ring data from Finnish Lapland has been used to construct chronologies of tree-ring width, maximum latewood density, and stable carbon isotope ratios for the past 7.5 kyr and to reconstruct variations in summer temperature and cloud cover over the same period. Dendrochronological cross-dating allows an exact calendar date to be assigned to these palaeoclimatic estimates.

1. JOHDANTO

Paleoklimatologia on geotieteen ala joka tutkii muinaisia ilmaston vaihteluita (Bradley 1999). Pohjimmiltaan tällainen tutkimus perustuu epäsuoriin, ilmaston menneitä vaihteluita indikoiviin tietolähteisiin kuten sedimenteistä määritettyihin siitepölykoostumuksen vaihteluihin, tai niin ikään sedimenttien tai jäätikkökairausten pohjalta mitattaviin fysikaalisiin tai kemiallisiin muuttujiin. Menneen ilmaston oloihin päästään kiinni myös historiallisia säästä kertovia havaintoja sekä syvien kairareikien lämpötilamittauksia analysoimalla. Mainituista indikaatiodatoista kuitenkin vain osa mahdollistaa vuodentarkan paleoklimatologian, millä tässä yhteydessä tarkoitetaan ilmastoestimaattien sijoittamista tietylle, varmennetulle historialliselle kalenterivuodelle. Tällaisten vuodentarkkojen aineistojen pohjalta voi olla mahdollista arvioida esimerkiksi vuoden 1601 jKr ”suuren olkivuoden” aikaisten kesäkuukausien lämpötilaa, pilvisyyttä, saapuvan auringon säteilyn määrää ja/tai sateisuutta, ja verrata niitä muiden kyseisestä historiallisesti tunnetusta katovuodesta kertovien tietojen suhteen.

Vuodentarkkuuteen paleoklimatologiassa voidaan päästä paitsi historiallisten sää-, fenologia- ja maataloustietojen avulla, myös erityisesti dendrokronologian eli puiden vuosilustotutkimuksen keinoin. Vuodentarkkuus pohjautuu tieteenalan lähtökohtana toimivaan dendrokronologiseen ristiinajoitukseen, joka puolestaan perustuu lämpötiloissa, kosteus- ja säteilyoloissa vuodesta toiseen tapahtuviin puun kasvua vastaavan laajoilla eliömaantieteellisillä alueilla samankaltaisesti ohjaaviin vaihteluihin. Näiden samankaltaisten ja erityisesti samanaikaisten muutosten vaikutuksia puun kasvuun voidaan mitata lähtökohtaisesti vuosilustojen leveysvaihteluina, ja saatuja puukohtaisia lustonleveyssarjoja analysoida aikasarja-analyysin avulla (Fritts 1976). Yksittäisten aikasarjojen sekä niiden ja jo ristiinajoitettujen keskiarvoaikasarjojen väliset vertailut paljastavat sarjoihin mahdollisesti

jääneitä ajoitusvirheitä, joita voi syntyä tyypillisesti puun rungon tietyltä sektorilta puuttumaan jääneen vuosikasvun eli luston tapauksessa. Tämän tutkimuksen alkuvaiheen jälkeistä varsinaisesti paleoklimatologista tutkimusta tehdäänkin juuri keskiarvoaikasarjoihin eli dendrokronologian tapauksessa puulustokronologioihin perustuen.

Suomen oloissa paleoklimatologisesti merkittävää puulustodataa on kerätty erityisesti Lapista. Syitä tähän on monia. Lähellä pohjoista metsänrajaa ilmastonvaihteluiden rooli yhtäältä voimistuu kasvunvaihtelua ohjaavana tekijänä, toisaalta terävöityy kyseeseen tulevien ilmastomuuttujien määrän suhteen. Paleoklimatologisessa mielessä Lapin puiden kasvunvaihtelu onkin erityisen tarkka kesäajan lämpötilavaihteluiden indikaattori. Toinen oleellinen syy on Lapin puumateriaalin, erityisesti männyn (*Pinus sylvestris* L.) hyvä säilyvyys ja subfossiilisina säilyneiden runkojen saatavuus erityisesti pienten järvien pohjasedimenteistä (kuva 1). Erotuksena kelopuusta tällainen materiaali on säilynyt vieläkin kauemmin erityisen vähähappisissa oloissa. Useampien tuhansien liekorunkojen lustonnäytteiden perusteella Lapin alueelle on koostettu yhtäjaksoinen puulustokronologia vuodesta 5634 eKr alkaen (Helama et al. 2008). Subfossiilisen lustomateriaalin systemaattisen keräämisen aloitti Lapissa professori Matti Eronen jo 1970-luvulla (Eronen 1979). Tänä päivänä Lapin pitkä puulustokronologia onkin eräs pisimpiä maailmassa, koostuen lähinnä maamme kolmen pohjoisimman kunnan, Enontekiön, Utsjoen ja Inarin alueita kerätystä materiaalista. Tämän materiaalin merkitys kasvaa edelleen tarkoin arkistoituna kokonaisuutena jolloin kyseistä lusto lustolta risriinajoitettua puunainesta voidaan jatkoanalysoida alati kehittyvien tutkimusmenetelmien keinoin.

Seuraavassa Lapin dendrokronologisia aineistoja käsitellään moniparametrisenä paleoklimatolisena arkistona, erityisesti lustonleveyksiin sekä puunaineen tiheys- ja isotooppimittauksiin pohjautuen.

Kuva 1: Maastotyötä eräällä Ylä-Lapin järvellä (kuva: Hannu Herva).

2. KRONOLOGIOITA JA REKONSTRUKTIOITA

Lapin männyn lustonleveyskronologioiden yleisenä piirteenä on niiden riippuvuus keskikesän, erityisesti heinäkuun lämpötilasta (Hustich & Elfving 1944), toissijaisena riippuvuussuhteena esiintyy talvikauden leutouden positiivinen korrelaatio (Helama et al. 2005). Kesälämpötilojen vuodesta toiseen tapahtuvasta vaihtelusta selittyy tätä dataa hyväksi käyttäen noin 40 prosenttia havaitusta vaihtelusta. Tarkoitusta varten on Karasjoen asemalta

saatavilla lämpötilahavaintoja yhtäjaksoisesti 1870-luvulta lähtien ja tilastollinen tarkastelu voidaankin siten reilusti yli sadan vuoden ajalle. Mikäli tarkastelu suoritetaan samalle aikajaksolle mutta pitempiaikaisten vaihteluiden suhteen voidaan lämpötiloista selittää tätä huomattavasti korkeammalla selityskertoimella R^2 = 0.75-0.95 (Helama et al. 2010).

Lustojen leveyksien lisäksi on Lapista analysoitu erityisesti kesäpuun (vuosiluston tummempi keskikesän jälkeen muodostuva solukko) maksimitiheyden ja lämpötilavaihteluiden välisiä suhteita. Kyseessä on dendroklimatologinen parametri jota on kirjallisuudessa käytetty usein ennallistettaessa eli rekonstruoitaessa kesäajan lämpötilaolojen vaihteluita. Tätä lustoparametria käyttäen voidaan vuodesta toiseen havaitusta kesäajan (kesä-elokuu) keskilämpötilasta selittää noin 65 prosenttia (esim. Matskovsky & Helama 2014). Maksimitiheys onkin lustonleveyttä huomattavasti tarkempi paleoklimatologinen indikaattori, toisaalta datan tuottamiseen tarvittava röntgenlaitteisto sekä analysointia edeltävä näytteiden virhelähdeherkempi esikäsittely vaativat huomattavasti suuremman työpanoksen, kuin valomikroskoopin avulla yksinkertaisimmillaan tapahtuva lustonleveyksien mittaus (Helama et al. 2012).

Kolmas viimeaikaisista Lapin aineistoista tuotetuista ja analysoiduista lustoparametreista on $^{13}C/^{12}C$ -isotooppisuhde (eli $\delta^{13}C$). Tämän parametrin vaihtelut muodostuvat yhtäältä kasvin kokemien kuivuusvaihteluiden ja siten sen lehden (neulasen) huulisolujen toimintaa ohjaavista vaikutuksista, toisaalta kasvin vastaanottaman valon määrän ja siten yhteyttämisen välisenä vuorovaikutussuhteena siten, että veden puute aiheuttaa positiivisen, puute valosta negatiivisen $\delta^{13}C$:n poikkeaman (Francey & Farquhar 1982). Lappi kuuluu yleensä alueeseen jolla männyn vuosilustoista tuotettujen $\delta^{13}C$-kronologioiden on todettu edustavan eritoten jäljempää eli saapuvan valon vaihteluissa tapahtuvaa ja sen yhteyttämiselle aiheuttamia muutoksia.

Paleoklimatologisestssa kontekstissa voidaan alueen $\delta^{13}C$-kronologioita käyttää indikaattorina joko auringon säteilyssä tai (epäsuorana indikaationa) pilvisyydessä tapahtuneille muutoksille. Selityskertoimet (R^2) vaihtelevat ennallistettavasta aikajänteestä riippuen noin 50 ja 85 prosentin välillä (Helama et al. 2018a, 2018b). Lapin pitkän puulustokronologian avulla on Helsingin yliopiston Ajoituslaboratorion ja Luonnonvarakeskuksen välisenä konsortiona tuotettu ja vuosikymmenten tarkkuudella analysoitu $\delta^{13}C$-kronologia vuodesta 5500 eKr lähtien (kuva 2). Tähän kronologiaan pohjautuen on alueen pilvisyysvaihteluita ennallistettu samalle ajanjaksolle siten että kronologian kunkin vuosikymmenen $\delta^{13}C$-arvo on määritetty vähintään viiden eri puun välisenä keskiarvona (Helama et al. 2018a).

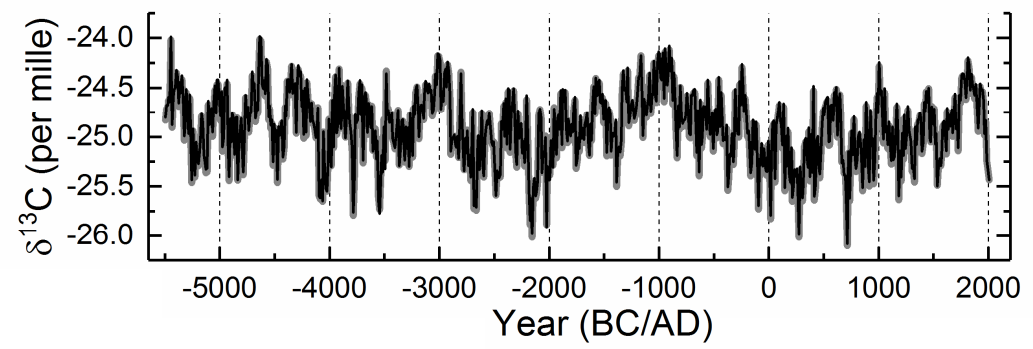

Kuva 2: Lapin $\delta^{13}C$-kronologia (5500 eKr – 2010 jKr) (Helama et al. 2018a).

KIITOKSET

CARATE- ja QUANOMAL-konsortioissa tehtyä tutkimusta on tukenut Suomen Akatemia.

LÄHTEET

Bradley, R.S., 1999. Paleoclimatology: reconstructing climates of the Quaternary, Academic Press, London.

Eronen, M., 1979. The retreat of pine forest in Finnish Lapland since the Holocene climatic optimum: a general discussion with radiocarbon evidence from subfossil pines, *Fennia*, **157**, 93-114.

Francey, R.J. ja G.D. Farquhar, 1982. An explanation for the $^{12}C/^{13}C$ variations in tree rings, *Nature* **297**, 28-31.

Fritts, H.C., 1976. Tree Rings and Climate. Academic Press, London.

Hustich, I. ja G. Elfving, 1944. Die Radialzuwachsvariationen der Waldgrenzkiefer, *Soc. Scient. Fenn., Comm. Biologicae*, **9(8)**, 1-18.

Helama, S., K. Mielikäinen, M. Timonen ja M. Eronen, 2008. Finnish supra-long tree-ring chronology extended to 5634 BC, *Norsk Geogr. Tidsskr.*, **62**, 271-277.

Helama, S., M. Lindholm, J. Meriläinen, M. Timonen ja M. Eronen, 2005. Multicentennial ring-width chronologies of Scots pine along north-south gradient across Finland, *Tree-Ring Res.*, **61**, 21-32.

Helama, S., M. Macias Fauria, K. Mielikäinen, M. Timonen ja M. Eronen, 2010. Sub-Milankovitch solar forcing of past climates, *Geol. Soc. Am. Bull.*, **122**, 1981-1988.

Matskovsky, V.V. ja S. Helama, 2014. Testing long-term summer temperature reconstruction based on maximum density chronologies obtained by reanalysis of tree-ring data sets from northernmost Sweden and Finland, *Clim. Past*, **10**, 1473-1487.

Helama, S., Y. Bégin, M. Vartiainen, H. Peltola, T. Kolström ja J. Meriläinen, 2012. Quantifications of dendrochronological information from contrasting microdensitometric measuring circumstances of experimental wood samples. *Appl. Radiat. Isotopes* **70**, 1014-1023.

Helama, S., L. Arppe, M. Timonen, K. Mielikäinen ja M. Oinonen, 2018a. A 7.5 ka chronology of stable carbon isotopes from tree rings with implications for their use in palaeo-cloud reconstruction, *Global Planet. Change* **170**, 20-33.

Helama, S., L. Arppe, J. Uusitalo, J. Holopainen, H. M. Mäkelä, H. Mäkinen, K. Mielikäinen, P. Nöjd, R. Sutinen, J.-P. Taavitsainen, M. Timonen ja M. Oinonen, 2018b. Volcanic dust veils from sixth century tree-ring isotopes linked to reduced irradiance, primary production and human health, *Sci. Rep*. **8** (1339).

Borehole muography – A new geophysical tool

M. Holma[1], P. Kuusiniemi[1,2,3], K. Loo[3], J. Joutsenvaara[1,2,4], M. Aittola[1,2], T. Enqvist[1,3], P. Jalas[4] and A. Virkajärvi[1]

[1] Muon Solutions Oy, Perkas 8, FI-67100 Kokkola, Finland, marko.holma@muon-solutions.com
[2] Arctic Planetary Science Institute, Lihtaajantie 1 E 27, FI-44150 Äänekoski, Finland
[3] Department of Physics, P.O. Box 35, FI-40014 University of Jyväskylä, Finland
[4] Kerttu Saalasti Institute, University of Oulu, Pajatie 5, FI-85500 Nivala, Finland

Abstract

The present work provides a brief overview to the current state of muography. Special attention is paid to description of some of the key concepts and terms as well as to the role of simulations in muography. With the additional short treatment of issues concerning borehole muon detectors, which represent one the newest techniques within the muography method, the present paper works as an introduction to borehole muography.

1. INTRODUCTION

Muons are short-living (2.2 μs half-life) elementary particles that are generated at the heights of 20-30 km in the atmosphere resulting from interactions between atmospheric nuclei and high-energy cosmic particles (also called cosmic rays). This process is continuous and offers a never-ending reservoir of muons on ground and – very importantly – beneath the ground. Many muons have energies high enough to penetrate many metres within the bedrock, and some for hundreds of metres. A small fraction of muons have even greater energies, in fact up to several magnitudes higher than that achieved using the world's largest and most powerful particle accelerator, the Large Hadron Collider (LHC at CERN) in Geneva, Switzerland. The research field exploiting muons for determining rock density inhomogeneities, or inhomogeneities in any other material for that matter, is called **muography**.

Muography is a technique that provides means to see through solid or liquid materials similar to X-rays, but in a much greater scale. This is carried out by comparing the number of muons detected in a given survey point to that of the predicted within a time span of the survey. If the material in the field of "seeing" is totally homogenous, the measured angular distribution of muons is statistically homogenous too. However, if there are notable density contrasts in the volume of rocks of interest, the muon data reveal variations. The denser the object, the more muons it absorbs before they ever reach the muon detector. Hence the attenuation of muons in various directions can be associated with the density variations in the media.

Muons are actually the second most penetrative (known) particles in the Universe, just after neutrinos. However, whereas the latter are notoriously difficult to catch due to their very weak interaction strength with any material, a trace of a passing muon can be detected relatively easily. Nevertheless, only the GeV range (and beyond) muons have the capacity to pass through material effectively before stopping or decaying into their daughter particles.

Herein we place emphasis on the portable muon detectors and especially on borehole muon detectors (BMDs). As muon detectors represent some of the most unfamiliar brand of new geophysical tools, the surrounding theoretical concepts are not yet widely understood by many in the geoscientific community. In this paper, hence, a special attention is paid for the concept definitions (marked in bold). As typical for an emerging scientific discipline, the related terms are not universally agreed upon. In this case, also, many terms still have way too many synonyms for effective transfer of ideas and research results. A major example of this problem is the name of the discipline itself, for which there exists various synonyms, including at least muography, muon imaging, muon radiography, muon tomography and muon geotomography. True enough, not all of these terms are equal in meaning. For readers interested to dive deeper in the realm of general muography, we recommend recent papers from Kaiser (2019) and Tanaka and Oláh (2019) and references therein.

2. DIFFERENT TYPES OF MUOGRAPHY AND RELATED CONCEPTS AND TERMS

The term muography is an umbrella term for **muon radiography** (2D muon imaging) and **muon tomography** (3D muon imaging). **The so-called time-sequential (or time-lapse) muography** can be based on the utilisation of either of the two main form of muography. Regarding geosciences, all the mentioned versions of muography can be used both on the surface (for example, transilluminating volcanoes) and underground (for example, lithological and ore exploration studies). However, the size of the given muon detector dictates where and how it can be used.

The portable muon detectors (MDs) have now been developed to the point they can be transported just about anywhere relatively easily. Such MDs can be handled by one or two persons and transported by car or by helicopter (or similar means) as is with the largest mobile versions. These types of MDs are commonly called **muon telescopes**. The smallest range instruments currently developed are cylindrical in shape and specifically designed to fit most standard-size boreholes. Small MDs have certain important differences comparing to larger portable MDs and due to the smaller size of the former, these differences have both advantages and disadvantages. For the former, these instruments fit boreholes where the larger ones are not even meant to fit. This fact naturally provides an almost endless supply of underground study sites, keeping in mind that boreholes are many times more abundant than, for example, tunnels. Thus, the **borehole muon detectors** (BMD) are not as diverse and accurate in their capabilities as the larger MDs, because of, for example, their limited angular resolution and reduced statistics. A combined use of both types of MDs would likely provide the best coverage and resolution in some underground study sites.

By far the simplest muographic method is a density analysis based solely on the number of detected muons in a given depth. This kind of study tells the average density of the media as a function of depth. The deviations from the homogeneous standard model imply more (or less) dense material than expected. However, this simple method is seldom accurate enough for

locating the exact coordinates for interesting objects (for example, dense orebodies). Nevertheless, it may well proof to be effective enough for solving some specific research tasks such as long-term hydrological studies with the time-sequential method.

3. SIMULATIONS

In addition to conducting the measurement there are a plenty of things that need to be well understood before the analysed measured data can lead to the reliable results and convincing conclusions. Simulations are a major part of that process. In general, there are three key issues where simulations play a crucial role: i) muon generation in the atmosphere, ii) muon energy loss (or stopping power) in different media and iii) the detector response.

Cosmic-ray induced muons are secondary particles originating from interactions of other cosmic-ray particles in the atmosphere. Simulations are used to obtain the properties of expected on-ground muon flux and their energy and angular distributions. Thanks to over 100 years of cosmic-ray measurements an extensive amount of data are available and turned into well-defined simulation tools.

The energy loss of muons in a given media they are traversing through depends (heavily) on the (nuclear/electronic) composition, the density of the media, and on the energy of muons. This material property is called **stopping power** and it determines the ranges of muons in different materials. Stopping powers (or muon ranges) in all materials are not readily available, but can be simulated with the cutting-edge particle simulation tools.

So, many interactions occur before a muon finally hits the detector, but even if it does it is not by any means always detected. If the muon hits the detector it (eventually) produces an electronic signal which is registered. Due to the limited geometrical properties of the detector and given detection technology, the detection efficiency is never 100%. Understanding and validating these kinds of effects requires simulations and calibrations.

In the most modern approaches, the extensive air-shower (EAS) simulation code CORSIKA (Heck, 1998) is used to obtain the surface flux of muons while stopping powers and detector response are studied and simulated with GEANT4 (Agostinelli et al., 2003). However, these state-of-the-art and up-to-date packages require a significant amount of computing power.

4. PRINCIPLES AND APPLICATIONS OF BOREHOLE MUOGRAPHY

Borehole muography is still in its infancy and hence a lot of development can be anticipated and is indeed required until the technique reaches maturity needed for it to enter the markets. However, this process can be speeded up by applying the existing technology to as many different geological settings as possible and by alternating the survey setups to find optimal combinations for best performance.

Borehole muography can be applied anywhere were boreholes are available. The technique works quickest when the survey points are within the vertical depth of few hundreds of metres from surface. In such depths the survey durations range from days to weeks. In addition, the average density of the overlying rock column and desired resolution affect the total survey duration. It can be speculated that borehole muography is still applicable in slightly below 1

km depth, but in this case the survey durations are already exceedingly long (at least many months, perhaps even years). However, the advantage from going deeper is a very attractive one: the deeper the survey is conducted, the greater the volume of rocks from which the density information is extracted. Survey setup needs hence to be optimised for any given project.

It is relatively easy to find interesting test applications for BMDs (Holma & Kuusiniemi, 2018). It can be, and in some cases already have been, applied to soil layering and groundwater studies, weathering crust studies, ore exploration (Muon Solutions' in-house data), lithology and rock boundary studies, structural geological research, and so on. Long-term monitoring at the spent nuclear fuel and carbon dioxide geostorage sites are another two examples in which muography may well be one part of the monitoring solution. In these cases, a network of BMDs could form a continuous observation system specially adjusted to alarm if the system or its parts detect unexplainable density declines (potential leaks).

5. SUMMARY

Even if the borehole muon detectors (BMDs) are not as diverse and accurate in their capabilities as larger muon telescopes, they are very versatile tools in their own right, or more precisely, are likely to be. It is true that currently we are only witnessing the first wave of such tools and there remains a lot to learn about the best practices, setups and competencies and also about the limits of their operating behaviours. Once more experience has been gained, many capability upgrades are likely to be incorporated to BMDs. At the same time their usage may get more applications, including coupling with muon telescopes as some sort of satellite probes. Such developments should publicise borehole muography and, if the BMDs operate as efficiently as needed, set the technique and its instruments permanently to the toolbox of geophysics.

REFERENCES

Agostinelli, S., J. Allison and K. Amako *et al.*, 2003. Geant4 - a simulation toolkit. *Nuclear Instruments and Methods in Physics Research Section A*, **506(250)**, doi: 10.1016/S0168-9002(03)01368-8.

Heck, D., Knapp, J., Capdevielle, J.N., Schatz, G. and Thouw, T., 1998. CORSIKA: A Monte Carlo Code to Simulate Extensive Air Showers. *Report FZKA*, **6019**. (https://www.ikp.kit.edu/corsika/70.php)

Holma, M. and P. Kuusiniemi, 2018. Underground muography: The raise of geoparticle physics as a soil, orebody and rock realm imaging method. *Institute of Seismology, University of Helsinki*, Report **S-67**, 27-30.

Kaiser, R., 2019. Muography: overview and future directions. *Philosophical Transactions of the Royal Society A*, **377**, 20180049, doi: 10.1098/rsta.2018.0049.

Tanaka, H.K.M. and L. Oláh, 2019. Overview of muographers. *Philosophical Transactions of the Royal Society A*, **377**, 20180143, doi: 10.1098/rsta.2018.0143.

Suihkuvirtausmallinnus jäteveden purun suunnittelussa

T. Huttula[1] ja J. Tanttari [2]

[1] Aurinkokatu 7 D 41, 80140 Joensuu, timohuttula829@gmail.com
[2] Elomatic Oy, juha.tanttari@elomatic.com

Abstract

Computational flow and transport models have been utilized in Finland since 1970's. They have proven to be very use-full tools in combating eutrophication and in planning water construction projects as well as predicting the fate of harm-full substances. The spatial resolution of the models has improved remarkably during the decades. Also many chemical and biological processes have been included into models as more data have been available. Still the near field of the release site has been treated in a rather approximative way. This because the physics of the release plumes is quite challenging. Also very fine spatial resolution is needed to describe pipes and diffusers. We used a modern computational fluid dynamics (CFD) code, STAR-CCM+ for predicting the behavior of a waste water plume in Lake Kemijärvi, Finland. The work was related to the environmental permitting of a new biorefinery at the lake. The task was to find an out optimum site and way to lead purified waste waters to the lake. A traditional advective dispersive lake model was already applied to the lake for rough scaling of the problem. The new application included diffuser description and eight simulation scenarios were selected. They presented the most challenging hydrological and meteorological conditions. The model application included also a pore water application as a special attention was paid to the under water dam in the middle of the lake. After successful work practical solution was recommended for the customer.

Auroral substorm energetics from 1993 to 2016

I. Jaakonaho[1] and E.I. Tanskanen[1]

[1]Aalto University, Finland, iina.jaakonaho@aalto.fi

Abstract

Auroral substorms are a common phenomenon in the northern and the southern auroral regions such as Finland. The influence of the varying solar wind and interplanetary magnetic field (IMF) extends from the near-Earth space down to the surface. Disturbances, observed as geomagnetic storms and substorms, arise from the solar wind energy input and dissipation in the magnetosphere and ionosphere. In order to be able to prepare for space weather effects, we need to understand their variation in different time scales, as well as the dependence on the conditions in the Sun and near-Earth space. We studied substorms and their energetics from 1993 to 2016 and found out that the yearly total ionospheric dissipation was two times larger in 1994 and 2003 than other examined years. Furthermore, the superimposed seasonal dissipation profile for the solar cycle 24 was almost flat while the solar cycle 22 closely followed classical seasonal pattern having the largest dissipation in spring and fall.

1. INTRODUCTION

Magnetospheric energy budget have been examined by studying single events (e.g. Akasofu, 1981) and years (Tanskanen et al. 2002). According to the current view, ionospheric processes have a major role in the energy dissipation during substorms (Lu et al. 1995; Tanskanen et al. 2002), replacing the previous view of the ring current being the dominant channel. Several empirical methods have been formulated for estimating the energy dissipated through the two main ionospheric sinks: Joule heating (JH) and electron precipitation (ep) (e.g. Ahn et al. 1983).

Over the years the analysis methods have developed to allow the analysis of longer time scales (Tanskanen, 2009), increasing from several years to several solar cycles (SC). Tanskanen et al. (2011) studied substorm parameters and variation during a 16-year period from 1993 to 2008. They observed signs of both seasonal and solar cycle dependence in the substorm number, duration and peak amplitude. This study examines the variation of substorm energy dissipation using the same methods and data, expanding the examined period to include also the more recent years. The analysis is based on ground-based magnetic observations during a 24-year period from 1993 to 2016, overlapping three solar cycles.

2. METHOD

This study examines substorms that occurred during a 24-year interval from 1993 to 2016. Substorms are identified from the one-minute westward electrojet index IL (Kallio et al.

2000). The index is formed by computing the negative envelope of the magnetic X-component measured by an array of ground-based magnetometers. The value at each timestep represents the maximum negative deviation from the quiet time baseline. The IL data is collected from stations belonging to the IMAGE network, a longitudinal magnetometer chain centered in Fennoscandia (Viljanen and Häkkinen, 1997; Syrjäsuo et al. 1998). Substorms are identified from the IL time series using a high-throughput substorm search engine SSeeker by Tanskanen (2009). The analysis covers substorms occurring between 1600 and 0300 UT, around the local midnight of the IMAGE longitudes, which is the optimal time interval for the network to estimate the AL index (Kauristie et al. 1996).

3. RESULTS

Interannual and seasonal variation of substorm energies were analyzed by computing average and total dissipation through Joule heating and electron precipitation on both yearly and monthly level. The average Joule dissipation of the entire data set was 1.34×10^{15} J and the average electron precipitation energy 0.561×10^{15} J.

Interannual variation was examined by computing the total energy dissipation of all substorms for each year (Figure 1). The largest dissipation was observed in 1994 and 2003, during the declining phases of solar cycles 22 and 23. The same years have also previously been found having the most intense and longest substorms in the study of Tanskanen et al. (2011). The least energetic substorms, as well as the smallest total dissipation, occurred in 2009 during the minimum of solar cycle 24.

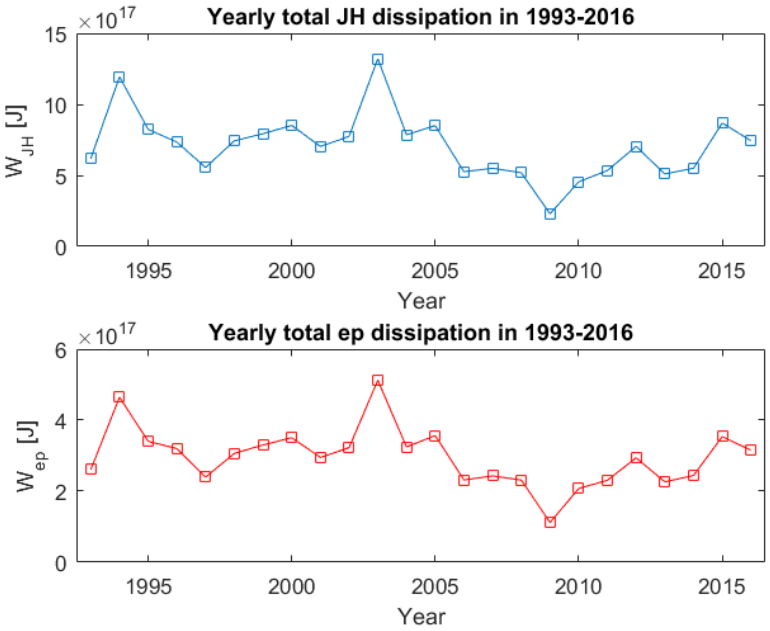

Figure 1: Yearly Joule heating (top) and electron precipitation (bottom) energy dissipated by substorms during 1993-2016.

The seasonal energy dissipation was analyzed by superposing all 24 years and calculating the average and total substorm energies for each month. This revealed that the most energetic substorms, on average, occurred during late spring and summer. The smallest average energies were observed during winter, with a minimum in December. In accordance with

Tanskanen et al. (2011), the seasonal pattern of average substorm energies showed a clear winter-summer asymmetry, most likely affected by long summer substorms. On the other hand, the variation of the monthly total dissipation showed more pronounced spring and fall maxima. The fall peak was higher and the spring peak wider, whereas summer and winter months had almost equally low values. A possible cause for the pattern might be the trend of substorm intensity peaks around equinoxes and smaller substorm occurrence during summer.

The examined 24-year period covers parts of three solar cycles: the declining phase of solar cycle 22 (1993-1996), the entire solar cycle 23 (1997-2008) and most of solar cycle 24 (2009-2016). The declining SC22 was found to be the strongest and SC24 the weakest in terms of both average and total monthly energies. As seen in Figure 2, SC22 showed signs of the spring-fall maximum pattern, but they were not as clearly seen in the following two cycles. The average substorm energies of SC23 and SC24 were largest in summer, while the total dissipation had only moderate equinox maxima in SC23 and almost none in SC24. The profiles of both cycles were overall flatter than SC22.

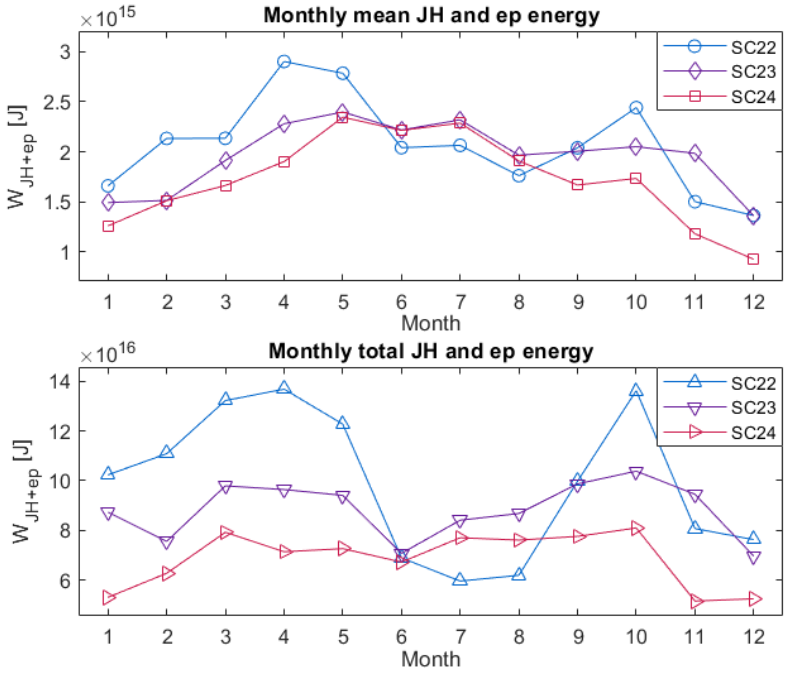

Figure 2: Seasonal energy dissipation from combined Joule heating and electron precipitation, calculated as monthly average (top) and monthly total (bottom) dissipation for solar cycles 22 (1993-1996), 23 (1997-2008) and 24 (2009-2016).

4. CONCLUSIONS

Substorm energy dissipation through two main ionospheric energy sinks was examined for a period from 1993 to 2016. Substorms were identified from the IL index using a search engine introduced by Tanskanen (2009), and estimations for the two-hemisphere Joule heating and electron precipitation energy dissipation were calculated for all the identified events. The largest yearly dissipation was found in 1994 and 2003 and the smallest in 2009, while the seasonal profiles had signs of the winter-summer asymmetry and equinox maxima. Different solar cycles showed distinctive seasonal characteristics, SC22 being the strongest and having more pronounced spring and fall peaks than SC23 and SC24.

It must be remembered that the superposed seasonal profiles only show highly averaged and general trends while individual years may have very distinctive patterns. However, the averaged patterns may reveal characteristics and dependencies that are only visible in longer time scales. Long-term analysis of magnetospheric energies and other space weather parameters is important for studying the evolution of space climate and its impacts.

REFERENCES

Ahn, B.H., S.I. Akasofu, and Y. Kamide, 1983. Joule heat production rate and the particle energy injection rate as a function of the geomagnetic indices AE and AL. *J. Geophys. Res.,* **88**, 6275-6287.

Akasofu, S.I., 1981. Energy coupling between the solar wind and the magnetosphere. *Space Sci. Rev.,* **28**, 121-190.

Lu, G., A.D. Richmond, B.A. Emery and R.G. Roble. 1995. Magnetosphere-ionosphere-thermosphere coupling: Effect of neutral winds on energy transfer and field-aligned current. *J. Geophys. Res.,* **100**, 19643-19660.

Kallio, E.I., T.I. Pulkkinen, H.E.J. Koskinen, A. Viljanen, J.A. Slavin, 2000. Loading-unloading processes in the nightside ionosphere. *Geophys. Res. Lett.,* **27**, 1627-1630.

Tanskanen, E.I., T.I. Pulkkinen, H.E.J. Koskinen and J.A. Slavin, 2002. Substorm energy budget during low and high solar activity: 1997 and 1999 compared. *J. Geophys. Res.,* **107**, A6.

Tanskanen, E.I., 2009. A comprehensive high-throughput analysis of substorms observed by IMAGE magnetometer network: Years 1993-2003 examined, *J. Geophys. Res.,* **114**, A5.

Tanskanen, E.I., T.I. Pulkkinen, A. Viljanen, K. Mursula, N. Partamies, and J.A. Slavin, 2011. From space weather toward space climate time scales: Substorm analysis from 1993 to 2008. *J. Geophys. Res.,* **116**, A00134.

Syrjäsuo, M., T.I. Pulkkinen, P. Janhunen, A. Viljanen, R.J. Pellinen, K. Kauristie, H.J. Opgenoorth, S. Wallman, P. Eglitis, P. Karlsson, O. Amm, E. Nielsen, and C. Thomas, 1998. Observations of substorm electrodynamics using the MIRACLE network. *Substorms-4*, **238**, 111.

Viljanen, A., L. Häkkinen, 1997. IMAGE magnetometer network, *Satellite-Ground Based Coordination Sourcebook,* **1198**, 111.

Kauristie, K, T.I. Pulkkinen, R.J. Pellinen, and H.J. Opgenoorth, 1996. What can we tell about global auroral-electrojet activity from a single meridional magnetometer chain? *Annales Geophysicae*, **14**, 1177-1185.

Mesospheric Monitoring of Ozone above the Polar Vortex (MeMO)

J. Jia[1], T. Ulich[1], A. Kero[1], R. Kivi[2], P. T. Verronen[2], K. Nilsen[1] and E. Sarkar[1]

[1] Sodankylä Geophysical Observatory, University of Oulu
[2]Space and Earth Observation Centre, Finnish Meteorological Institute

Abstract

Satellite and ground-based ozone measurements have been widely used to monitor ozone and many other atmospheric trace gases. However, most of the ozone monitoring instruments have limited measurement response at the altitude over 70 km. The Ku-band radiometer MOSAIC measures the emission line at 11.07GHz, providing ozone density in the mesosphere and the lower thermosphere. MOSAIC is portable, inexpensive, and independent from the solar radiation. The 11.07 GHz emission line is sensitive to the second ozone maximum at 92 km and to the third ozone peak at around 72 km in the polar regions. Thus, MOSAIC is optimal to be investigated and distributed within the Polar cap to provide continuously day and night ozone monitoring, which fills the gap of the satellite and traditional ground-based measurements. Moreover, the observed ozone data is crucial in helping to understand the space weather induced ozone variation in the upper atmosphere, and its influence to the lower atmosphere within Polar Vortex. In this presentation, the MeMO project is introduced. The instrument development and data analysis are reported.

Interpretation and 3D-visualization of Electromagnetic Exploration Data

J. Jokinen[1] **and S. Elo**

[1] Loop and Line Oy, jarkko@loopandline.fi
seppo.elo@pp.inet.fi

Abstract

We present 3D images of electromagnetic (EM) exploration data and models. The specific EM multi-frequency sounding system consists of a controlled source transmitter (large fixed loop antenna) and a moving receiver. The receiver has three orthogonal coils detecting amplitude variations of the magnetic field generated by the transmitter antenna (primary field) and the electric currents induced in the ground (secondary field). The method uses 41 different frequencies with the results divided into in-phase and quadrature (out-of-phase) components. Each measured station has 246 independent EM variables. Data is interpreted by means of realistic petrophysical parameters and 3D-structures.

The basic rule considering harmonic electromagnetic waves in conductive media is that low frequencies penetrate deeper than high frequencies. From this point of view a low frequency map reflects deeper conditions than a high frequency map. Each frequency map can be projected onto a characteristic depth below the ground surface and together all the projected frequency maps produce a 3D image. The depth level of each frequency map can be estimated, calculated (skin depth value) or transformed (apparent resistivity versus depth). After theoretical interpretation, also simulated data and interpreted structures can be imported into the same image. 3D images in pdf format are an effective and easy-to-use tool in modelling and geological interpretation.

1. INTRODUCTION

Electromagnetic measurements are mostly done for mapping electrical conductivity in the soil and bedrock. The low-altitude airborne electromagnetic measurements by the Geological Survey of Finland, covering the whole Finnish territory, were done with two frequencies and two vertical coplanar coils mounted on the wingtips of the aircraft. This high quality in-phase and quadrature data offers a depth penetration of about 60 m. Some EM methods with a helicopter carrying a powerful pulse transmitter reach deeper levels. Airborne conductivity maps offer a lot of information and drilling targets, but all conductors will not be found in this way. Exploration of deep targets needs more accurate and useful methods. The effective solution is an EM system with a large fixed transmitter loop and a moving receiver. In practice, the "moving receiver" remains stationary while measuring. A low noise level, a long measuring period at each station and a large transmitter loop form a strong combination for deep EM exploration. This arrangement is not new, it has been used for a long time with

borehole devices. Measurements at the ground surface, multi-frequency sounding and a new way to visualize data in 3D increase the usefulness of the set-up.

2. 3D IMAGING OF ELECTROMAGNETIC DATA

EM interpretation of Finnish exploration targets is rarely an easy task due to the complex lithological formations, but also due to a wide range of ambiguity in theoretical modelling. One basic arrangement is presented in Fig. 1. The results obtained with the highest frequency are presented just below the ground surface as a horizontal layer. Other frequency maps are positioned below it at depths which increase as the frequency decreases. Each map layer shows lateral variation, and vertical variation is visualized by means of iso-surfaces, which are calculated from all the frequency data (41 frequencies), not only from data shown as horizontal layers.

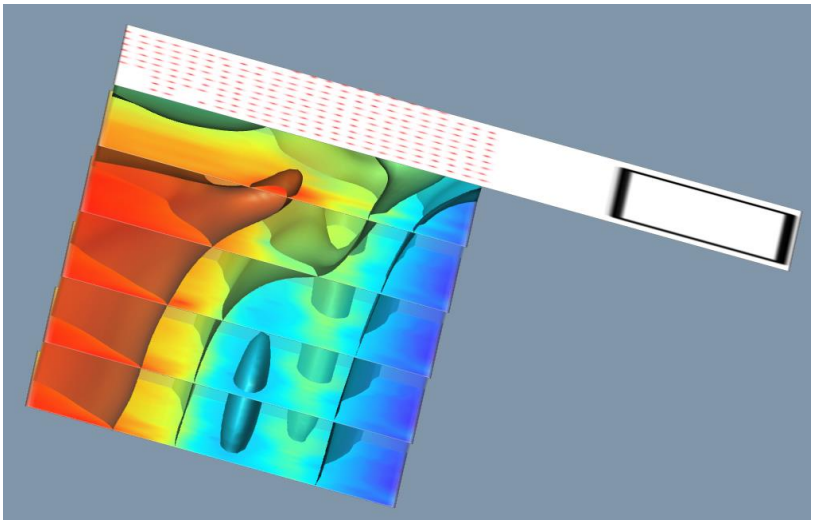

Figure 1: 3D-map of horizontal (radial) secondary field component. The black square is transmitter loop and red dots are measuring stations. Lengths of loop sides are 800 and 500 meters. Line separation is 100 meters and station spacing is 50 meters. Distance from transmitter to the nearest measuring stations is 400 meters.

Data is visualized as an 3D image by means of Voxler program and then transformed to pdf-format. The 3D PDF format can be easily shared and viewed by freeware programs like Adobe Acrobat Reader DC, in which user has many options to manipulate the 3D image such as to rotate viewing direction, to make objects visible or invisible, to select the render mode or the lighting scheme, to measure distances etc. In Voxler, layers and iso-surfaces can be transformed to other coordinate systems or exported in file formats suitable to other software.

Konenäön käyttö näkyvyyshavainnoinnissa

H. Juntti[1], J. Kentala[1] ja N´. Puttonen[1]

[1] Ilmatieteen laitos, heikki.juntti@fmi.fi

Abstract

A pilot study for researching the possibilities to measure meteorological visibility at airport by using cameras was conducted at Rovaniemi airport. Existing automated methods for visibility measurements often give misleading information especially when diamond dust, patches of fog or runway snow removal occurs. A method developed by Varjo and Hannuksela (2014) was applied at Rovaniemi airport for a test period of five months. The results were promising and showed that the method has potential in removing dramatically misleading observations of scattering measurements.

1. JOHDANTO

Meteorologinen näkyvyys on merkittävä sääsuure erityisesti ilmailussa. Lentoasemilla laskeutuvilla koneilla on erilaisia miniminäkyvyyksiä riippuen koneiden varustelusta, lentoaseman varustelusta ja lentäjän kelpuutuksista. Perinteisesti näkyvyyden mittaus on tehty ihmissilmin, mutta yhä enenevässä määrin sitä, samoin kuin muutakin havaintotoimintaa, on automatisoitu. Yleisesti käytetyt automaattiset mittarit perustuvat valon etusirontamittausperiaatteeseen (Laine, 2014) ja ne toimivat varsin hyvin silloin, kun näkyvyys on homogeeninen lentoaseman alueella. Tilanteissa, joissa esiintyy sumua vain osassa kenttää tai kentän kunnossapidon aiheuttama lumipöly osuu mittalaitteisiin sekä säässä, jossa ilmassa on jääkiteitä mittarit antavat usein virheellisiä havaintoja.

Tässä tutkimuksessa selviteltiin mahdollisuuksia arvioida vallitsevaa meteorologista näkyvyyttä konenäön avulla. Ideana on yrittää automaattisesti simuloida ihmisen tapaa havainnoida näkyvyyttä. WMO määritelmän mukaan meteorologinen näkyvyys on etäisyys, jolta tumma kohde (esim. metsän reuna) erottuu harmaata taustaa vasten (esim. taivas). Ilmatieteen laitos hyödynsi tässä tutkimuksessa Oulun Yliopiston Tietotekniikan osastolla kehitettyä menetelmää, joka on kuvattu seikkaperäisesti Sami Varjon ja Jari Hannukselan julkaisussa (Varjo ja Hannuksela, 2014).

2. KONENÄÖN KÄYTTÖ NÄKYVYYDEN ARVIOINNISSA

Konenäön avulla näkyvyyttä voidaan arvioida 1) hahmontunnistuksen avulla tai 2) kuvan kontrastin perusteella. Koska havaintoja tarvitaan myös yöllä, on tarve pystyä kuvaamaan myös pimeän aikaan. Pilottitutkimuksessa sovellettiin kuvaukseen HDR (High Dynamic

Range) tekniikkaa, jossa lopullinen kuva kootaan useasta eri valotuksilla kuvatuista kuvista. Näin voidaan lisätä kuvan dynamiikkaa sekä pimeän suuntaan, että runsaan valon suuntaan.

Hahmontunnistukseen perustuvan menetelmän periaate on yksinkertaisesti sen testaamista näkyykö kuvissa tunnetuilla etäisyyksillä sijaitsevat kohteet vai eivät. Jos kohde näkyy kuvassa, tiedetään että näkyvyys on ainakin kohteen ja kameran välinen etäisyys. Jos taas kohde ei näy, näkyvyys on vähemmän kuin kameran ja kohteen välinen etäisyys. Vaatimus näkyvyyden arvioimisen onnistumiselle on, että kiintopisteitä on sopivasti monella etäisyydellä ja ne ovat selvärajaisia. Tämä onkin usein haasteena menetelmän käytölle havaintoasemilla.

Kontrastiin perustuvan menetelmässä käytettiin Varjon ja Hannukselan kehittämää työnkulkua. Siinä **piirrevektorit** muodostettaan suodatetuista **HDR-kuvista**, joita varten kameralla otetaan kuvia eri valotusajoilla. Otettujen kuvien määrä riippui valaistuksen määrästä. HDR-kuvat muodostetaan laskemalla kuvien valotusajoilla painotetut intensiteetit yhteen. Sen jälkeen muodostettuun HDR-kuvaan käytetään **Retinex-suodatusta**, jolla pyritään korostamaan kuvan reunoja sekä normalisoimaan valaistuksen määrää. Retinex suodatetusta kuvasta saadaan laskettua **piirrevektorit**, joiden avulla koulutus suoritetaan. Piirrevektorit muodostetaan laskemalla yhteen HDR-kuvien Retinex suodatetut intesiteetit vaakasuunnassa ja ottamalla kuvasta gradientti y-suunnassa. Saatuja piirrevektoreita käytetään näkyvyysluokkien koulutuksessa. Näkyvyys saadaan **tukivektorikoneeseen (Support Vector Machine)** perustuvan luokittelun avulla, jossa piirrevektorit luokitellaan manuaalisen näkyvyyshavainnon perusteella. Tukivektorikoneessa käytetään RBF-kernelifunktiota (Radial Basis Function), jonka tarvitsemat parametrit C ja gamma, optimoitiin molemmille pilottiprojektissa käytetyille kameroille erikseen. (Varjo ja Hannuksela, 2014).

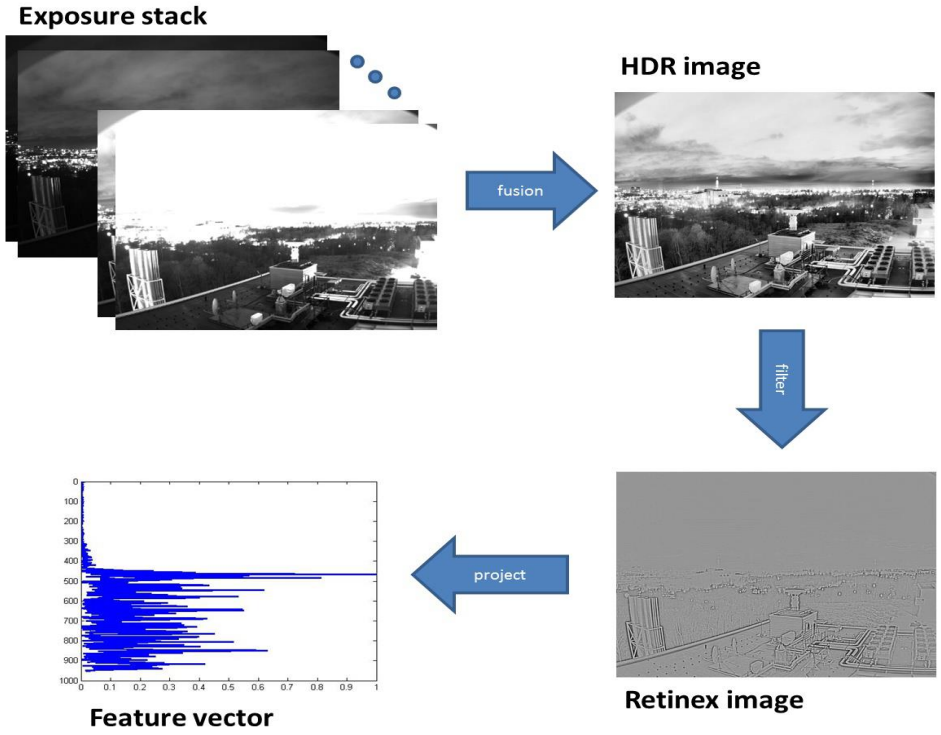

Kuva 1: Työn kulku kontrastiin perustuvassa menetelmässä (Varjo ja Hannuksela 2014)

3. PILOTTITUTKIMUKSEN TULOKSIA

Pilottijärjestelmään kuului 2 kameraa, jotka oli suunnattu vastakkaisiin suuntiin lentokentällä. Kuvaamiseen liittyviä ongelmia, joita ratkottiin mittauksen alussa olivat valotukseen ja HDR ajoituksiin liittyvät ongelmat. Lapissa aurinko paistaa yöllä suoraan linssiin, mikä voi tuhota kameran kennon. Talvella puolestaan kamerakotelon ikkunaan tuiskuava lumi ja vesi tekevät kuvista ajoittain käyttökelvottomia, joita kotelon lämmityksellä pyrittiin ratkaisemaan.

Järjestelmä koulutettiin vertaamalla kuvia manuaalisiin havaintoihin. Koulutusmateriaalia kerättiin 5 kk ajalta ja koulutukseen käytettiin n. 11 000 kuvaa/kamera. Molemmilla menetelmällä saatuja näkyvyysarvioita verrattiin manuaalisiin näkyvyyshavaintoihin, joita lentokentällä tehdään. Menetelmää testattiin n. 2700 kuvan avulla vertailemalla niitä tehtyihin näkyvyyshavaintoihin.

Havaittiin, että kameranäkymällä on suuri vaikutus koulutuksen onnistumiseen. Osoittautui, että maisemassa olisi saanut olla enemmän selkeitä kohteita esim. rakennuksia. Metsänreunan erottaminen kameralla harmaasta taivaasta osoittautui varsin haastavaksi varsinkin kauempana ollessaan. Metsällä ja maisemalla on Suomessa tapana lisäksi olla tyystin erilainen kesä- ja talviaikaan. Ehkä osittain tästä johtuen kontrastiin perustuvalla menetelmällä saatiin parempia tuloksia kuin hahmontunnistuksen menetelmällä.

Kontrastiin perustuvan menetelmän tulokset ovat lupaavia. Niiden avulla kyettiin merkittävästi parantamaan erityisesti näkyvyysalueen 500 m – 6 km havaintojen osuvuutta oikeaan ICAO luokkaan. ICAO:n Annex 3:n mukaan kriittiset näkyvyyden raja-arvot ilmailille ovat: 5000m, 3000m, 1500m, 800m, 600m, 350m and 150m (ICAO ???).

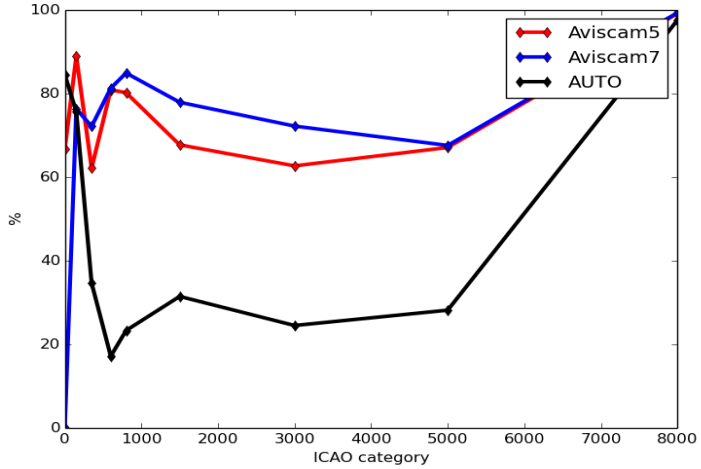

Kuva 2: Pilottitutkimuksessa kontrastiin perustuvalla menetelmällä konenäöllä arvioidun näkyvyyden osuminen samaan lentosään näkyvyysluokkaan. Aviscam 5 ja 7 ovat eri suuntiin katsovia kameroita ja AUTO automaattisen näkyvyyshavainnon osuvuus aiemman 3 vuoden tutkimusaineiston perusteella. Huom. Vertailujaksot kameroiden ja AUTO havaintojen välillä ovat erit.

4. KONENÄÖN MAHDOLLISUUKSISTA NÄKYVYYDEN ARVIOINTIIN

Kokeilujakson lyhyyden vuoksi tuloksista ei voida tehdä kovin pitkälle meneviä johtopäätöksiä, mutta niiden perusteella menetelmä vaikuttaa mahdolliselta tavalla parantaa näkyvyysmittaukset laatua. Yksinomaiseksi mittausmenetelmäksi se ei ainakaan välttämättä sovellu, mutta sen avulla olisi mahdollista korjata selvästi virheellisiä havaintoja tilanteissa, joissa, sirontamittarit harhautuvat kokonaan.

Hahmontunnistukseen perustuvia näkyyvden havaintomenetelmiä on myytävänä jo kaupallisena sovelluksena. Niiden toimivuudesta Suomen talvisessa ja vähän kiintopisteitä omaavassa maisemassa ei ole kokemusta.

5. LOPUKSI

Haasteena kaikissa koneoppimiseen perustuvissa menetelmissä on koulutuksen järjestäminen. Kouluttaminen vaatii suuren aineiston erilaissa mahdollisissa näkymissä (eri vuodenajata, valaistukset, säätyypit ja niiden voimakkuudet) tehtyjä havaintoja ja koska näkymä on jokaisella havaintopaikalla lisäksi erilainen, pitää se tehdä jokaiselle havaintopaikalle erikseen. Menetelmä on kuitenkin lupaava ja jatkotutkimukset sen soveltamiseksi näkyvyyshavainnointiin olisivat aiheellisia

KIITOKSET

Erityiset kiitokset Sami Varjolle, Jari Hannukselalle ja Olli Silvenille tämän tutkimuksen mahdollistamiselle ja korvaamattomalle avulle, joka mahdollisti menetelmän tieteellisen pohjan. Juha Ylioinaalle suuret kiitokset ideoinnista, josta koko hanke sai alkunsa. Kiitokset myös Ilmatieteen laitoksen havaintotoiminnalle ja etenkin Lasse Latvalle, Antti Poikiselle, Veikko Postilalle, Antti Aarvalle laitteiston instrumentoinnista ja avusta teknisten haasteiden ratkaisemisessa.

LÄHTEET

Laine, S., 2014: Tuotantotestauksen kehittäminen, Optiset säänmittausanturit, Opinnäytetyö, Lahden ammattikorkeakoulu, Tekniikan ala, Tietotekniikan koulutusohjelma, **48**, 2-7.

Varjo, S. ja J. Hannuksela, 2014. Image Based Visibility Etimation During Day and Night. *Conference: ACCV 2014 Workshops*, Singapore, Volume: **LLCN 9010**.

Annex 3 – Meteorological Services for International Air Navigation, ICAO 2018.

Snow research in Sodankylä

A. Kontu[1], L. Leppänen[1], H-R Hannula[1], J. Lemmetyinen[1] and J. Pulliainen[1]

[1] Finnish Meteorological Institute, Space and Earth Observation Centre, anna.kontu@fmi.fi

Abstract

This paper describes the snow research activities of Finnish Meteorological Institute in Sodankylä, Finland. We present the infrastructure that is currently available for studies of snow and soil frost and give a review of research done using the data.

1. INTRODUCTION

The Finnish Meteorological Institute's Arctic Space Centre (FMI-ARC) in Sodankylä has a long history as a meteorological measurement station with daily snow depth records dating back to 1911. Nowadays the research focus of Sodankylä station is the monitoring of hydrological and carbon cycles and atmospheric gases. The aim of snow research is to develop models and algorithms for satellite remote sensing and satellite calibration/validation studies. For that purpose, the station has significant infrastructure of continuous, coincident and collocated measurements.

Passive microwave remote sensing of snow water equivalent (SWE) suffers from poor spatial resolution (tens of km), as well as from uncertainties in the modelling of the effect of forests, soil, and snow structure. In short, numerous other parameters in addition to the desired SWE affect snow microwave emission, most important being snow wetness and scattering particle size. The research goal is to find methods of overcoming these shortages and inaccuracies through better modelling and new algorithms.

Remote sensing using active microwave sensors (radar) is one way to increase the spatial resolution of satellite SWE products, but typically at the cost of temporal resolution or coverage. Currently there are no active microwave algorithms no algorithms for hemispherical scale yet, but several methods are in development and under study.

2. INFRASTRUCTURE

The current setup of snow remote sensing instruments includes three radiometers, a radar and a hyperspectral camera in a 24-m tower monitoring a sparse pine forest on mineral soil. Reference measurements include a weather station, soil temperature and moisture stations, automated SWE measurement, snow temperature profile, dendrometers for tree trunk diameter, tree trunk temperature and CO2 flux. In addition, manual measurements of snow structure are performed weekly.

The instrument setup includes two European Space Agency's (ESA) ELBARAII radiometers (1.4 GHz), one in 21 m height and another at ground level. They are reference instruments for ESA SMOS mission, and have been used to map soil frost. Another radiometer located at 21 m measures on frequencies (10.65, 18.7, 21, 36.5 GHz) typically used in remote sensing of SWE. The motivation for these measurements is to develop better microwave emission models for boreal forests in satellite grid cell scale. In addition, the connection of soil frost, snow and forest to CO2 flux from the area is studied to develop means for satellite measurements of CO2 flux of boreal forest.

A 1-10 GHz radar, originally designed for stationary measurements of snow backscatter, has now been upgraded with rotation and position control system allowing SAR measurements. It is used in development of new active or combination of active/passive methods for snow mapping.

A hyperspectral camera (500-900 nm) will be mounted on the same movement system with the radar. On campaign basis it can be mounted in a UAV allowing hyperspectral measurements of a larger area.

3. MANUAL MEASUREMENTS

Weekly manual snow pit measurements (Leppänen et al., 2016) are performed in the forest close to the 24-m tower to study the temporal changes in snow structure (layers, grain size, specific surface area, temperature, density).

4. REVIEW OF RESEARCH

The measurement data of FMI-ARC station has been used to develop new methods for mapping soil frost (Rautiainen et al. 2016), to enhance microwave snow modelling (Maslanka et al. 2016; Lemmetyinen et al. 2010) and L-band snow models (Lemmetyinen et al., 2016; Schwank et al., 2014), for retrieval of snow properties from active and passive microwave observations (Lemmetyinen et al. 2018; Lin et al. 2016; Leinss et al. 2015), in physical snow models (Kontu et al. 2017; Krinner et al. 2018; Leppänen et al. 2015).

REFERENCES

Kontu, A., J. Lemmetyinen, J. Vehviläinen, L. Leppänen, and J. Pulliainen, 2017. Coupling SNOWPACK-modeled grain size parameters with the HUT snow emission model. *Remote Sens. Environ.*, **194**, 33-47.

Krinner G., et al., ESM-SnowMIP: assessing snow models and quantifying snow-related climate feedbacks, 2018. *Geosci. Model Dev.*, **11**, 5027-5049.

Leinss, S., A. Wiesmann, J. Lemmetyinen, and I. Hajnsek, 2015. Snow water equivalent of dry snow measured by differential interferometry. *IEEE J. Sel. Top. Appl. Earth Obs. Remote Sens*, **8**, 3773-3790.

Lemmetyinen, J., C. Derksen, H. Rott, G. Macelloni, J. King, M. Schneebeli, A. Wiesmann, L. Leppänen, A. Kontu, and J. Pulliainen, 2018. Retrieval of effective correlation length and snow water equivalent from radar and passive microwave measurements, *Remote Sensing*, **10**.

Lemmetyinen, J., M. Schwank, K. Rautiainen, A. Kontu, T. Parkkinen, C. Mätzler, A. Wiesmann, U. Wegmüller, C. Derksen, P. Toose, A. Roy, and J. Pullainen, 2016. Snow density and ground permittivity retrieved from L-band radiometry: Application to experimental data, *Remote Sens. Environ.*, **180**, 377-391.

Lemmetyinen, J., J. Pulliainen, A. Rees, A. Kontu, Y. Qiu, and C. Derksen, 2010. Multiple-layer adaptation of HUT snow emission model; Comparison with experimental data, *IEEE Trans. Geosci. and Remote Sens.*, **48(7)**, 2781-2794.

Leppänen, L., A. Kontu, H. Hannula, H. Sjöblom, and J. Pulliainen, 2016. Sodankylä manual snow survey program, *Geosci. Instrum. Method. Data Syst.*, **5**, 163-179.

Leppänen, L., A. Kontu, J. Vehviläinen, J. Lemmetyinen, and J. Pulliainen, 2015. Comparison of traditional and optical grain-size field measurements with SNOWPACK simulations in a taiga snowpack, *J. Glac.*, **61(225)**, 151-162.

Lin, C.-C., B. Rommen, N. Floury, D. Schüttemeyer, M. Davidson, M. Kern, A. Kontu, J. Lemmetyinen, J. Pulliainen, A. Wiesmann, C. Werner, C. Mätzler, M. Schneebeli, M. Proksch, and T. Nagler, 2016. Active microwave scattering signature of snowpack – Continuous multiyear SnowScat observation experiments, *IEEE J. Sel. Top. Appl. Earth Obs. Remote Sens.*, **9(8)**, 3849-3869.

Maslanka, W., L. Leppänen, A. Kontu, M. Sandells, J. Lemmetyinen, M. Schneebeli, M. Proksch, M. Matzl, H.-R. Hannula, and R. Gurney, 2016. Arctic Snow Microstructure Experiment for the development of snow emission modelling, *Geosci. Instrum. Method. Data Syst.*, **5**, 85-94.

Rautiainen, K., T. Parkkinen, J. Lemmetinen, M. Schwank, A. Wiesmann, J. Ikonen, C. Derksen, S. Davydov, A. Davydova, J. Boike, M. Langer, M. Drusch, and J. Pulliainen, 2016. SMOS prototype algorithm for detecting autumn soil freezing, *Remote Sens. Environ.*, **180**, 346-360.

Schwank, M., K. Rautiainen, C. Mätzler, M. Stähli, J. Lemmetyinen, J. Pulliainen, J. Vehviläinen, A. Kontu, J. Ikonen, C. Ménard, M. Drusch, A. Wiesmann, and U. Wegmüller, 2014. Model for microwave emission of a snow-covered ground with focus on L band, *Remote Sens. Environ.*, **154**, 180-191.

Geophysical research at Oulu Mining School: challenges and solutions

E. Kozlovskaya[1,2], K. Moisio[1], J. Okkonen[1], N. Afonin[1], J. Nevalainen[1]

[1] University of Oulu, Oulu Mining School, elena.kozlovskaya@oulu.fi
[2] Geological Survey of Finland

Abstract

Exponential population growth, urbanization, and the subsequent constantly growing demand for metals, minerals and rock aggregates pose the key challenges to mankind in the 21st century. As a response to these challenges development of raw materials sector and mining industry is required. Rapid warming of the Arctic attracts more businesses and activities to the area and in particular, mining in the Arctic Region is expanding in Finland as well as in other Arctic countries due to increasing need of mineral resources. In response to needs of rapidly growing mining industry in Finland, a new faculty, Oulu Mining School (OMS), was organized at the University of Oulu in 2014. In 2018, the OMS as a separate research unit was merged with the Faculty of Technology. The Oulu Mining School aims to integrate scientific disciplines along the value chain from exploration to mining and mineral processing. The OMS concentrate on the research and education in geosciences: geology and mineralogy, quaternary geology, mining engineering and mineral processing and applied geophysics. Tasks of applied geophysics at different stages of life-cycle of a mine include search for new mineral deposits and their detailed investigation, contribution to economic and technical evaluations which confirm the feasibility of a mining project, rational exploitation of deposit, monitoring, renewing mineable reserves and mitigating the negative impacts of mining (surface subsidence, emissions and waste, lowering of the water table etc.). In the phase of mine closure the geophysics helps in stabilisation, re-cultivation and re-naturalisation of mining environment.
Reorganization of geophysics at Oulu University required significant revision of the existing research directions and education programs. Development of applied geophysics has been always driven by technology development and the 21th century applied geophysics is not only consuming new technologies, but it largely initiates their development. New developments in sensor technologies and wireless communications, computer science, new satellite missions for observing the solid Earth, new technologies of data processing have put new challenges before specialists in applied geophysics. In response to these challenges, applied geophysics research at OMS is concentrating on the following main topics:

1) *Advanced methods of geophysical exploration*
2) *Mining geophysics that is a new research direction connected with geophysical measurements in mines.*
3) *Geophysical modeling, inversion and joint interpretation of geophysical and geological information.*

A specific area of applied geophysics research at OMS is investigating impact of extreme weather and climate change in the Arctic on mining infrastructures and operations. Mining in

cold climate conditions is a challenging task and may result in negative impacts on both the environment and on local communities, if the environmental issues are not treated in proper way. Geophysical techniques are traditionally used in environmental studies and new measurement technologies open new opportunities for application of geophysics.

DigiMAG method and historical magnetic recordings for better magnetic environment understanding

O. Kärhä[1]

[1] Aalto University, otto.karha@aalto.fi

Abstract

The main goal of this project is compare magnetic disturbances in the island and inland locations by using the currently existing magnetic observations and recordings by SMA network (35 stations). Magnetic disturbances are compared from two inland observatories Abisko and Sodankylä to two island magnetometers in Bear and Hopen islands. We compare the disturbance amplitude in X, Y and Z direction and estimate the effect of local conductivity structure to the measurements. We will present the idea behind the custom-build digitization devise and show examples of the recently digitized data. Recorded data consist of 620 film reels. Each reel contains about two months of data from one station. The total length of the all reels is 20 km. The quality of the data is excellent and a resolution of 0.1 nT can be achieved. The ultimate goal is to extend the ground magnetic data (1) to the locations that are not covered by the current magnetometers and (2) to include data from solar cycles 20 and 21 which is partly missing from World Data Centres.

Solar UV radiation in Arctic and Antarctic sites measured by ground instruments and satellites

K. Lakkala[1,2], M. Aun,[2,3], J. Kujanpää[1], N. Kalakoski[1], O. Meinander[1], R. Sanchez[4], A. Arola[2], A. Heikkilä[2], I. Ialongo[1], J. M. Karhu[1], T. Karppinen[1], A. Redondas[5], J. Tamminen[1]

[1] Finnish Meteorological Institute, Space and Earth Observation Centre, kaisa.lakkala@fmi.fi
[2] Finnish Meteorological Institute, Climate Research Programme
[3] University of Tartu, Estonia
[4] Servicio Meteorológico Nacional, Argentina
[5] Spanish Agencia Estatal de Meteorología, Tenerife, Spain

Abstract

The Finnish Meteorological Institute (FMI) measures solar UV radiation in both Arctic and Antarctic sites. Spectral UV measurements started in Sodankylä, 67°N, in 1990, and the time series is one of the longest in northern high latitudes. Multifilter UV measurements started in Marambio, 64°S, in 2017. They continue the time series of the Antarctic NILU-UV network, which was established in cooperation between Spanish Agencia Estatal de Meteorología (AEMET), Argentinean Direccíon Nacional del Antártico–Instituto Antártico Argentino and FMI. Both Sodankylä and Marambio are located at polar areas which suffer from stratospheric ozone loss during spring time. As total ozone is one of the main factor affecting the amount of solar UV radiation reaching the Earth's surface, ozone loss is expected to be seen as increased UV levels. Marambio's measurements showed that UV index can be 12 during low total ozone episodes in late spring, while in Sodankylä UV indices in the spring don't exceed those measured in the summer. In this work, the time series of both locations are shown. In addition to ground measurements, the FMI is responsible for three satellite-derived UV products: 1) EUMETSAT Offline UV is generated in the framework of the Satellite Application Facility on Atmospheric Composition Monitoring (AC SAF), 2) OMI UV product uses the measurements of the Ozone Monitoring Instrument aboard the NASA EOS-Aura satellite launched in 2004 and 3) the TROPOMI UV product uses the measurements of the Tropospheric Ozone Monitoring Instrument (TROPOMI) aboard the Copernicus Sentinel-5 precursor satellite launched in 2017. Inhomogeneous surface and low sun increase the uncertainty of satellite UV retrievals at high latitudes, and ground measurements are essential for validation of satellite UV products and thus development of satellite UV processors. Validation results are shown for Arctic and Antarctic sites.

Green Minerals Project – Exploration Techniques for Flake Graphite

S. Leinonen[1]

[1] Geologian tutkimuskeskus, seppo.leinonen@gtk.fi

Abstract

The global market of battery minerals are getting strongly upwards. Manufacturers in EU have announced that they will increase significantly production of electric vehicles in coming years. New investments set major challenges to exploration as well to mining and mineral processing industries. Green Minerals project, years 2018-2019 focuses on developing prospecting of flake graphite and lithium pegmatites. The project tests ground geophysical methods locating graphite deposits, geochemical prospecting is found more effective for Li-pegmatites. One of the objectives is also to improve beneficiation techniques, also tests Finnish graphite in Li-ion batteries. Project is funded by Business Finland. Consortium consists of Geologian tutkimuskeskus, Fennoscandian Resources Ab Oy and Keliber Oy.

1. BACKGROUND

Global usage of high quality flake graphite rises remarkably in coming years, especially demand of so-called battery-grade graphite. The Finnish bedrock has a great potential for commercially exploitable flake graphite. There has been small-scale mining in previous decades in East-Finland. Potential areas for prospecting are high metamorphic schist belts (Ahtola and Kuusela, 2015). In these regions are the highest potential to find coarse flaked graphite 100-1000 µm. For battery use grain size is milled down to 15 µm. After flotation anode grade graphite needs to be purified by chemical-thermal processes > 99% C.

2. ACTIVITIES

Most of the conductive anomalies of bedrock are caused by graphite. Green Minerals project tests ground geophysical methods and data processing procedures to find new ways to classify resource qualities of flake graphite from less valued amorphous types. During the first project year there were electromagnetic profile measurements with GEM-2 and Max-Min, also ERT, Electrical resistivity tomography method was tested. Magnetic measurements were made by GEM GSM 19 Overhouser. For the interpretation of results numerous petrophysical analysis have been made from the drill cores. Ground geophysical surveys continue also in the second project year 2019. Results will be published in the beginning of 2020.

REFERENCES

Ahtola, T. and J. Kuusela, 2015. Esiselvitys Suomen grafiittipotentiaalista. *Geologian tutkimuskeskus, Arkistoraportti,* **88**, 14 s.

Lumen mikrorakenteen mittauksiin ja mallinnuksiin perustuva tutkimus Sodankylässä

L. Leppänen[1], A. Kontu[1], J. Lemmetyinen[1] ja J. Pulliainen[1]

[1] Ilmatieteen laitos, Avaruus- ja kaukokartoituskeskus, leena.leppanen@fmi.fi

Abstract

Snow microstructure is essential for many research applications related to improvement of interpretation of remote sensing observations. Measurements of the snow microstructure are performed at the Arctic Space Centre of Finnish Meteorological Institute in Sodankylä since 2006 with a traditional method and since 2012 with an instrument based on reflectance of near-infrared laser. Error analysis of traditional grain size and specific surface area (SSA) measurements were conducted, resulting generally larger bias for the traditional grain size. A novel portable instrument for spectral reflectance observations was tested for the snow observations. An empirical relationship was found between SSA and the reflectance derived parameter. Field observations of traditional grain size and optical grain size derived from SSA were compared to SNOWPACK model simulations. The optical grain size had larger bias to the simulated optical grain size than the traditional grain size to the traditional grain size simulation. However, correlation coefficient was better for the optical grain size. Consequently, agreement scores between the measurements and the simulations resulted better values for the traditional grain size than the optical grain size. Effective grain size retrieved from HUT microwave emission model was compared to the SNOWPACK simulations resulting smaller bias with the simulated optical grain size than with the simulated traditional grain size. HUT model simulations of microwave emission had annually varying bias to microwave emission observations resulting need of scaling of the SNOWPACK simulations prior to applying the simulated grain sizes to snow water equivalent retrievals.

1. JOHDANTO

Lumen mikrorakenteella tarkoitetaan kiteiden kokoa, muotoa, sidoksia ja sijoittumista toistensa suhteen. Mikrorakenne on tärkeä säteilyn siroamisen ja heijastumisen kannalta sekä mikroaalloilla että optisilla aallonpituuksilla. Näin ollen mikrorakenteen mittaukset ovat tärkeitä optisen ja mikroaaltokaukokartoituksen kannalta. Lumen mikrorakenne on perinteisesti mitattu kiteen suurimpana halkaisijana. Parin viimeisen vuosikymmenen aikana on kehitetty menetelmiä, joilla mikrorakennetta voidaan mitata esimerkiksi infrapunasäteilyn heijastumisen avulla. Lumen mikrorakenneteen evoluutiota voidaan simuloida fysikaalisilla malleilla. Lumen ominaisuuksien globaali havainnointi on mahdollista kaukokartoituksen avulla. Passiivisia mikroaaltoradiometrejä käytetään lumen vesiarvon havainnointiin. Näiden havaintojen tulkintaan käytetään mikroaaltoemissiomalleja, jotka simuloivat luonnollista

mikroaaltoemissiota lumen ominaisuuksien perusteella. Tutkimus perustuu Ilmatieteen laitoksen Arktisessa Avaruuskeskuksessa Sodankylässä tehtäviin mittauksiin lumen rakenteesta, mittauksiin optisilla ja mikroaaltolaitteilla sekä niiden tukimittauksiin (Leppänen et al., 2016; Leppänen et al., 2018).

2. MENETELMÄT

Perinteisesti lumen kidekokoa on mitattu arvioimalla keskimääräisen kiteen halkaisija millimetriruudukkoa käyttäen (Fierz et al. 2009). Mittaus tehdään paljaalla silmällä ja apuna voi käyttää suurentavaa linssiä. Menetelmä on herkkä havaitsijasta aiheutuville virheille. Lisäksi kiteiden erottaminen lumipenkasta muuttaa lumen mikrorakennetta. Sodankylässä mittaus tehdään lisäksi käyttäen makrokuvausta, jossa lumikiteet kuvataan millimetriruudukkoa vasten ja kuvat analysoidaan myöhemmin. Modernimpi tapa mitata lumen mikrorakennetta on määrittää lumen pinta-alan ja massan suhde (specific surface area, SSA). SSA kuvaa lumen kolmiulotteista mikrorakennetta paremmin kuin perinteinen kidekoko. Maastomittauksiin soveltuvia menetelmiä on kehitetty perustuen lähi-infrapunasäteilyn heijastuvuuden ja SSA:n riippuvuuteen (Domine et al. 2006). Tällainen mittalaite on IceCube, jota on käytetty Sodankylässä vuodesta 2012 lähtien. IceCube mittaa aallonpituudeltaan 1310 nm infrapunalaserin säteilyn heijastumista luminäytteen pinnasta, josta SSA lasketaan perustuen kalibrointimittauksiin ja mallinnukseen. QualitySpec Trek (QST) kannettava spektrometri mittaa heijastunutta säteilyä 350-2500 nm aallonpituuksilla. Mittaus tehdään kosketuksissa lumeen, joten laitteessa on sisäinen valonlähde.

Mikroaaltoradiometri on passiivinen laite, joka mittaa luonnollista mikroaaltosäteilyä eli kirkkauslämpötilaa. Kuivan lumen tapauksessa havaittavan mikroaaltosäteilyn määrään vaikuttaa muun muassa lämpötila, mikrorakenne ja vesiarvo. Sodankylässä on käytössä useita radiometrejä, jotka havaitsevat säteilyä eri taajuuksilla (Leppänen et al. 2018). HUT emissiomallia käytetään kirkkauslämpötilojen simulointiin lumesta mitattujen parametrien avulla (Pulliainen et al. 1999; Lemmetyinen et al., 2010). Puoli-empiirinen malli simuloi yksi tai moni kerroksisen lumipeitteen, jossa kerrokset määritellään syvyyden, lämpötilan, tiheyden, kosteuden, kidekoon, suolaisuuden ja vesiarvon avulla. Efektiivinen kidekoko lasketaan minimoimalla simulaatioiden ja havaintojen välinen ero.

Lumen rakenteen muutosta voidaan simuloida fysikaalisilla lumimalleilla, kuten SNOWPACK (Lehining ja Bartelt 2002). Mallin käyttämät parametrit ovat ilman lämpötila, suhteellinen kosteus, tuulen nopeus ja suunta, tuleva ja lähtevä lyhytaaltoinen säteily, lumen syvyys, lumen lämpötila ja maaperän lämpötila. Mallin simuloimien kerrosten määrä kasvaa lumen syvyyden mukana. Malli käyttää kahta parametria kiteiden muodon määrittämiseen. Kiteen kasvu on joko lämpötilan, muodon ja kidekoon funktio tai kasvun määrittää alkuperäinen kidekoko, massavuo kerrosten välillä, massa vuo kerroksen sisällä, kasvava kidekoko ja lumen syvyys riippuen olosuhteista. Optinen kidekoko on määritetty joko muotoa kuvaavien parametrien tai perinteisen kidekoon funktiona (Vionnet et al. 2012).

3. TULOKSET

Perinteisen kidekoon havaitsijasta johtuvaa virhettä tutkittiin makrokuvien perusteella. Kolmen havaitsijan arvioiden vaihtelu oli suurinta lumikuopan pohjalla, jossa näytteet sisälsivät monen kokoisia kiteitä. IceCube mittauksen kalibroinnin vaikutus oli maksimissaan

noin 0.1 mm SSA:sta laskettuun optiseen kidekokoon. Mittauksen toistettavuutta tutkittiin mittaamalla samaa näytettä kolme kertaa peräkkäin. Keskimääräinen suhteellinen keskihajonta oli 2 %. Näytteenottamisen aiheuttamaa virhettä tutkittiin ottamalla näyte kolmesti kahdesta eri kidetyypistä olettaen että lumi oli näissä kohdissa homogeenistä, jossa keskimääräinen suhteellinen hajonta oli 3 %. (Leppänen et al. 2015; Leppänen ja Kontu, 2018)

QST laitetta testattiin lumimittauksiin keväällä 2017. Mittaukset tehtiin kahdesti suoraan lumikuopan seinämästä, kerran IceCube näytteistä ja kahdesti molemmista. Mitatuista spektreistä käytettiin aallonpituuksia 1160 nm ja 1260 nm, joiden perusteella laskettiin empiirinen vakio Q. SSA:n ja Q:n välille löytyi lineaarinen yhteys. Tulevaisuudessa voidaan mahdollisesti hyödyntää QST laitetta lumen mikrorakennemittauksissa, mutta lisätutkimuksia tarvitaan. (Leppänen ja Kontu, 2018)

SNOWPACK malli simuloi tyypillisesti enemmän kerroksia kuin mittauksissa havaitaan. Siitä johtuen kerroksittainen vertailu ei ollut mahdollista, vaan painotettuja keskiarvoja käytettiin. Optisen kidekoon mittaukset ja simulaatiot riippuvat paremmin toisistaan kuin perinteisen kidekoon tapauksessa, mutta simulaation ja mitatun välinen ero on optisella kidekoolla suurempi (Kuva 1a). Sen seurauksena optisella kidekoolla mittausten ja simulaatioiden vastaavuus (agreement score) oli huonompi kuin perinteisen kidekoon tapauksessa. (Leppänen et al. 2015; Kontu et al. 2017)

HUT emissio mallilla laskettua efektiivistä kidekokoa verrattiin SNOWPACK mallin simuloimiin kidekokoihin (Kuva 1b). Efektiivinen kidekoko oli lähempänä simuloitua optista kidekokoa kun perinteistä. HUT mallin kirkkauslämpötila simulaatio poikkesi havainnosta vähemmän kun käytettiin SNOWPACK mallin simuloimaa optista kidekokoa simuloidun perinteisen kidekoon sijaan. Jotta simulaatioita voitaisiin käyttää HUT mallin kanssa tehokkaasti, ne tarvitsisivat vuosittain eri skaalauskertoimen. (Kontu et al. 2017).

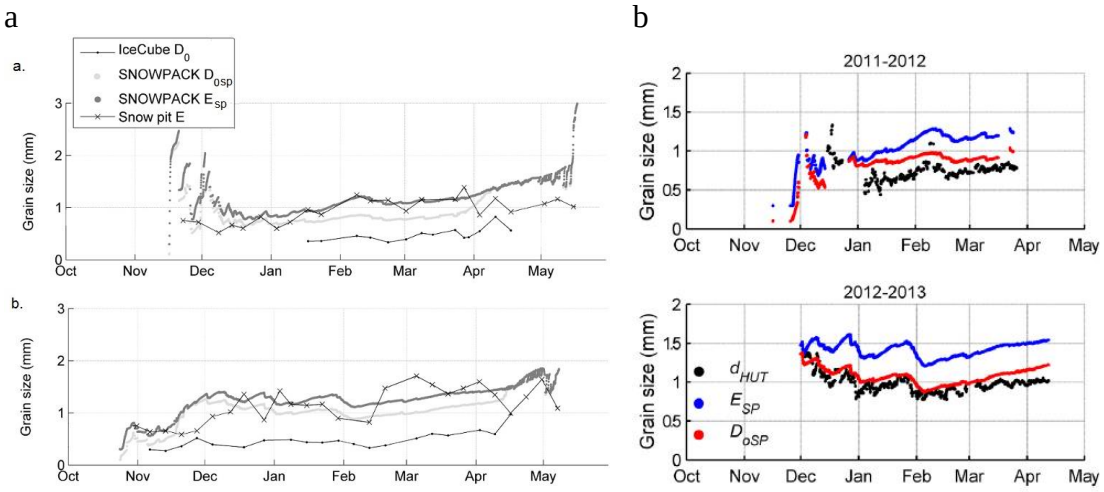

Kuva 1: a) Mitattu perinteinen (x) ja optinen (.) kidekoko sekä SNOWPACK simuloitu perinteinen (tumma) ja optinen (vaalea) kidekoko talvelle 2011-2012 yllä ja 2012-2013 alla (Leppänen et al., 2015). b) SNOWPACK perinteinen (sininen) ja optinen (punainen) kidekoko sekä efektiivinen kidekoko HUT mallista (musta) (Kontu et al. 2017).

4. YHTEENVETO

Arktisessa Avaruuskeskuksessa Sodankylässä tehdään kattavia lumikuoppamittauksia lumen rakenteesta sekä havaintoja optisilla ja mikroaaltolaitteilla. Lisäksi käytössä on kattavat automaattiset tukimittaukset ja meteorologiset mittaukset. Mikrorakenteen mittauksia on hyödynnetty fysikaalisten lumimallien ja mikroaaltoemissiomallien validointiin, mikroaaltomallinnuksen kehittämiseen ja optisten mittausten tulkinnan kehittämiseen. Paperissa esiteltiin mittauksiin perustuen tutkittua mikrorakennemittausten virhettä, uuden laitteen sopivuutta mikrorakennemittauksiin, mikrorakenteen simulaatioiden validointia sekä mikroaaltoemissiomallilla lasketun efektiivisen kidekoon ja mikrorakennesimulaatioiden vastaavuutta.

KIITOKSET

Kiitämme Arktisen Avaruuskeskuksen henkilökuntaa mittauksissa avustamisesta.

LÄHTEET

Domine, F., R. Salvatori, L. Legagneux, R. Salzano, M. Fily ja R. Casacchia, 2006. Correlation between the specific surface area and the short wave infrared (SWIR) reflectance of snow. *Cold Regions Science and Technology*, **46(1)**, 60-68.

Kontu, A., J. Lemmetyinen, J. Vehviläinen, L. Leppänen, L ja J. Pulliainen, 2017. Coupling SNOWPACK-modeled grain size parameters with the HUT snow emission model. *Remote Sensing of Environment*, **194**, 33-47.

Lehning, M., P. Bartelt, B. Brown, C. Fierz ja P. Satyawali, 2002. A physical SNOWPACK model for the Swiss avalanche warning. Part II: snow microstructure. *Cold Reg. Sci. Technol.*, **35(3)**, 147-167.

Leppänen, L., A. Kontu ja J. Pulliainen, 2018. Automated Measurements of Snow on the Ground in Sodankylä. *Geophysica*, **53(1)**, 43-62.

Leppänen L., A. Kontu, H.-R. Hannula, H. Sjöblom ja J. Pulliainen, 2016. Sodankylä snow survey program. *Geosci. Instrum. Method. Data Syst.*, **5**, 163-179, doi:10.5194/gi-5-163-2016.

Leppänen, L., A. Kontu, J. Vehviläinen, J. Lemmetyinen ja J. Pulliainen, 2015. Comparison of traditional and optical grain size field measurements with SNOWPACK simulations in a taiga snowpack. *J. Glaciol.* **61(225)**, doi: 10.3189/2015JoG14J026.

Pulliainen, J., J. Grandell ja M. Hallikainen, 1999. HUT snow emission model and its applicability to snow water equivalent retrieval. *IEEE Transactions on Geoscience and Remote Sensing*, **37(3)**, 1378-1390.

Vionnet, V., E. Brun, S. Morin, A. Boone, S. Faroux, P. Le Moigne, E. Martin, J.-M. ja Willemet, 2012. The detailed snowpack scheme Crocus and its implementation in SURFEX v7.2. *Geosci. Model Dev.*, **5**, 773-791.

Petrophysical properties of the Kylylahti Cu-Au-Zn sulphide mineralization and its host rocks

T. Luhta[1], S. Mertanen[2], E. Koivisto[1], S. Heinonen[2] and COGITO-MIN work group

[1] University of Helsinki, Department of Geosciences and Geography
tuija.luhta@helsinki.fi
[2] Geological Survey of Finland, P.O. Box 96, FI-02151 Espoo, Finland

Abstract

This work (Luhta, 2019) presents a new set of petrophysical laboratory measurements made on 209 samples from the Kylylahti mine and 30 ores samples from several mining sites in the Outokumpu district. The work was aimed to provide a solid base for accurate interpretation of already existing geophysical exploration data, and to new seismic data collected in 2016 during the COGITO-MIN (COst-effective Geophysical Imaging Techniques for supporting Ongoing MINeral exploration in Europe) project. The sample set covered most common rock types found in the Outokumpu district: ophiolite-derived ultramafic massifs, the so called Outokumpu assemblage rocks, and also black schists and mica schists surrounding the massifs. The ultramafic massifs in the area contain several polymetallic (Cu-Co-Zn-Ni-Ag-Au) semimassive-to-massive and disseminated sulphide mineralizations.

The petrophysical parameters measured were density, seismic P-wave velocity, porosity, magnetic susceptibility, intensity of remanent magnetization, inductive resistivity, galvanic resistivity and chargeability. Additional parameters calculated from the measurements were seismic impedance, Königsberger (Q) ratio and induced polarization (IP) estimates.

The density data divides the Kylylahti rocks in three categories: 1) Massive and semi-massive sulphide mineralizations with an average density of 3750 kg/m^3, 2) Outokumpu assemblage rocks with densities close to 3000 kg/m^3 and 3) Kalevian rocks, mica schist and black schist, with densities a bit under 2800 kg/m^3. Sulphide disseminations are common in both Outokumpu assemblage carbonate-skarn-quartz rocks and black schists, elevating the densities when abundant. The average P-wave velocities for almost all Outokumpu assemblage rock types, including the sulphide mineralizations, are a bit over 6 km/s. Soap stones, mica schists and black schists have lower P-wave velocities, around 5.5 km/s. Overall, the porosity of the samples was very low.

Most of the Kylylahti rocks belong to paramagnetic group (susceptibilities under 2000 µSI). Serpentinites and tremolitic calc silicate rocks belong to strongly magnetic group. Both have low Q ratios, thus the magnetic mineral is most probably coarse-grained magnetite. The rocks rich in disseminated sulphides had high susceptibility and high Q ratios, thus the disseminated sulphides are probably mostly monoclinic pyrrhotite. Kylylahti sulphide

mineralizations and black schists are both conductive, as well as rocks rich in disseminated sulphides. The rocks containing disseminated sulphides have high IP estimates. Conductivity of the black schists is due to graphite and to some extent due to disseminated sulphides.

Comparison of physical properties of ore samples from different mine sites in the Outokumpu district reveals the differences in their mineralogy. Throughout the Outokumpu district, the physical properties of ore samples change with changing proportions of pyrite, pyrrhotite and magnetite. This change follows the metamorphic zoning in the Outokumpu district, also evidenced by the physical properties of Outokumpu district serpentinites. Metamorphic grade in the Outokumpu district varies from low amphibolite facies in the east to upper amphibolite facies in the west.

Based on the results, the sulphide mineralizations should produce a detectable reflection against any background due to their high density. Also the other Outokumpu assemblage rocks have a clear contrast against the mica schists and black schists. Furthermore, soap stones in contact with other Outokumpu assemblage rocks form a reflecting contact.

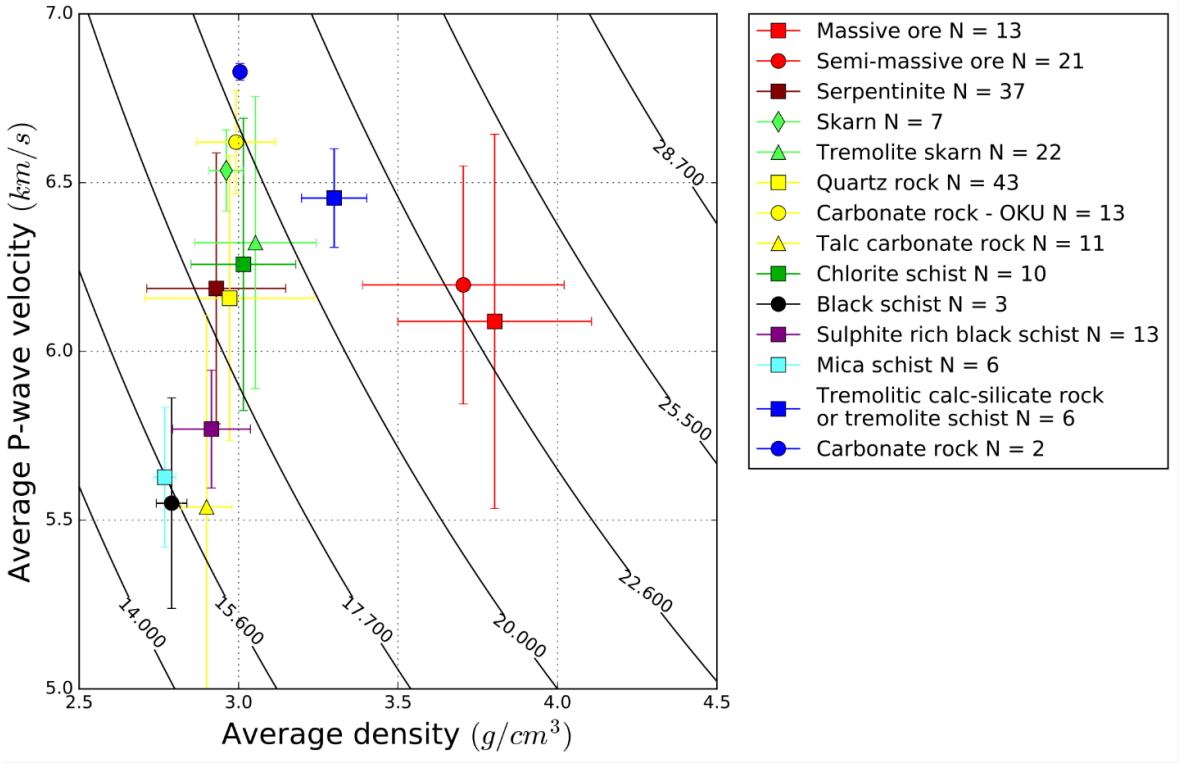

Figure 1: Average densities and P-wave velocities on samples from Kylylahti mine. Standard deviation shown as errorbars. Also seismic impedance isolines are shown, their spacing corresponding to 0.06 reflection coefficient, generally regarded as large enough to produce a detectable reflection.

REFERENCES

Luhta, T., 2019. Petrophysical properties of the Kylylahti Cu-Au-Zn sulphide mineralization and its host rocks, *University of Helsinki, Master´s thesis*, 95 p.

High frequency VLF banded emissions observed at Kannuslehto: Geomagnetic analysis

E.L. Macotela[1], F. Němec[2], J. Manninen[1], T. Turunen[1], O. Santolík[3,2], and I. Kolmašova[3,2]

[1] Sodankylä Geophysical Observatory, University of Oulu, Sodankylä, Finland, edith.macotelacruz@oulu.fi
[2] Faculty of Mathematics and Physics, Charles University, Prague, Czechia
[3] Department of Space Physics, Institute of Atmospheric Physics, The Czech Academy of Sciences, Prague, Czechia

Abstract

The VLF technique, which uses the propagation of Very Low Frequency (VLF) radio waves, provides the outstanding possibility of investigating the response of both the lower ionosphere and magnetosphere to a diversity of transient and long-term physical phenomena originating on Earth (e.g. lightning discharges) and space (e.g. solar flares). In this work, data obtained by the VLF radio receiver located in Kannuslehto, Northern Finland, is used to find natural VLF emissions at frequencies above 16 kHz. We analysed the campaign carried out in 2013. We found banded emissions which can be observed either in high frequency ranges, between 16 and 39 kHz, or spanning from low to high frequency ranges, i.e, from 0-39 kHz. Their times of occurrence are between 20:00 – 24:00 MLT. These events last from 5 to 80 minutes. The events are mostly observed when the AE index < 400 nT. We also analysed magnetometer data from locations near Kannuslehto and we found that the events are occurring before substorms or when no substorms are observed. Another characteristic is that the banded emissions have stronger left-handed polarization than right-handed polarization.

1. INTRODUCTION

The term very low frequency (VLF) radio waves is defined by the range 3-30 kHz. However, the VLF technique, which is employed to monitor radio waves, can operate in any subset of a wider frequency band that can extend from 3 Hz up to even 50 kHz. The VLF technique is an important tool used to study changes in the properties of the magnetospheric plasma (using natural emissions) and ionospheric conductivity (using transmitting signals from navigation systems) caused by a diversity of transient or long-term physical phenomena originating in the Earth or in space (e.g., Macotela et al., 2019).

A major reason for the scarce number of reports and studies on natural emissions at frequencies above 16 kHz, and using ground-based receivers, is that such frequencies are also used by navigation transmitters, which block possible detections. However, some of those transmitters operate sporadically, opening up frequency windows to find new natural VLF

emissions that were not reported before. Thus, the aim of the present study is to examine the broadband VLF data between 16-39 kHz, recorded at Kannuslehto, to look for VLF emissions not reported in previous literature.

2. OBSERVATIONS

In this study, the broadband VLF data from the Kannuslehto (KAN) VLF receiver is used. This receiver is located in northern Finland (67.74° N 26.27° E; L-value = 5.5) running under the operation of the Sodankylä Geophysical Observatory (SGO) (Manninen, 2005). The receiver is composed of two square loop antennas. The antennas, electronics and acquisition software were all developed and implemented at SGO. The Kannuslehto receiver is one of the most suitable VLF data sources in polar latitudes, and it is the most sensitive receiver in the world. The sensor registered natural and man-made VLF emissions during different campaigns since 2006, in the radio band of 0.2-39 kHz and with a sampling frequency of 78.125 kHz. The receiver is very sensitive, with 1 ADC unit approximately equal to 100 aT. Furthermore, the system is calibrated before the acquisition. All these characteristics make the data very reliable and they are very advantageous even when analysing weak events.

Many naturally occurring VLF waves at frequencies above 4–6 kHz could not be studied in the past because strong atmospherics (sferics) hide all such waves. Sferics originate in lightning discharges and propagate thousands of km in the Earth-ionosphere waveguide. To study the high frequency emissions, we have to apply special digital tools which filter out the strong impulsive sferics. That process uncovers completely new types of high frequency VLF emissions with various unusual spectral structures that have never been seen before. More information about the sferics removal technique can be found in Manninen et al. (2016). In this study we use spectrograms after filtering. We also remove the narrowband transmitter signals and Power Line Harmonic Radiations (PLHRs).

Figure 1 shows examples of banded VLF emissions observed in high frequencies obtained on 5 (left panel) and 20 (right panel) December 2013, respectively. Both panels show 1 hr polarization spectrograms in the frequency range 0.2-39 kHz. The right-handed circular power is indicated by reddish colours, while the left-handed circular power is indicated by bluish colours. The horizontal white lines indicate the removed radio transmitter signals. The left panel shows 40 min (16:30 – 16:50) VLF emissions spanning in all frequency ranges. During the time of the event no impulsive auroral hiss is observed. The right panel presents 1 hour (18:00 – 19:00 UT) of banded emissions observed in all frequency ranges. VLF auroral hiss emissions are also observed at the time in which the banded emissions are occurring. This panel also shows that the behaviour of the observed waves is not constant. There seems to be an important change at about 18:25, just when the auroral hiss ends.

In total we found 11 events, some of them were observed at high frequencies only and others were observed in the whole frequency range recorded by KAN. The banded emissions can last up to 80 minutes, with a typical duration between 5 and 30 minutes. The diurnal distribution of the events shows that these occurred in the evening, from 20:00 to 24:00 MLT, it means during the local darkness. Regarding the geomagnetic conditions, we found that the events are observed mostly during quiet geomagnetic periods, i.e., KP < 4, Dst > -30 nT, ap < 30 nT, and AE-index < 400 nT. Figure 2 (upper panel), where time 0 indicates the middle

time of the events. The lower panel of Figure 2 shows the x-component of magnetometer data at Kevo (KEV), Finland. This site is located 226 km to the north of KAN.

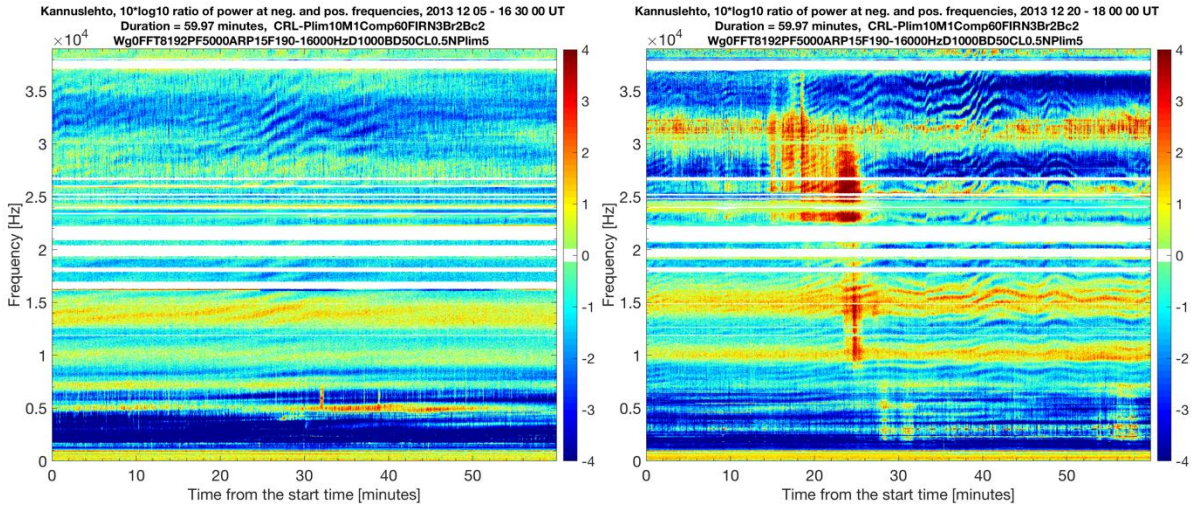

Figure 1: One-hour polarization spectrogram for the frequency range 0.2-39 kHz of right-handed circular power (dark red) and left-handed circular power (dark blue) on 5 December 2013, starting at 16:30 UT (left panel) and 20 December 2013, starting at 18:00 UT (right panel). The white horizontal lines represent the removed signals from navigation transmitters.

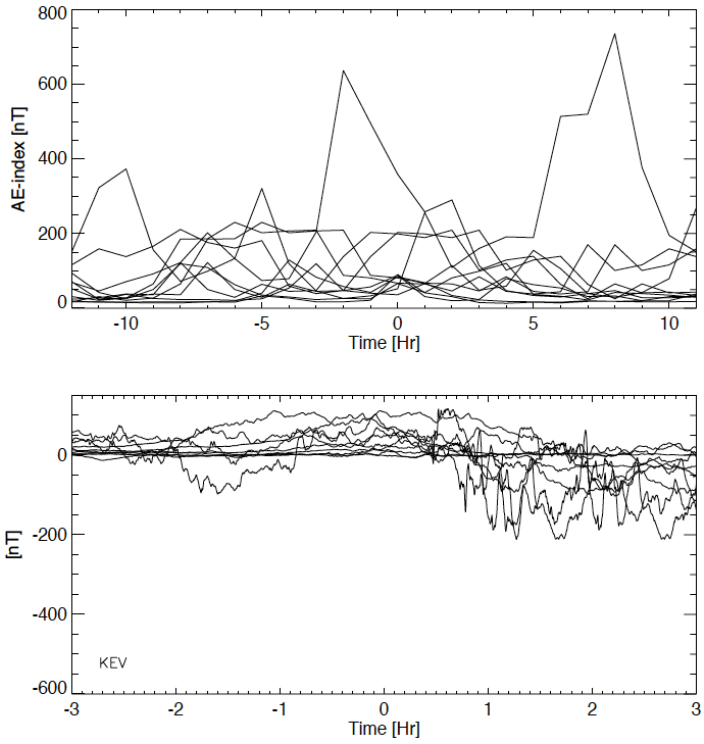

Figure 2: Geomagnetic conditions. AE index (upper panel) and the x-component of magnetometer data at KEV (Finland, at 226 km to the north of KAN). Time 0 indicates the middle time of the events.

Figure 2 reveals that the events are observed during quiet periods, or before the start of substorms. Performing the same analysis using magnetometer measurements at Sodankylä, 44

km to the south of KAN, we found the same results. We would like to point out that the Sodankylä and KEV magnetometers are at the same longitude as KAN receiver. Finally, computing the average value of the ratio of polarization in the frequency range 25-37 kHz, we found that the events are characterized by a stronger left-handed polarization than a right-handed polarization.

3. FINAL COMMENTS

In this study, VLF natural emissions observed in high frequency ranges are analyzed. We found that some of the emissions are only observed in high frequency ranges (above 16 kHz), while others are observed in all the frequencies recorded at KAN (0.2-39 kHz). The results suggest that the majority of the band separations are constant, i.e., they do not vary significantly as a function of time and frequency. The frequency drift also is quite constant as a function of time. The frequency separation of the emissions is clearly related to the event formation and it will be investigated in detail in the future.

Regarding the geomagnetic analysis, we expected that strong geomagnetic disturbances can penetrate deeply in the magnetosphere, i.e., to the regions of strong geomagnetic field, which ensures a shift of wave processes related to cyclotron resonance to higher frequencies (Ermakova et al., 2016). However, we found that the banded emissions are occurring during quiet geomagnetic activity. Thus, more analysis using all the VLF campaigns at KAN is needed.

ACKNOWLEDGEMENTS

This research is supported by Suomen Kulttuurirahasto (grant: 00180689), and Oulun yliopiston tukisäätiö (grant: 20180003). Data availability is described at http://www.sgo.fi/Data/VLF/VLF.php.

REFERENCES

Ermakova, E., A. Yahnin, T. Yahnina, A. Demekhov, and D. Kotik, 2016. Sporadic geomagnetic pulsations at frequencies of up to 15 Hz in the magnetic storm of November 7–14, 2004: features of the amplitude and polarization spectra and their connection with ion–cyclotron waves in the magnetosphere. *Radiophys. Quantum Electron.*, **58**, 547-560, doi:10.1007/s11141-016-9628-3.

Macotela, E. L., M. Clilverd, J. Manninen, T. Moffat-Griffin, D. Newnham, T. Raita and C. Rodger, 2019. D-region high-latitude forcing factors. *Journal of Geophysical Research: Space Physics*, **124**, doi: 10.1029/2018JA026049.

Manninen, J, 2005. *Some aspects of ELF–VLF emissions in geophysical research*. PhD dissertation, Sodankyla Geophys. Obs. Publ., **98**.

Manninen, J., T. Turunen, N. Kleimenova, M. Rycroft, L. Gromova, and I. Sirviö, 2016. Unusually high frequency natural VLF radio emissions observed during daytime in Northern Finland. *Environ. Res. Lett.*, **11**, doi: 10.1088/1748-9326/11/12/124006.

Simultaneous Kannuslehto and ARASE satellite ELF-VLF observations

J. Manninen[1], C. Martinez-Calderon[2] and T. Turunen[1]

[1] Sodankylä Geophysical Observatory, Sodankylä, Finland, Jyrki.Manninen@oulu.fi
[2] Department of Geophysics, Graduate School of Science, Tohoku University, Sendai, Japan

Abstract

The ERG (Exploration of energization and Radiation in Geospace) project is a mission to elucidate acceleration and loss mechanisms of relativistic electrons around Earth during geospace storms. The project consists of the satellite observation team, the ground-based network observation team, and the integrated data analysis/simulation team. After the launch, ERG was nicknamed to ARASE.

All satellite projects observing the geospace need also reliable and high-quality ground-based data in order to explain different kinds of events observed by the satellites. ARASE satellite is having several particle instruments, plasma wave instrument, and magnetic field instrument. Often, we should be able to separate spatial and temporal features from our observations. In this case, we can often use ground-based data to find out the differences.

In this presentation, we will show ground-based ELF-VLF observations during the winter campaigns of ARASE. The first campaign was organized in the end of March and beginning of April in 2017. Other campaigns have been made in 2017, 2018, and 2019. One interesting event is shown in Figure 1. Another example is shown in Figure 2.

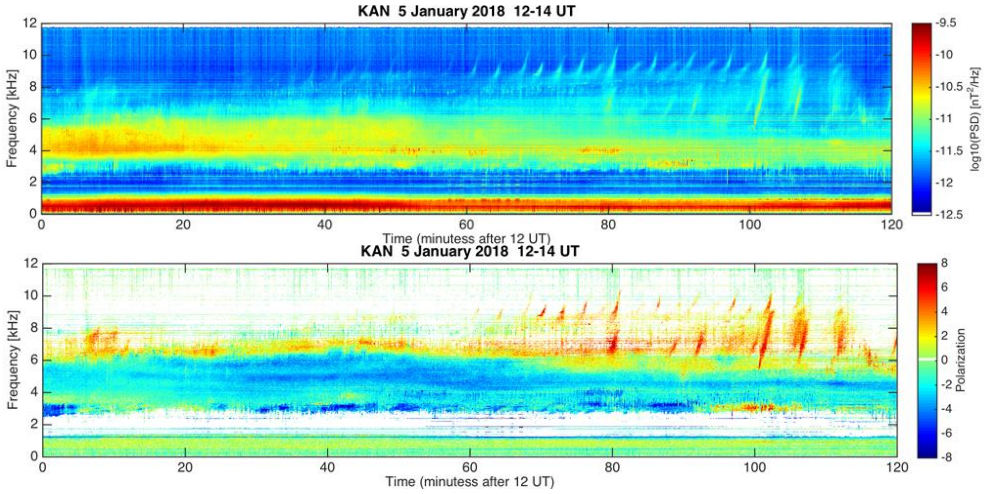

Figure 1: ELF-VLF total power and polarization plots observed at Kannuslehto at 12-14 UT on 5 January 2018. Emissions reach the frequencies up to 10.5 kHz. Yellow and red colours refer to right hand polarization while green and blue colours mean left hand polarization.

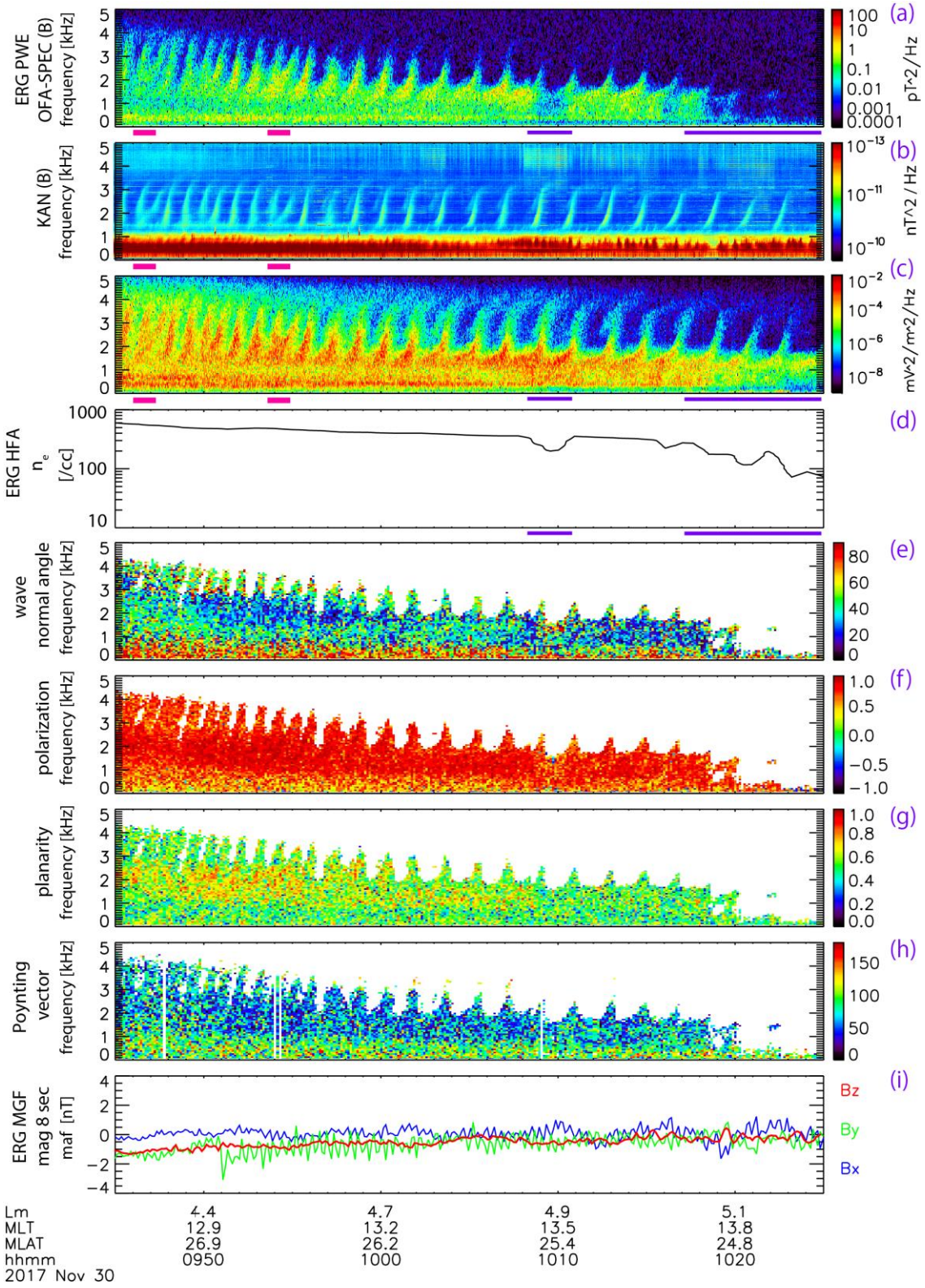

Figure 2: Power spectrum density of magnetic field at (a) KAN and (b) ERG, and electric field at (c) ERG. (d) Cold plasma density from ERG. (e) Normal wave angle, (f) polarization sense, (g) wave planarity and (h) Poynting vector from ERG data. Magnetic field variations from ERG in MFA coordinates (j). These were observed at 22:30-23:30 UT on 30 Nov 2017.

Winter climate change affects subnivean conditions and conifer seedling survival in boreal forest

F. Martz[1], J. Vuosku[1], M. Männistö, S. Stark[2], A. Ovaskainen[1] and P. Rautio[1]

[1] Natural Resources Institute Finland (Luke), Rovaniemi, Finland, francoise.martz@luke.fi
[2]Arctic Center, University of Lapland, Rovaniemi, Finland

Abstract

Frequency of rain-on-snow events and winter warm spells is increasing in high latitudes and is forecasted to further increase in the future. By decreasing the insulation capacity of the snowpack and causing ice layers or ground ice encasement (IE), those events lead to changes in the subnivean environment. To test for the effect of such changing overwintering conditions on boreal forest, we established a snow manipulation experiment in a coniferous forest in Northern Finland with planted Norway spruce and Scots pine seedlings. Four snow manipulation levels were applied for three consecutive years: ambient conditions, artificial IE, snow compaction and complete snow removal. Soil temperature, frost and gases were recorded. After three years of snow manipulation, IE, snow compaction or snow removal led to increased seedling mortality compared to ambient snow cover. Norway spruce appeared more resistant than Scots pine to adverse winter conditions. Our results demonstrate a negative impact of winter climate change on boreal forest regeneration and productivity.

1. INTRODUCTION

Air temperatures and precipitation are predicted to continue increasing in the future, especially at high latitudes and particularly so during winter. In contrast to air temperatures, changes in soil temperatures are more difficult to predict, as the fate of the insulating snow cover is crucial in this respect. Soil conditions can also be affected by rain-on-snow events and warm spells during winter, resulting in freeze–thaw cycles, compacted snow or ice encasement. Ice layers under or within the snow restrict the soil-atmosphere gas exchange which, in addition to changing soil temperature, will modify the overwintering conditions of plants. Little is known about the influence of the snow cover on CO_2 and O_2 in soil, and the potential consequences these might have on overwintering conifer seedlings. Given that the snow-covered period can last more than half a year in boreal ecosystems, this creates a major gap in the understanding of how climate warming will affect boreal ecosystem functioning.

2. MATERIAL AND METHODS

We established a snow manipulation experiment following a randomized block design with 10 blocks in a Scots pine forest (xeric- sub-xeric site) near the Arctic Circle close to the city of Rovaniemi (Tavivaara, 66°25 '35"N 25°41'42"E) (see Martz et al. (2016) for a detailed description of the field site. Four study plots with similar exposure, hydrological status and

vegetation were selected within each of the 10 blocks and randomly assigned to the following treatments: 1) ambient (**AMB**) with no treatment, 2) induction of IE (**IE**, artificially created by snow watering), 3) no snow cover (**NoSNOW**: roofs and low walls made of translucent white plastic were positioned over the plots to prevent natural snow fall or drifted snow) and 4) compaction of snow cover (**COMP**: snow compaction by hand). The snow manipulation were performed as described in Martz et al (2016) during three consecutive winters, from the autumn 2013 to the spring 2016. Both types of seedlings were planted in plots (1 m x 3 m) were divided into three sections: two subplots (A and B) separated by a buffer zone (see Martz et al, 2016). All seedlings in B subplots were used to record growth and health in 2014. Due to sampling in the spring 2015, only half of the seedlings in the subplots B were used to record growth and health in 2015 and 2016 (totally 50 seedlings/treatment for each species).
All the environmental variables (air and soil temperature, snow depth, snow water equivalent, soil frost depth and upper unfrozen ground, O_2 and CO_2 concentrations in soil) were measured as described in Martz et al. (2016) (due to space limitation, only soil frost, soil gases and seedling mortality are reported in this abstract). The methylene blue tubes used to measure the depth of soil frost were installed in all treatment plots (5), in three blocks in winter 2013-2014 and in five blocks in subsequent winters.

3. RESULTS

As expected, complete snow removal exerted a considerable influence on soil temperatures and removal of the insulating snow cover led to deeper soil frost (Fig. 1). IE or snow compaction lead to an situation intermediate between snow removal and an ambient snow cover. Soil started to thaw from the surface earlier in the NoSNOW plots due to the lack of snow and consequent change in albedo (not shown).

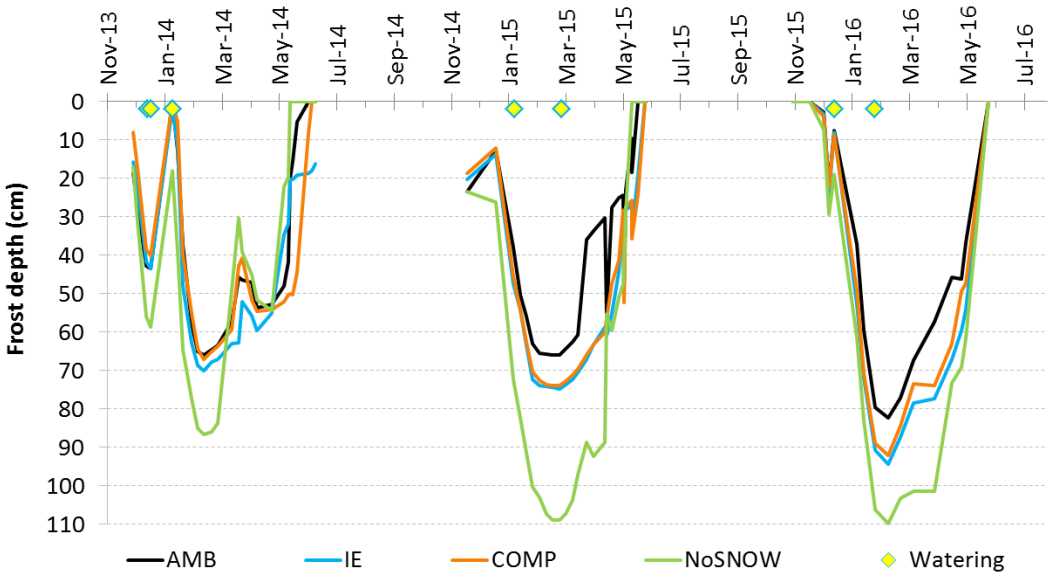

Figure 1: Effect of snow manipulation on the depth of soil frost. Values are means of 3 (winter 2013-2014) or 5 blocks (winters 2014-2015, 2015-2016). Occurrences of snow manipulation (snow watering and compaction) are indicated by yellow diamonds.

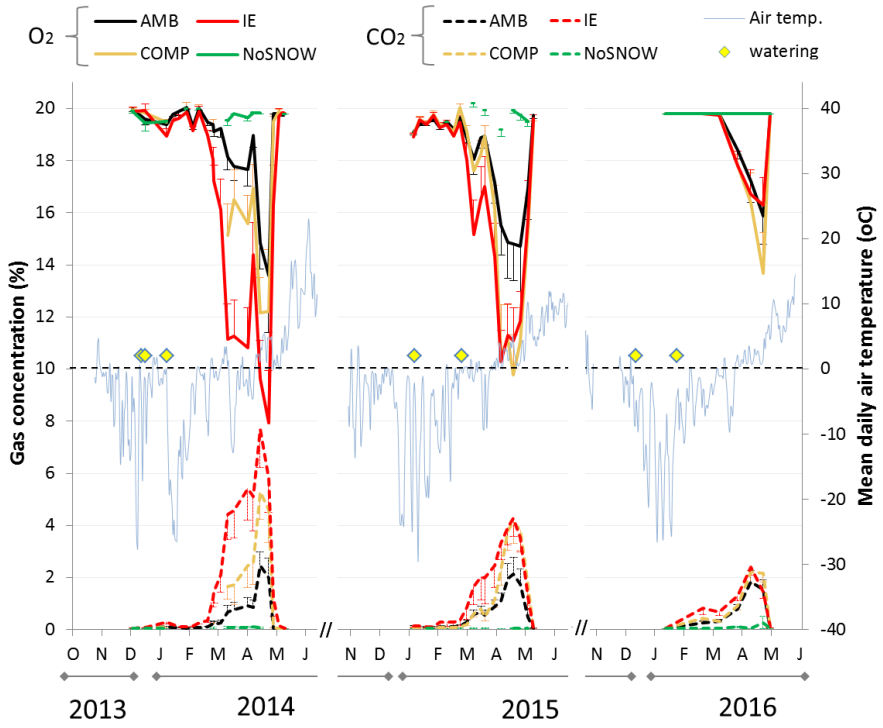

Figure 2: Effect of snow manipulation on the concentration of O_2 (solid lines) and CO_2 (dotted lines) in the humus layer. Occurrences of snow manipulation (snow watering and compaction) are indicated by yellow diamonds. Values are means ± SE (n=10).

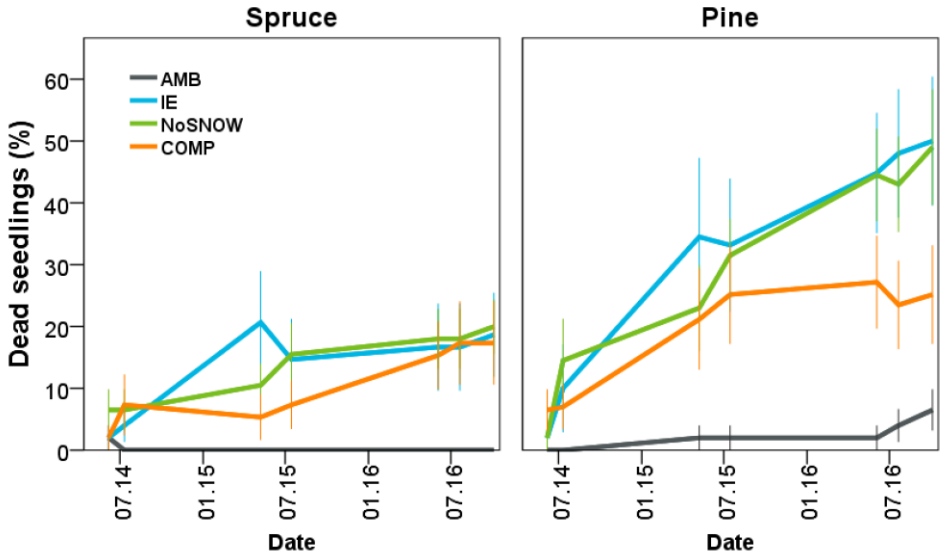

Figure 3: Effect of snow manipulation for three consecutive years on the mortality of Norway spruce and Scots pine seedlings. Values are mean ± SE (n=10).

Analysis of gas samples collected in the humus layer (2-cm deep) throughout the winter showed large seasonal changes in CO_2 and O_2 concentrations and, above all, significant treatment effects (Fig. 2). The treatment effects were the strongest during the first winter 2013-2014, likely due to the particular weather conditions this year (several warm spells in early 2014, naturally icy conditions, see Martz et al., 2016). Generally, the decrease in O_2 was correlated with the accumulation of CO_2 (not shown).

In general, seedling mortality was very low in ambient conditions at the field site (AMB plots) (Fig. 3). Three consecutive winters of snow manipulation significantly affected the mortality of seedlings. The mortality rate of spruce was similar whatever the snow manipulation treatment (IE, COMP, NoSNOW). Scots pine seedlings appeared more vulnerable to adverse snow conditions than Norway spruce. At the opposite to Norway spruce, the quality of the snow cover mattered, with IE and complete snow removal leading to 50% mortality compared to 6.8% under an ambient snow cover.

3. FINAL COMMENTS

Soil microbes are essentials for growth and survival of trees in boreal forest. Analysis of soil fungal and bacterial communities in the field experiment described in this study indicated that microbial communities in acidic northern boreal forest soil may be insensitive to direct effects of changing snow cover after one winter of snow manipulation (Männistö et al, 2018).
Although further studies are needed to determine which of the winter stresses caused the most damaging effects, our results show that denser snowpack or lack of snow cover due to winter warming could have a major impact on forest ecosystems. It might have a negative effect on forest growth and productivity that could partially counteract the positive growth effects due to increasing growing season temperatures.

Scots pine appeared to be more vulnerable than Norway spruce to changing overwintering conditions. Laboratory experiments carried out simultaneously with the field experiment showed that deciduous species (Downy birch) performed better in altered snow conditions than coniferous species (Domisch et al, 2018b; Domisch et al, 2018a). Altogether, our results support an effect of winter climate on species composition in future coniferous forests.

ACKNOWLEDGEMENTS

We are grateful to forest engineers Pekka Närhi, Tarmo Aalto, Aarno Niva, Raimo Pikkupeura and Eero Siivola for maintenance of the field experiment and help in sampling.

REFERENCES

Domisch, T. *et al.*, 2018a. Let it snow! Winter conditions affect growth of birch seedlings during the following growing season. *Tree Physiol.*, **tpy128**, doi:10.1093/treephys/tpy128.

Domisch, T. *et al.*, 2018b. Winter survival of Scots pine seedlings under different snow conditions. *Tree Physiol.*, **38**, 602-616. doi:10.1093/treephys/tpx111.

Martz, F. *et al.*, 2016. The Snow Must Go On: Ground ice encasement, snow compaction and absence of snow differently cause soil hypoxia, CO_2 accumulation and tree seedling damage in boreal forest. *PLoS ONE*, **11**, e0156620.

Männistö, M. *et al.*, 2018. Bacterial and fungal communities in boreal forest soil are insensitive to changes in snow cover conditions. *FEMS Microbiol.Ecol.*, **94**, fiy123-fiy123.

Hydrogeophysical approach for Characterization of Mining Wastes: Tailings Storage Facilities (TSFs)

R. Mollehuara-Canales[1], E. Kozlovskaya[1,2] , J.P. Lunkka[1], K. Moisio[1] and E. Banks[3]

[1] Oulu Mining School, University of Oulu, Finland, Raul.MollehuaraCanales@oulu.fi
[2] Geological Survey of Finland
[3] National Centre for Groundwater Research and Training, Flinders University, Australia

Abstract

This paper introduces the concept of hydrogeophysics with focus on characterization of mining waste repositories and the application of geophysical techniques for the determination of subsurface structural zones and hydraulic properties – key for quantitative hydrogeological models. We present the aspect of geophysical field application using a selected case study; a decommissioned tailings storage facility (TSF) of a former mine site in South Australia. We find that geophysical outputs can enable the reconstruction of the subsurface geometry and the quantification of hydraulic properties important for developing hydrogeological models.

1. INTRODUCTION

Constructed systems in the mining industry demand continuous characterization in order to comply with specifications and performance criteria. Tailings storage facilities (TSFs) for instance, are large waste repositories constructed for managing the impacts of the extractive activity, with the purpose to store and contain in perpetuity a mining waste generated in large quantities, tailings. Design, construction and operation of these facilities are a well-known practice in the industry, and these facilities seem to work well until some type of anomaly (e.g. seepage, erosion, surface or groundwater contamination) is detected with the potential to cause failure (i.e. environmental, physical, or operational) in the system. Historically, the performance of TSFs are prone to fail mainly due to hydrological-related causes either causing overtopping or failure in the embankment or dam (Oboni and Oboni 2016).

2. HYDROGEOPHYSICAL APPROACH FOR CHARACTERIZATION OF TSFs

Geophysics has received increased attention in applications related to hydrological flow and transport processes in the subsurface at the field and catchment scale. It is constantly evolving with new equipment and data processing capabilities, creating new opportunities to streamline field data acquisition on a continuum for the investigation of hydrogeological processes. This new research area falls in the realm of hydrogeophysics, an integrative approach combining

geophysical and hydrogeological principles for the investigation of parameters and processes important to subsurface investigations.

An early framework formulated by Binley et. al. (2010) considered geophysics for hydrogeologic investigations and proposed on the use of geophysical methods to allow for large scale aquifer characterisation and where hydrogeological techniques are limited.

Several geophysical techniques have been investigated for characterization of constructed facilities in mining waste repositories; among these, electrical resistivity tomography (ERT), ground-penetrating radar (GPR), induced polarization (IP), self-potential (SP), electromagnetic induction (EMI), and seismic methods. Recent applications in TSFs have demonstrated promising results in mapping anomalies within the structure of the dam, embankment or dyke, with a few attempts to characterize the internal structure of the deposit (Martín-Crespo et al. 2018; Olivier et al. 2017; Cortada et al. 2017).

The approach in Figure 1 expands on the hydrogeophysical framework by Binley et al. (2010), with application to mining environments, and aims to leverage proxy measurements of non-invasive geophysical techniques in the investigation of constructed mining waste repositories for the determination of subsurface structural zones and hydrological properties – key for quantitative hydrogeological models.

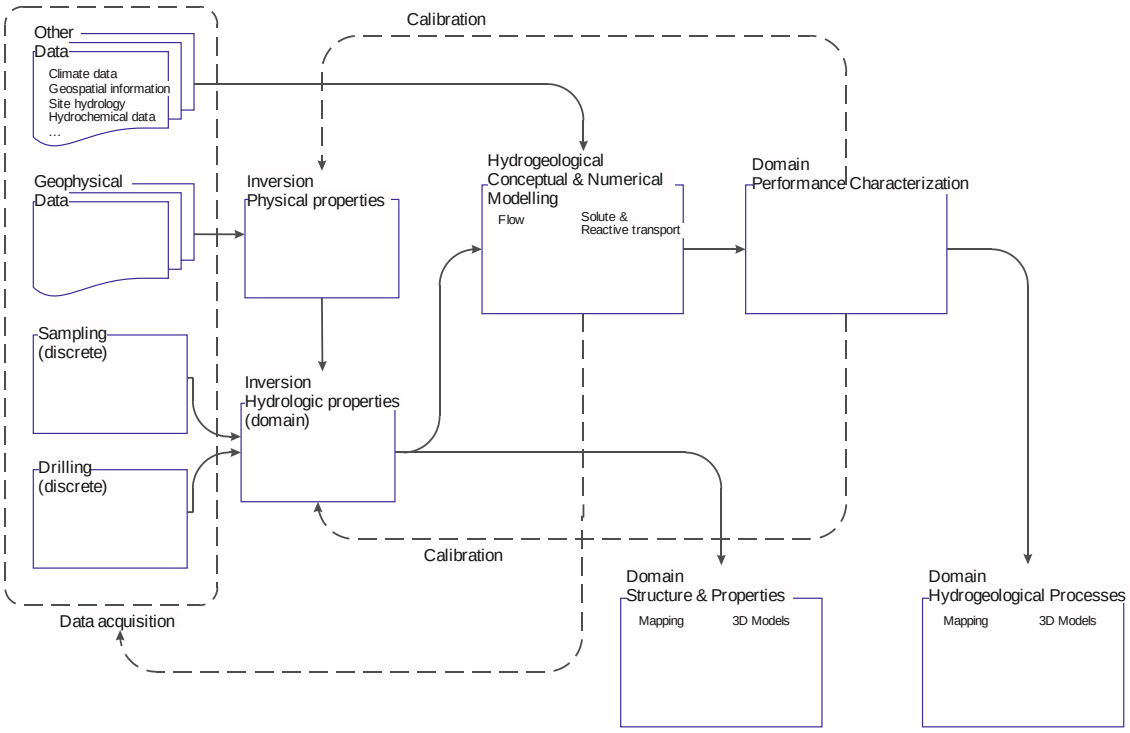

Figure 1: Hydrogeophysical proposal for characterization of mining wastes - TSFs

3. THE GEOPHYSICAL INPUT

The case study tailings material is a reject of a pyrite enrichment process that has separated a fine clayey sandy waste containing around 1-2 % sulphides. The tailings and the pore water in situ are expected of high electrical conductivity in contrast with natural ground soil.

The geophysical survey at the surface of the mine tailing deposit consisted on ground-penetrating radar (GPR), and electrical resistivity tomography (ERT). The data acquired by geophysical methods is validated with field measurements and ground truth data available on site.

The GPR survey was carried out following a continuous path along the embankment and transverses covering the surface of the facility. GPR data were acquired using 80MHz, 160MHz and 450MHz antennas. In Figure 2, a section of the radargram is analyzed to locate the interfaces at the upper region of the impoundment. Soil wave transmission velocity is corrected with the hyperbole curve fitting in order to determine the depth profile. Further data processing estimates the dielectric constant of the in-situ material for inferring moisture content in the subsurface.

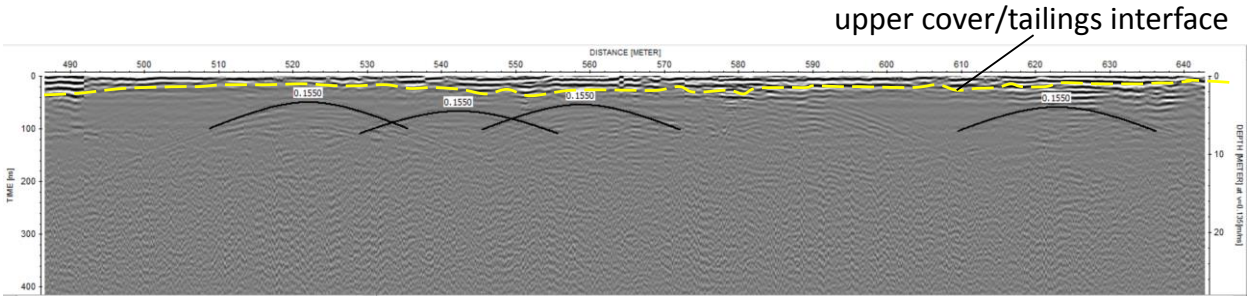

Figure 2: Imaging of the impoundment subsurface with an 80MHz ground penetrating radar antenna.

The ERT survey on the embankment slope and on top of the tailings consisted of five electrical data profiles using dipole-dipole, and werner-schlumberger arrays. All profiles used 96 electrodes positioned with a 2.5 m and 5 m electrode spacing. Electrical resistivity model is effective to locate the interface between the unsaturated and saturated zones in the tailings impoundment. Existing piezometers along the path of each transect allows for measurements of the water level during the survey. Measurements of the hydraulic head throughout the surface of the TSF provide with information to pinpoint localised recharge areas and mounding of the water table which are contrasted with the electric resistivity survey as shown in Figure 3.

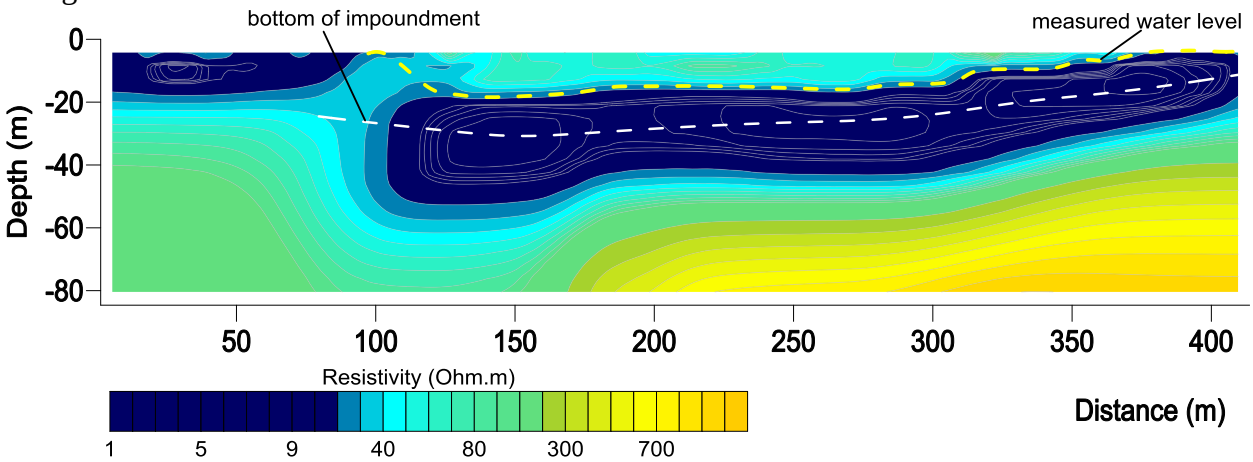

Figure 3: Modeled electrical resistivity section defines the water level interface in the subsurface of the impoundment. Bottom of impoundment is approximated from site reports.

4. CONCLUSIONS

The proposal formulates a whole-domain approach for applying hydrogeophysics for the interpretation of properties, structure, and hydrogeological processes of mining waste repositories. Geophysics can complement data that are sparse or unavailable about the subsurface and for assisting the evaluation of hydrological processes with implications for water quality and environmental health.

By leveraging advances in geophysical and hydrogeological techniques, we can establish a novel characterisation methodology of TSFs and similar structures that is integrative, less resource demanding and safe. Geophysics can image subsurface in 2D and 3D with high spatial resolution, up to a depth of few tens of meters. For instance, quantitative information from the subsurface such as porosity and water content can be obtained by establishing a relationship between geologic and geophysical properties at a field scale.
This approach has the potential to be adopted in other areas of the mining cycle facing the same challenges (i.e. waste management, rehabilitated mine sites, closure and post-closure).

ACKNOWLEDGMENTS

The project is cofounded by the Marie Curie I4Future program and Oulu Mining School; and has received research funding from K.H. Renlund foundation. Acknowledgments to Dr Huade Guan and Dr Patrick Hesp in the National Centre for Groundwater Research and Training at Flinders University Australia for hosting and providing the field research equipment. Thanks also to the executives and staff at the Brukunga mine site in South Australia for providing access to the site for fieldwork research.

REFERENCES

Binley, A., G. Cassiani, and R. Deiana, 2010. Hydrogeophysics : Opportunities and Challenges. *Bollettino Di Geofisica Teorica Ed Applicata*, **51**, 267-284.

Cortada, U., J. Martínez, J. Rey, M.C. Hidalgo, and S. Sandoval. 2017. Assessment of Tailings Pond Seals Using Geophysical and Hydrochemical Techniques. *Engineering Geology*, **223**, 59-70.

Martín-Crespo, T., D. Gómez-Ortiz, S. Martín-Velázquez, P. Martínez-Pagán, C. de Ignacio, J. Lillo and Á. Faz, 2018. Geoenvironmental Characterization of Unstable Abandoned Mine Tailings Combining Geophysical and Geochemical Methods (Cartagena-La Union District, Spain). *Engineering Geology*, **232**, 135-146.

Oboni, F. and C. Oboni, 2016. A Systemic Look at Tailings Dams Failure Process. In: *Tailings and Mine Waste 2016, Keystone, Colorado, USA, October 2-5, 2016,* https://www.riskope.com/wp-content/uploads/2016/10/Paper-17.

Olivier, G., F. Brenguier, T. de Wit and R. Lynch, 2017. Monitoring the Stability of Tailings Dam Walls with Ambient Seismic Noise. *The Leading Edge* **36(4)**, 350a1-350a6. https://doi.org/10.1190/tle36040350a1.1.

What role for targeted geoengineering to mitigate climate change?

J. Moore[1]

[1]Arctic Global Change Unit, University of Lapland, john.moore@ulapland.fi

Abstract

Dangerous human-induced climate warming is underway. If we stop all greenhouse gas emissions today the climate will still warm and the oceans will still rise. The greenhouse gases already in the atmosphere have a long residence time and critical thresholds in the Earth's natural systems have been crossed. Geoengineering is deliberate human intervention to counter warming and sea level rise. For example, engineering projects to stabilise the Antarctic Ice sheet. This is a proposal for research, it is neutral about the findings. That is the research may show that doing geoengineering is worse than living with greenhouse gases alone. This is a very interdisciplinary subject area covering the natural sciences (impacts of geoengineering and likely success against climate change), engineering (feasibility and implementation) and social sciences and law (international governance of such schemes).

How Hemispheric Polar Field Reversal Sets the Timing and Shape of the Solar Cycle

A. Muñoz-Jaramillo[1]

[1] Southwest Research Institute, Boulder, CO, USA, amunozj@boulderswri.edu

Abstract

The solar cycle is a phenomenon that simultaneously presents a significant level of randomness, and an incredible regularity. This dichotomy lies at the root of the impossibility of making multi-cycle predictions, but the remarkable capability we have of pinning down a cycle's properties once its underway. One of the most important pieces of information that is currently used for solar cycle prediction is the strength of the polar fields during the minimum prior to the predicted cycle. However, we only have direct measurements of the polar fields during the last 45 years and they paint an incomplete, and overly simplified, picture of this important relationship.

In this presentation I take advantage of a century of polar faculae measurements (as a proxy of polar magnetic flux), to illustrate how the dynamics of polar field reversal, the interaction between the Northern and Southern hemispheric cycles, and the interaction of each cycle with the one that came before, give shape to each solar cycle in a remarkably regular way. We will discuss how the polar field may not be the only determinant of the observed cycle amplitude and how this discrepancy comes to be. Then we will discuss how the moment of polar field reversal plays a critical role on timing the onset of the next solar cycle. Finally, we will discuss how all this can be put together to make better and more detailed solar cycle predictions, and the kind of information that he next generation of model-driven cycle predictions needs to strive for to enable earlier and better cycle predictions.

Geomagnetic history of the Grand Modern Maximum: Centennial evolution of geomagnetic activity and geomagnetic storms

K. Mursula[1], T. Qvick[1], L. Holappa[1] and V. Filppa[1]

[1] ReSoLVE Centre of Excellence, Space Climate Research Unit, University of Oulu, Finland, kalevi.mursula@oulu.fi

Abstract

The 20th century marks a period of exceptionally high solar activity, now termed the Grand Modern Maximum. Sunspot activity increased from a low level at the beginning of the century to a maximum during solar cycle 19 in the late 1950s, then settled to a slightly lower level during cycles 20-23, and reduced to a significantly lower level during the soon-ending cycle 24. The Sun has two forms of geo-effective variability that are the main drivers of overall geomagnetic activity (GA) and of geomagnetic storms: coronal mass ejections (CME) and high-speed solar wind streams (HSS). The occurrence frequency and heliolatitudinal distribution of these drivers vary fairly systematically over the solar cycle. CMEs closely follow the sunspot cycle, while HSSs arise from large coronal holes, which maximise in the declining phase of the solar cycle. CMEs cause most of the large storms, but HSSs produce most of geomagnetic activity in most years. Here we study the centennial evolution of geomagnetic activity and geomagnetic storms, which give new information about the long-term evolution of solar magnetic fields, in particular the occurrence of large coronal holes and CMEs, respectively. We determine the temporal occurrence of storms of different intensity (weak, moderate, large) and study GA in different seasons, which depicts differences in the occurrence of polar and low-latitude coronal holes.

1. GEOMAGNETIC ACTIVITY AT HIGH LATITUDES

The highest values of solar wind speed at the Earth's orbit are observed during the declining phase of the solar cycle, when high-speed streams from the equatorward extensions of polar coronal holes extend to low heliographic latitudes. High-speed streams have the largest relative effect on geomagnetic activity at high latitudes, and solar wind speed is the main driving parameter of high-latitude GA (Finch et al. 2008; Holappa et al. 2014).

We use here the horizontal magnetic field measurements at Sodankylä observatory (67.37° GGlatitude, 26.63° GGlongitude; 64° GMlat and 119° GMlong) in order to obtain a long-term proxy of the seasonal solar wind speed (V) since 1914. The magnetic disturbances in the midnight sector are caused by variations of the westward electrojet, whose strength is mainly controlled by the HSSs (Finch et al. 2008). Thus, in order to obtain the best proxy for HSSs,

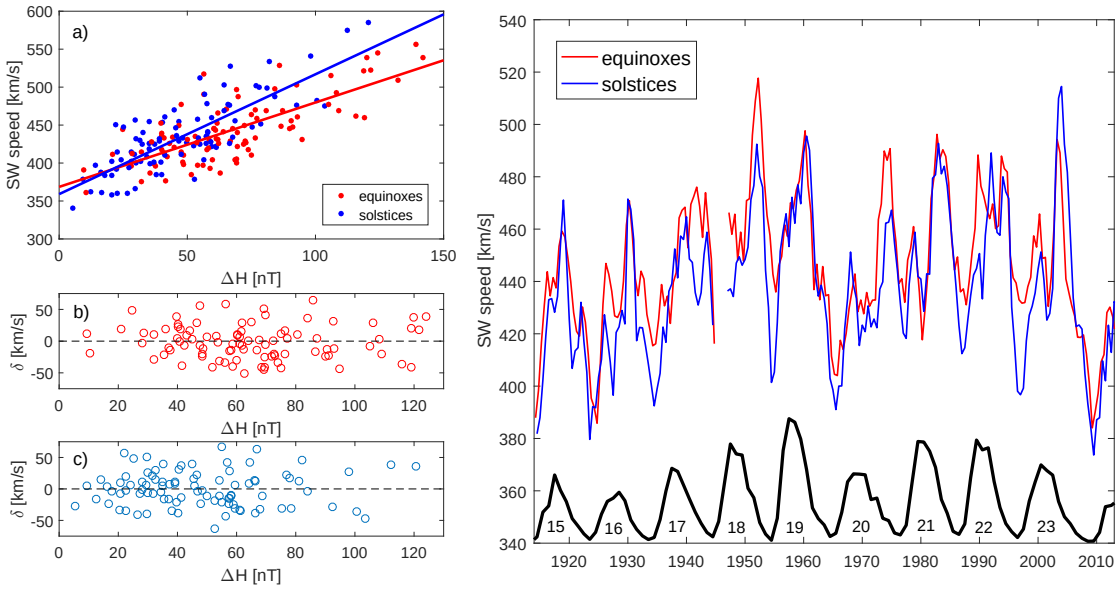

Figure 1: Left: a) Scatter plot between seasonal means of ΔH and solar wind speed during equinoxes (red dots) and solstices (blue dots), together with their best-fit lines; b) Residuals of regressions as a function of ΔH for equinoxes and c) solstices. Right: Three-point running means of the reconstructed solar winds speeds for equinoxes and solstices. Annual sunspot numbers and solar cycle numbers are included below for reference.

we limit the data to the 20-23 UT (22-01LT) interval. As a monthly-averaged measure of geomagnetic activity, we use the disturbance parameter ΔH, which is calculated as the difference between the monthly average of night-time H of all days and the monthly average of quiet days. Then we calculate the seasonal (ordered by the Earth's heliographic latitude) averages of the monthly ΔH values for spring (Feb-Apr), summer (May-Jul), fall (Aug-Oct) and winter (Nov-Jan).

Figure 1 depicts the correlation between the monthly values of ΔH and the measured solar wind speed 1964-2014 separately for solstice (summer and winter) and equinox (spring and fall) months (left panels), and the solstice and equinox means of the solar wind speed reconstructed from this correlation in 1914-2014 (right panel) (Mursula et al. 2017). Using separate correlations for solstice and equinox is necessary to account for the different ionospheric conductivity in different seasons, which leads to the well known semiannual variation of geomagnetic activity (Lyatsky et al. 2001). Figure 1 (panels b and c) show the fit residuals $\delta = V$(measured) - V(predicted) as a function of ΔH for equinoxes and solstices, respectively. The residuals lie symmetrically around zero for the whole range of ΔH, indicating a homoscedastic distribution of errors.

Figure 1 (right) shows that a short period of typically 1-2 years of high values of solar wind speed (HSS) occurs always in the declining phase of the solar cycle, thus verifying a similar basic evolution of solar magnetic fields over the whole GMM. However, interesting differences are seen in the centennial evolution of geomagnetic activity between solstices and equinoxes. Cycle 19, which marks the sunspot maximum of the Grand Modern Maximum, was exception-

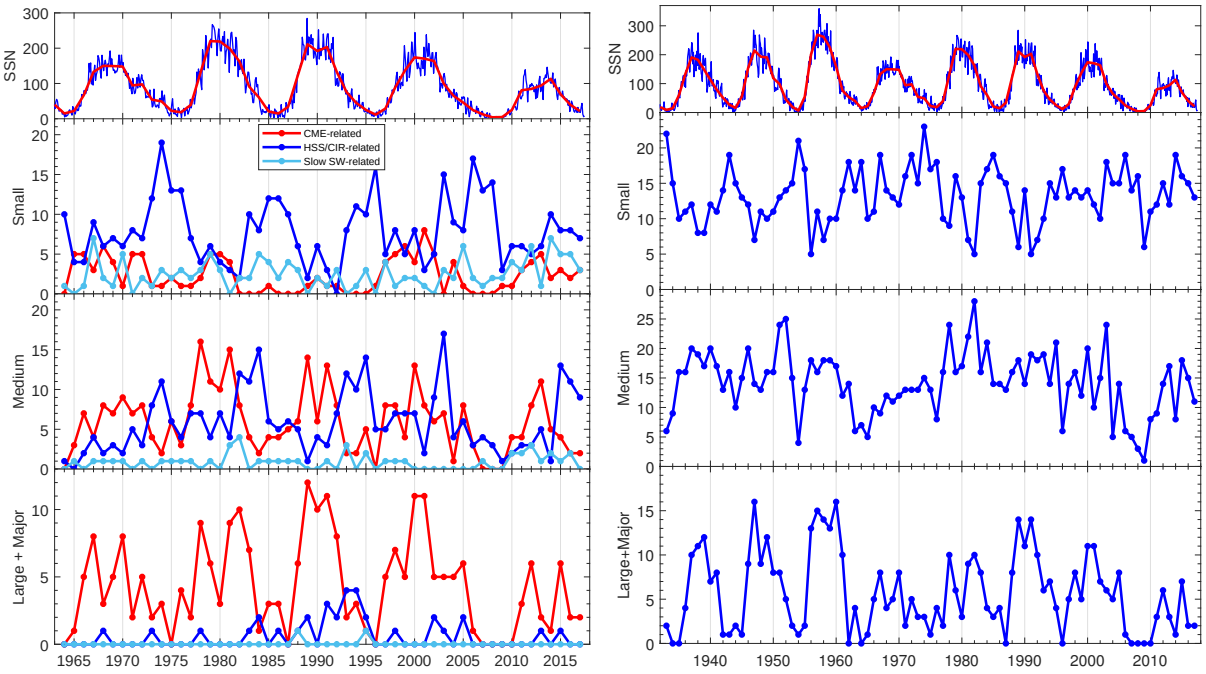

Figure 2: Left: Annual numbers of small, medium and large/major geomagnetic storms in 1964-2017 divided according to their solar wind drivers (CME, HSS, slow wind): Right: Annual numbers of small, medium and large/major geomagnetic storms in 1932-2017. Sunspots are included in both at top.

ally strong during equinoxes. Since equinoctial activity is more closely related to polar coronal holes and their extensions, this is in line with the result (Mursula et al. 2015) that polar fields were exceptionally strong in the declining phase of cycle 18, verifying the basic tenet of solar dynamo theory of the poloidal-to-toroidal field transition (so called Ω mechanism) (Babcock, 1961). On the other hand, solstice GA maximised during the declining phase of cycle 23, in agreement with the exceptional evolution of the solar magnetic field and the occurrence of persistent low-latitude coronal holes during this cycle (Gibson et al. 2009). Isolated equatorial or low-latitude coronal holes lead to a larger relative fraction of Earth-bound HSS close to solstices, at low heliographic latitudes. Thus, the observed differences in GA between the seasons corresponding to low vs. high heliographic latitudes can be used to study the occurrence and the approximate location of persistent coronal holes.

2. GEOMAGNETIC STORMS

We have used the the Dxt index (Karinen and Mursula, 2005) to study the occurrence of geomagnetic storms throughout the GMM. Figure 1 (left) shows the annual number of small, medium and large storms in 1964-2017. We have further separated the storms according to their solar wind drivers, as given by the classification by Richardson et al. (2006). Small storms are clearly dominated by the HSS-related storms and their occurrence maximises in the late declining phase of each cycle. Typically 15-20 small storms, i.e. more than one per solar rotation,

are found in the most active year of each cycle. On the other hand large storms are dominated by CMEs and occur fairly well in accordance with sunspot cycle. Some 10 large storms are typically found in the most active year of each cycle, except for the ongoing cycle where the number of large storms has reduced roughly by factor of two. Note also that no large storms occurred in the four years around the previous solar minimum.

Figure 1 (right) shows the annual number of small, medium and large storms in 1932-2017 without separation into solar wind drivers. (Such a separation can only be done after 1964). Small storm occurrence maximises in the late declining phase of each cycle. This indicates that HSSs were dominating the driving of small storms even in the early phase of GMM, during cycles 16-19. Also, large storms follow closely the sunspot cycle even in the early GMM, indicating that CMEs are their main source throughout the GMM. Interestingly, the number of large storms in the most active year of the cycle seems to be somewhat larger in the early GMM than later, and the total number of large storms is largest during cycle 19, the peak sunspot cycle of GMM. Note also the momentary dropout of storms of all intensity classes during cycle 20 in 1960s. Currently, during cycle 24, the number of large storms is very small. However, not much reduction is seen in the number of small storms in SC24, but the year of maximum number of small storms is found in the early declining phase, which is exceptional.

REFERENCES

Babcock, H. W. (1961). The topology of the Sun‘s magnetic field and the 22-year cycle, *Astrophys. J.*, **133**, 572–587.

Finch, I. D., M. L. Lockwood and A. P. Rouillard (2008). Effects of solar wind magnetosphere coupling recorded at different geomagnetic latitudes: Separation of directly-driven and storage/release systems, *Geophys. Res. Lett.*, **35**, L21105.

Gibson, S. E., J. U. Kozyra, G. de Toma, B. A. Emery, T. Onsager and B. J. Thompson (2009). If the Sun is so quiet, why is the Earth ringing? A comparison of two solar minimum intervals, *J. Geophys. Res.*, **114(A13)**, A09105.

Holappa, L., K. Mursula, T. Asikainen and I. G. Richardson (2014). Annual fractions of high-speed streams from principal component analysis of local geomagnetic activity, *J. Geophys. Res.*, **119(6)**, 4544–4555.

Karinen, A., and K. Mursula (2005). A new reconstruction of the Dst index for 1932-2002, *Ann. Geophys.*, **23**, 475–485.

Lyatsky, W., P. T. Newell and A. Hamza (2001). Solar illumination as cause of the equinoctial preference for geomagnetic activity, *Geophys. Res. Lett.*, **28**, 2353–2356.

Mursula, K., R. Lukianova and L. Holappa (2015). Occurrence of high-speed solar wind streams over the grand modern maximum, *Astrophys. J.*, **801(1)**, 30.

Mursula, K., L. Holappa and R. Lukianova (2017). Seasonal solar wind speeds for the last 100 years: Unique coronal hole structures during the peak and demise of the Grand Modern Maximum, *Geophys. Res. Lett.*, **44(1)**, 30.

Richardson, I. G., et al. (2006). Major geomagnetic storms (Dst $\leq$ -100 nT) generated by corotating interaction regions, *J. Geophys. Res.*, **111**, A07S09.

The effect of magnetograph saturation and resolution on the observations of the photospheric magnetic field

N. Mäkinen[1], I. Virtanen[1] and K. Mursula[1]

[1]ReSoLVE Centre of Excellence, Space Climate research unit, University of Oulu, POB 3000, FIN-90014, Oulu, Finland
niina.makinen@oulu.fi, ilpo.virtanen@oulu.fi, kalevi.mursula@oulu.fi

Abstract

The magnetic field of the solar photosphere can be observed using the Zeeman splitting of spectral lines. These observations are important for both solar and heliospheric studies, including space weather and space climate, since they can be used as a boundary condition for models of the solar coronal and heliospheric magnetic fields. Unfortunately, the longest observations of the photospheric magnetic field have a rather low spatial resolution and are saturated above a fairly low magnetic field strength. We investigate here the importance of these shortages for the coronal field by studying several low harmonic coefficients calculated from the magnetic field observations (synoptic maps) of the modern, high-resolution SOLIS/VSM magnetograph. We find that moderate saturation and low spatial resolution do not have a significant effect on the low harmonic coefficients that are the most important for the coronal field model.

1. INTRODUCTION

Observations of the photospheric magnetic field (PhMF) started at Mount Wilson Observatory in 1950s, but digital data are available only from the late 1960s. The longest and most homogeneous series of PhMF observations has been measured at Wilcox Solar Observatory (WSO) since 1976 until today. However, these long-term data have a fairly low resolution and they are saturated above a certain, rather low field strength. As a result, complex magnetic field areas and high field intensities are poorly resolved at WSO. The more modern instruments like the SOLIS/VSM magnetograph do not suffer from saturation, and their much higher spatial resolution makes the observations more reliable.

The photospheric magnetic field also produces the magnetic field of the solar corona, which determines the structure of the heliospheric magnetic field, being largely responsible for space weather and space climate. Unfortunately, the coronal magnetic field cannot be directly measured because of the very low density of coronal plasma. Therefore, coronal modelling is one of the crucial tasks in space science. A widely used model for coronal magnetic field is the potential field source surface (PFSS) model (Altschuler et al., 1969), where coronal currents are neglected. This leads to a potential magnetic field, which can be presented in terms of a spherical harmonic expansion. It has been shown that only a few low harmonics are needed to

a coronal field which matches with observations of the heliospheric field (Wang, 2014; Koskela et al., 2017). The large-scale field is mainly produced by the axial dipole and octupole (Petrie, 2014; Zieger et al., 2019), and the axial quadrupole mainly contributes to the hemispheric asymmetry of the field, and leads to the southward shift of the heliospheric current sheet (Mursula and Hiltula, 2003; Virtanen et al., 2016). We investigate here the quality of the early observations by studying how the low harmonic coefficients that are calculated from modern high-accuracy data, respond to artificial saturation and spatial downgrading.

2. DATA AND THE PFSS MODEL

We use SOLIS/VSM synoptic (rotational) maps of the radial flux density that have 180×360 (sine-latitude - longitude) pixel resolution. In these maps the unobserved pixels at very high latitudes are interpolated using a cubic-polynomial fit. Here we neglect all maps that have any data gaps.

The PFSS model assumes a current-free corona up to a so-called source surface radius r_{ss}, where the field becomes radial. The potential field obeys the Laplacian equation $\nabla^2\phi = 0$, which can be solved in terms of spherical harmonics. The solution for the radial component of the magnetic field can be presented in the form

$$B_r(r,\theta,\phi) = \sum_{n=1}^{\infty}\sum_{m=0}^{n} P_n^m(\cos\theta)(g_n^m \cos m\phi + h_n^m \sin m\phi)C(r,n) \tag{1}$$

where θ is colatitude (polar angle) and ϕ longitude, $P_n^m(\cos\theta)$ are associated Legendre functions and $C(r,n)$ is the radial function. The coefficients g_n^m and h_n^m are solved from

$$\left\{ \begin{array}{c} g_n^m \\ h_n^m \end{array} \right\} = \frac{2n+1}{N}\sum_{i=1}^{X}\sum_{j=1}^{Y} B_r^{j,i} P_n^m(\cos\theta_i) \left\{ \begin{array}{c} \cos m\phi_j \\ \sin m\phi_j \end{array} \right\} \tag{2}$$

where $B_r^{j,i}$ is the radial component of the measured photospheric magnetic field, j and i are longitude and latitude coordinates of the data point, X and Y are number of data points in latitude and longitude direction and $N = XY$ is the total number of data points. Since h_n^m and g_n^m are closely related, only the latter are studied here. Moreover, we limit our study to the lowest harmonics of g_1^0, g_1^1, g_2^0 and g_3^0 only, since they have the largest effect on the solar large-scale field.

3. DATA PROCESSING

Babcock-type magnetographs like the one at WSO suffer from poor sensitivity of weak fields or saturation of strong fields. Saturation point depends on the wavelength used by the detector and the Landé g-factor of the observed spectral line. We artificially saturate the high-quality SOLIS/VSM data by assuming a simplified sinusoidal instrument response curve, where maximum is reached at saturation point B_s, beyond which the field decreases reaching zero at $2B_s$. This roughly corresponds to Babcock-type magnetograph where two boxcar-shaped detectors observing the left- and right-handed polarized light are located symmetrically with respect to center of the Gaussian-shaped spectral line core. This artificial saturation is applied to each

synoptic map using

$$B_{sat} = \begin{cases} \frac{B_s \sin\left(\frac{B}{B_s}\frac{\pi}{2}\right)}{\pi/2}, B < 2B_s \\ 0, B \geq 2B_s, \end{cases} \tag{3}$$

where B_{sat} is a new "saturated" field value, B_s is the chosen saturation point (value) and B is the original value of the pixel of interest. We test the effect using four different saturation points at $B_s = 50G$, $100G$, $200G$ and $500G$.

As another test we study the downgrading of spatial accuracy, by applying a two-dimensional average over a block of pixels. Actually, downsampled high-resolution data do not resemble the real low-resolution observations (Riley, 2014). However, a more realistic test method would be unnecessarily complicated. The saturated set and the original set are downsampled to resolutions of 30×72, 9×18, 6×12, 3×6 and 2×4. We then have six different resolutions and five levels of saturation, which gives us 30 data sets of 174 synoptic maps.

Harmonic coefficients g_1^0, g_1^1, g_2^0 and g_3^0 are then calculated for each data set. Figure 1 depicts the ratios (where sum is over all 174 maps)

$$\frac{\sum |g^m_{n(sat,res)}|}{\sum |g^m_n|}, \tag{4}$$

where $g^m_{n(sat,res)}$ are coefficients of the modified data sets and g^m_n the original coefficients. Since g_2^0 divides a sphere into three sections, it cannot be calculated for sets with resolution below 3×6. For the same reason g_3^0 is not calculated for sets with resolution below 6×12.

4. RESULTS

Figure 1 shows that for a fixed spatial scale the color (value of the ratio) is quite similar for all saturation levels. This demonstrates that saturation has, overall, only a rather small effect on the low harmonics included in the Figure 1. Axial dipole and axial octupole show hardly any difference (less than 10%) when saturation point changes. The equatorial dipole and quadrupole terms are more sensitive to saturation and show a notable change (about 20% and 30%. resp.) when $B_s = 100G$ and smaller.

Resolution has a more notable effect on the ratios depicted in Figure 1, but only when it decreases to a very small number of pixels. Axial dipole and quadrupole terms show a fairly steady decrease as resolution drops, with a large change seen only at 3×6, i.e. after a reduction of resolution by a factor of 3600. Octupole term is the most sensitive to spatial resolution, suffering a significant drop already at resolution 9×18 (reduction by 400). Equatorial dipole suffers least from saturation and can even slightly increase in downgrading.

Our results show that moderate instrument saturation is not a significant constraint. Most of the photospheric field is fairly weak and areas of large field intensity are very small. Therefore the areas which are affected by saturation are small and do not contribute significantly to the large-scale structure. Reducing the spatial resolution has a somewhat larger effect, but becomes significant only when resolution is made very coarse.

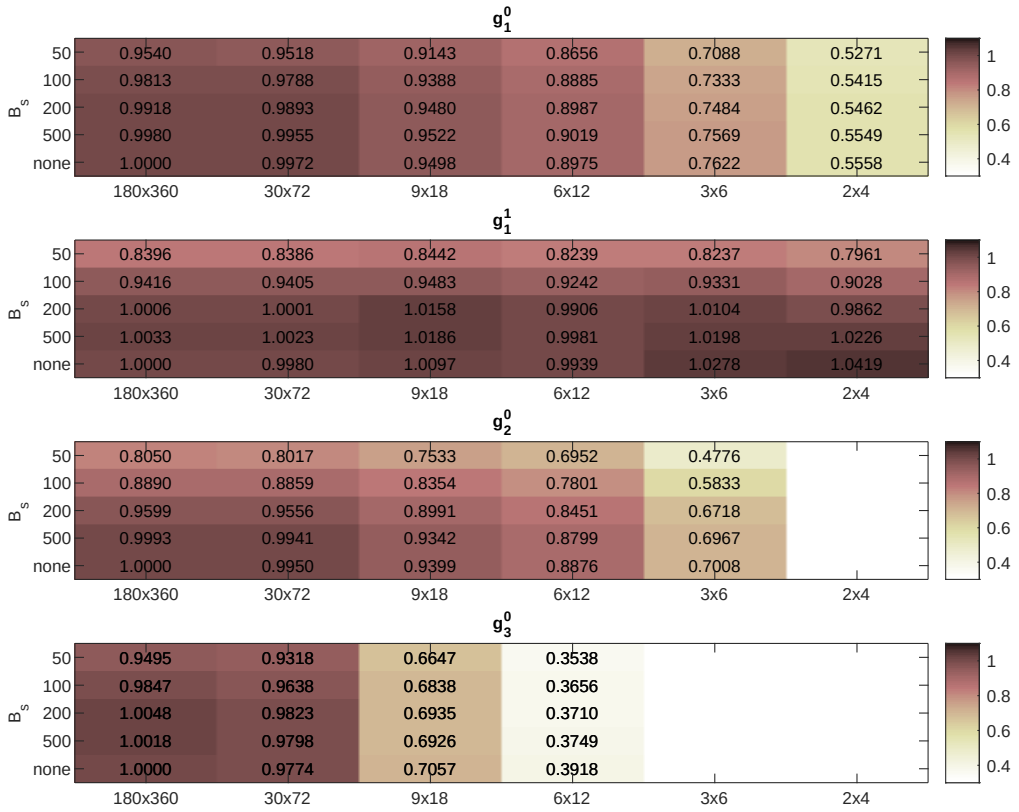

Figure 1: Ratios 4 (in color coding) between modified and original values of absolute harmonic coefficients of g_1^0, g_1^1, g_2^0 and g_3^0 calculated using SOLIS/VSM data. In each panel, y-axis gives the saturation point (none=original data) and x-axis the spatial resolution.

REFERENCES

Altschuler, M. D., and G. Newkirk, 1969. *Solar Physics*, **9 (1)**, 131-149.

Koskela, J., I. Virtanen, and K. Mursula, 2017. *The Astrophysical Journal*, **835 (1)**, 63.

Mursula, K., and T. Hiltula, 2003. *Geophys. Res. Lett.*, **30 (22)**, SSC 2–1-4.

Petrie, G., 2014. *The Astrophysical Journal*, **768 (2)**, 162.

Riley, P., et al., 2014. *Solar Physics*, **289 (3)**, 769-792.

Virtanen, I., and K. Mursula, 2016. *Astronomy & Astrophysics*, **591**, A78.

Wang, Y.-M., 2014. Solar cycle variation of the sun's low-order magnetic multipoles: heliospheric consequences *Space Science Reviews*, **186 (1-4)**, 387-407.

Zieger, B., and K. Mursula, 2019. *Astronomy & Astrophysics*, in press.

Luotausverkoston alueellisen kattavuuden vaikutus numeerisessa säänennustamisessa arktisilla alueilla

T. Naakka[1], T. Nygård[1], T. Vihma[1] ja R. Pirazzini[1]

[1] Ilmatieteen laitos, tuomas.naakka@fmi.fi

Abstract

The impact of spatial coverage of the radiosounding network in the Arctic on the quality of 850 hPa level temperature field in numerical weather prediction model products was examined by comparing operational analyses and 12-hour forecast from European Centre of Medium Range Weather Forecasts (ECMWF) with radiosonde observations from Integrated Global Radiosonde Archive (IGRA). Comparison showed that radiosoundings had a remarkable impact on improving operational analyses, but the impact had a large geographical variation. Especially, radiosoundings from islands (Jan Mayen and Bear Island) in the northern North Atlantic had a remarkable impact on analyses suggesting that those stations were critical for the quality of analyses and further for the quality of weather forecasts. Comparison between short forecasts, which were used as an estimate for the background field in data assimilation process, and observations showed that the density of the sounding network was not the most critical factor for the quality of background fields on the areas where the radiosounding network is tolerably dense. Instead, the weight of radiosonde observations in analyses seemed to have a much larger effect on the quality of background fields in comparison with observations.

1. JOHDANTO

Radioluotausverkosto on tärkeä osa säähavaintojärjestelmää Arktisella alueella. Radioluotaukset tuottavat luotettavia havaintoja ilmakehän lämpötila- tuuli- ja kosteusprofiileista tarkalla pystyresoluutiolla ja ovat siten tärkeä havaintojen lähde sääennustusmalleille. Luotausverkosto Arktisessa on kuitenkin harva: vain 76 luotausasemaa sijaitsee leveyspiirin 60°N pohjoispuolella, ja nekään eivät ole alueellisesti tasaisesti jakautuneet (Kuva 1). Tihein luotausverkosto sijaitsee Pohjois-Euroopassa ja Länsi-Venäjällä, kun taas keskisellä Jäämerellä ei ole yhtään luotausasemaa. On esitetty, että luotausasemien vähyys on osasyynä heikompi laatuisiin sääennusteisiin Arktisessa (Jung et al. 2016). Toisaalta syrjäisestä sijainnista ja ankarista olosuhteista johtuen luotausten suorittaminen etenkin Jäämerellä on sekä teknisesti vaikeaa että taloudellisesti kallista, joten onkin tärkeää selvittää, kuinka luotausverkoston alueellinen kattavuus vaikuttaa numeeristen sääennusteiden laatuun.

2. AINEISTO JA MENETELMÄT

Tutkimuksen aineistona on käytetty Euroopan keskipitkien sääennusteiden keskuksen (Europen Centre of Medium Range Weather Forecasts, ECMWF) operatiivisia analyyseja ja 12 tunnin ennusteita sekä radioluotauksia IGRA-arkistosta (Integrated Global Radiosonde Archive). Tutkimusjakso ulottuu tammikuusta 2016 syyskuuhun 2018. Tältä jaksolta on käytetty mallituotteita ja luotauksia ajanhetkiltä 00 UTC ja 12 UTC.

ECMWF käyttää säämallissaan 4-D variaatioassimilaatiojärjestelmää tuottamaan analyysin eli alkutilan numeerisille ennusteille. Assimilaatiossa ennakkokenttää korjataan havainnoilla. Ennakkokenttä perustuu aiempaan lyhyeen ennusteeseen ja näin ollen sisältää myös havaintojen informaation edellisistä assimilaatio sykleistä. Assimilaatiossa havaintojen vaikutus myös leivitetään havaintopisteen ympäristöön, jotta analyysi olisi fysikaalisesti johdonmukainen. Assimilaatio toistetaan kahdesti vuorokaudessa eli 12 tunnin välein. Tässä tutkimuksessa 12 tunnin operatiivista ennustetta käytetään estimaattina ennakkokentälle. 12 tunnin ennuste ei aivan täysin vastaa assimilaation oikeaa ennakkokenttää, sillä ECMWF ei käytä operatiivisia ennusteita assimilaation ennakkokenttänä.

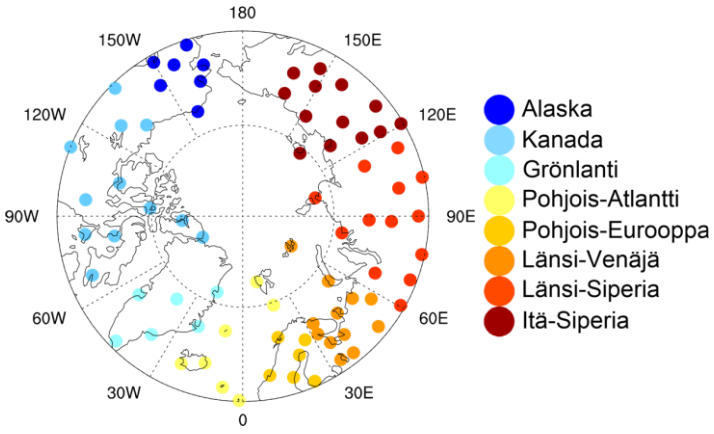

Kuva 1: Luotausasemat leveyspiirin 60°N pohjoispuolella ja niiden aluejako.

Tässä tutkimuksessa tarkastellaan ennakkokentän ja luotausten välisiä eroja, erityisesti erojen alueellista jakaumaa. Nämä erot kuvaavat tavallisesti ennakkokentän epävarmuutta, mutta voivat liittyä myös luotausten epätarkkuuteen. Lisäksi tarkastellaan ennakkokentän ja analyysin välisiä eroja. Nämä erot puolestaan kuvaavat havaintojen vaikutusta analyysiin. Kolmanneksi tarkastellaan ennakkokentän ja analyysin sekä analyysin ja havaintojen välisisten erojen suhdetta, joka kuvaa havaintojen painoarvoa assimilaatioprosessissa. Tutkimuksessa keskityttiin tarkastelemaan lämpötilaa 850 hPa painepinnalla, joka on tärkeä suure ilmamassojen ja niiden välisten rintamien tunnistamisessa.

3. TULOKSET

Erot ennakkokentän ja luotaushavaintojen välillä olivat pienimpiä Pohjois-Euroopan, Pohjois-Atlantin sekä Alaskan luotausasemilla tarkoittaen, että ennakkokentät olivat tarkimpia näillä alueilla (Kuva 2a ja 3). Suurimmat erot sen sijaan löytyivät Siperiasta viitaten epävarmempiin ennakkokenttiin tällä alueella, mutta myös huonompi luotausten laatu voi kasvattaa eroja havaintojen ja ennakkokentän. Merkittävää oli kuitenkin, että alueellinen vaihtelu erojen suuruudessa ennakkokentän ja havaintojen välillä ei riippunut luotausverkoston tiheydestä. Atlantilla, missä luotausverkosto on harva, erot olivat suhteellisen pienet verrattuna Siperiaan, missä luotausverkosto ei kuitenkaan ole varsin harva.

Erot ennakkokentän analyysin välillä kuvaavat havaintojen vaikutusta analyysissa. Näistä eroista ei kuitenkaan voida tunnistaa yksittäisten havaintojen vaikutusta analyysiin, koska

kaikki assimiloidut havainnot vaikuttavat ennakkokentän ja analyysin välisiin eroihin. Analyysin ja ennakkokentän välisten erojen alueellinen jakauma kuitenkin osoitti, että luotauksilla on huomatta merkitys analyysin korjaamisessa assimilaatio prosessissa. Erot ennakkokentän ja analyysin välillä olivat suurimat luotausasemien läheisyydessä (Kuva 2b). Toisaalta luotausten suurin vaikutus näyttäisi keskittyvän hyvin pienelle alueella luotausaseman läheisyydessä, mikä viittaisi siihen, että luotausasemaverkon tiheydellä saattaisi olla vaikutus analyysien ja sitä kautta seuraavan ennakkokentän laatuun, mitä ennakkokenttien ja luotausten välinen vertailu ei kuitenkaan osoittanut. Keskimäärin RMS-ero ennakkokentän ja analyysin välillä oli vain 0.1 K suurempi luotausasemilla kuin keskimäärin koko Arktisessa, mutta yksittäisillä luotausasemilla, kuten Jan Mayenin, Karhusaaren (Pohjois-Atlantilla) asemilla, RMS-ero oli 0.9 K ja 0.8 K suurempi osoittaen, että näiden asemien havainnoilla on merkittävä vaikutus analyysien tarkkuuden parantamisessa.

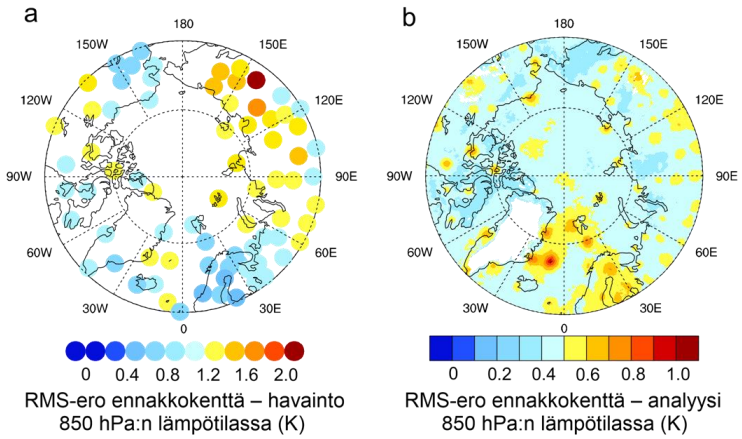

Kuva 2: RMS-erot luotausasemilla ennakkokentän ja havaintojen välillä (a) sekä koko Arktiksessa ennakkokentän ja analyysin välillä (b).

Luotaustenpainoarvoa assimilaationprosessissa arvioitiin vertailemalla ennakkokentän ja analyysin sekä havaintojen ja analyysin välisten erojen suhdetta. Asemilla, joilla erot keskimäärin havaintojen ja analyysin välillä olivat suuret ja toisaalta erot ennakkokentän ja analyysin välillä pienet, luotauksien painoarvo oli pieni, kun taas jos erot havaintojen ja analyysin välillä olivat pienet ja ennakkokentän ja analyysin välillä suuret, luotauksilla oli suuri painoarvo assimilaatioprosessissa. Keskimäärin arktisilla luotausasemilla erot ennakkokentän ja analyysien välillä olivat pienemmät kuin havaintojen ja analyysien eli analyysit ovat lähempänä ennakkokenttää kuin havaintoja. Kuitenkin Pohjois-Euroopan luotausasemilla erot havaintojen ja analyysin välillä olivat keskimäärin pienennät kuin ennakkokentän ja analyysin välillä tarkoittaen (Kuva 3a), että, Pohjois-Euroopassa analyysit nojasivat vahvasti luotaushavaintoihin.

Luotaushavaintojen painoarvolla ja luotausten ja ennakkokentän keskimääräisellä erolla oli selvä riippuvuus. Keskimäärin luotausten painoarvo oli sitä suurempi mitä lähempänä havainnot ja ennakkokenttä olivat toisiaan (Kuva 3b). Toisaalta myös muutamia poikkeuksia esiintyi. Jan Mayenin, Karhusaaren ja Barrow:n (Alaskassa) luotausasemilla luotausten painoarvo assimilaatiossa oli suuri vaikka erot ennakkokentän ja havaintojen välillä olivat suuret, joten näillä asemilla oli merkittävä vaikutus analyysien tarkkuuden parantamisessa.

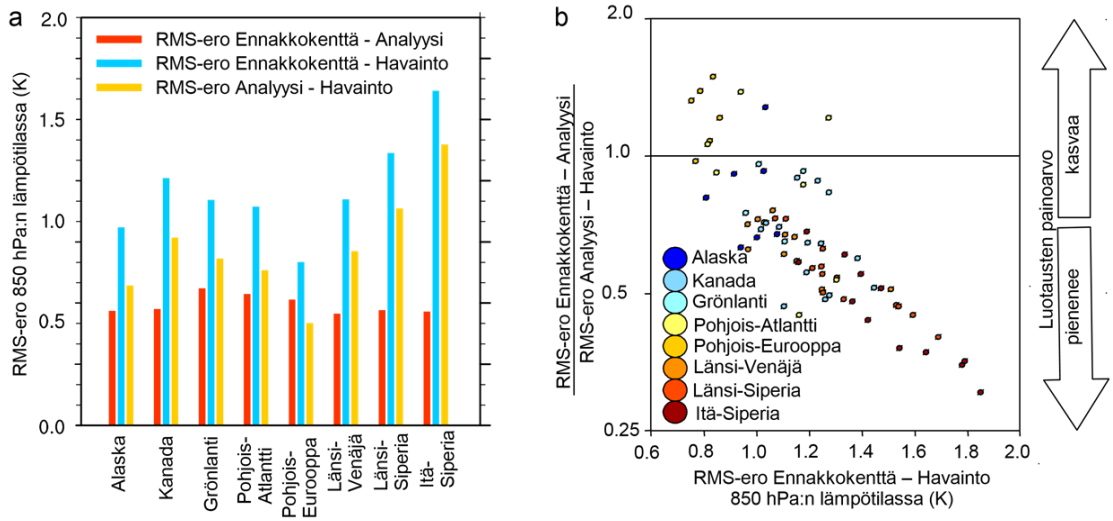

Kuva 3: Keskimääräiset RMS-erot luotausasemilla ennakkokentän ja analyysin välillä, ennakkokentän ja havaintojen välillä sekä analyysin ja havaintojen välillä (a). Ennakkokentän ja analyysin sekä analyysin ja havaintojen välisten RMS-erojen suhde ennakkokentän ja havaintojen välisen RMS-eron funktiona (b).

4. YHTEENVETO

Radioluotaukset auttavat merkittävästi parantamaan operatiivisia analyyseja, mutta luotausten vaikutus vaihtelee alueellisesti paljon. Erityisesti pohjoisella Atlantilla sijaitsevilta saarilta saaduilla luotaushavainnoilla on huomattava vaikutus analyyseihin, ja siksi nämä havaintoasemat ovat erityisen tärkeitä hyvien analyysien ja sitä kautta myös ennusteiden kannalta. Toisaalta luotausten suora vaikutus analyysiin keskittyi suhteellisen pienelle alueelle luotausaseman ympäristöön, mikä antaisi olettaa, että luotausverkoston tiheys vaikuttaisi analyysien laatuun ja sitä kautta seuraavan assimilaatiosyklin ennakkokentän tarkkuuteen. Ennakkokenttien tarkkuus, kun ennakkokenttiä verrattiin luotaushavaintoihin, ei kuitenkaan ensisijaisesti riippunut luotausverkoston tiheydestä vaan luotausten saamasta painoarvosta analyyseissa. Toisaalta ei voitu osoittaa, että riippuiko tämä luotaushavainnoille annetusta painoarvosta assimilaatioprosessissa vai luotausten laadun maantieteellisestä vaihtelusta. Tämä kuitenkin osoittaa, että luotaushavaintojen laadun arviointi sekä mahdollisesti radiosondien tarkkuuden parantamien olisi tärkeää parempien analyysien ja sitä kautta parempien numeeristen sääennusteiden kannalta.

KIITOKSET

Tämä tutkimus on osa INTAROS-projektia, joka on saanut rahoituksen Euroopan komission Horizon 2020 -ohjelmasta.

LÄHTEET

Jung, T., N.D. Gordon, P. Bauer, D. H. Bromwich, M. Chevallier, J. J. Day, J. Dawson, F. Doblas-Reyes, C. Fairall, H. F. Goessling, ja M. Holland, 2016. Advancing polar prediction capabilities on daily to seasonal time scales. *Bulletin of the American Meteorological Society*, **97(9)**, 1631-1647, DOI: 10.1175/BAMS-D-14-00246.1.

INFACT (Innovative, Non-Invasive and Fully Acceptable Exploration Technologies) - Geophysical aspect of the project.

J. Nevalainen[1], J.-P. Ranta[1], E. Kozlovskaya[1] and INFACT colleagues

[1] University of Oulu, Oulu Mining School, jouni.nevalainen@oulu.fi

Abstract

The rising demand for metallic raw materials in Europe and worldwide increases the need for finding new mineral deposits. Comparing depth of discovered mineral resources during previous centuries, new mineral deposits are being found deeper, and thus, resolution and depth penetration of geophysical methods needs to be developed. In addition, concern of environmental impact of mineral exploration and mining needs to be addressed by better communication between mining industry, government and stakeholders. INFACT (Innovative, Non-Invasive, Fully Acceptable Exploration Technologies) addresses to these challenges by supporting development of non-invasive geophysical exploration technologies and ensuring that stakeholders voices are heard. In addition, based on the review of the best practices used in the exploration and mining globally, "best practice" guidelines for doing exploration and mining within EU are developed. INFACT has received funding from European Union's Horizon 2020 research and innovation programme. In this extended abstract, main goals of the INFACT project are described with emphasis being the geophysical aspect of the project.

1. INTRODUCTION

It has been recognized in the EU that the energy usage must be reduced and CO_2 emissions need to be decreased (European Commission, 2018). To achieve this, new innovative, efficient, and green ways to produce energy are developed through wind, solar, nuclear fission energy and carbon capture solutions together with supporting the e-mobility (e.g. electric cars). However, it is often overlooked that most of crucial components for these technologies are manufactured from imported raw materials (European Commission, 2014). Based on the economic importance and supply risk of certain metals, European Union has listed 27 critical raw materials, which possess high supply risk but have high economic importance to EU (European Commission, 2017). For instance, rare-earth elements (REE) such as neodymium (Nd), dysprosium (Dy) and praseodymium (Pr) are crucial material of permanent magnets used in wind turbines and electric vehicles (European Commission, 2014). Majority of these REE metals (ca. 95%) are currently produced in China and their export is highly regulated (European Commission, 2014). From economical point of view, EU relies mainly on imported key materials that are vital to European industry and its competitiveness on global market (European Commission, 2014).

As many of the surficial deposits are been mined out, geophysics is becoming more important tool for discoveries of hidden and buried deposits. This brings challenges to exploration techniques to detect deep deposits from the surface in high enough accuracy. Exploration solely based on drilling in the early stages of the mineral exploration is expensive, and has a larger environmental footprint compared to many geophysical methods, and thus the decreasing the need for drilling at the early stages of exploration is important.

In addition, negative publicity due known environmental accidents, such as Talvivaara mine case in Finland, can lead in the clash between mining industry and environmental agencies and local stakeholders in the mining region (Litmanen et al., 2016; Sairinen et al., 2017). Such an incidents affect to the common opinion toward mining industry (Litmanen et al., 2016). The distrust between local stakeholders and the mining industry can be seen in the questionnaire results (Figure 1), where EU citizens were asked to rate companies in different fields by their responsibility towards society and country (European Commission, 2013).

INFACT project (Innovative, Non-Invasive and Fully Acceptable Exploration Technologies) was created to address both of these challenges. INFACT is an international project that involves operators from wide field including institutes focused in geosciences, technical development & exploration companies, social and environmental sciences, business model planners and mining companies. The coordinator for the project is Helmholtz Zentrum Dresden Rossendorf (HZDR). The project has received funding from the European Union‘s Horizon 2020 research and innovation programme. Project partners are shown in Figure 2. (INFACT, 2019).

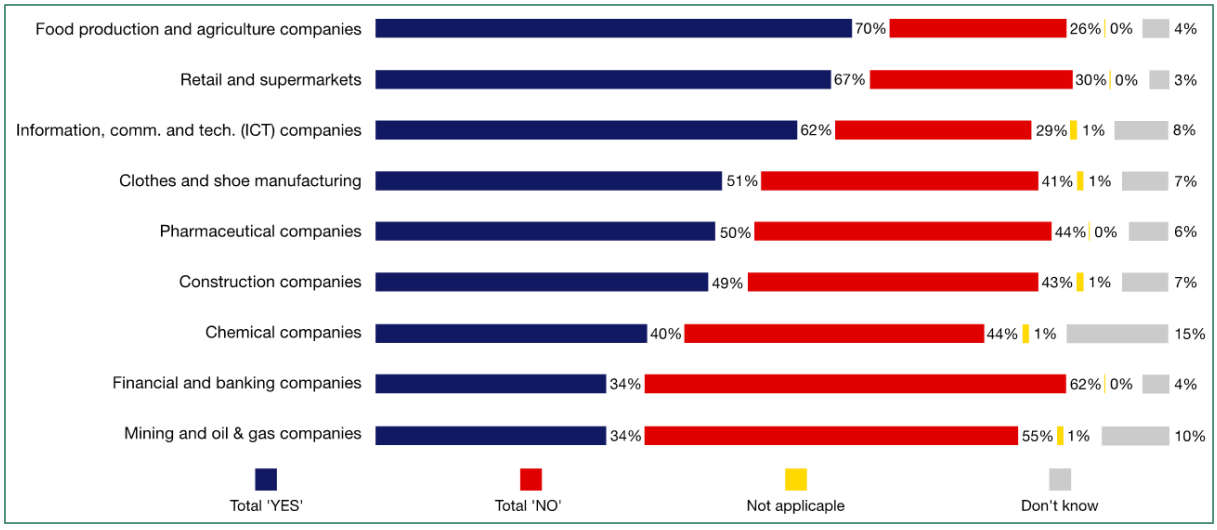

Figure 1: Survey results of the Flash Eurobarometer 363 for the question ”Do companies make effort to behave responsibly towards society in our country?”. Average values for the EU by type of industries (European Commission, 2013).

Figure 2: Partners of INFACT and their respective roles.

2. MAIN GOALS FOR INFACT

INFACT supports the development of non-invasive geophysical exploration technologies which potentially reduces the need of drilling during the early stages of mineral exploration. In this context, an idea for three reference sites for testing the geophysical exploration technologies is introduced. The sites are located in three countries within EU, Finland, Germany and Spain. The reference sites provides industry-relevant environments representing a variety of social, physical and technical challenges. The reference sites offer benchmarking targets to test sensitivity of geophysical instrumentation. Benchmarking target could be any geological feature that have either been directly detected by geological mapping or identified based on high-resolution geophysical ground surveys (INFACT, 2019).

During INFACT project, all reference sites are surveyed with state-of-art geophysical methods suitable to detecting site characteristic mineral deposit and other features such as overburden thickness. In addition, innovative technologies are tested during the project. These include for example, passive seismic and SQUID (superconducting quantum interference device) magnetic survey. Most of the surveys are done by airborne geophysical methods (e.g. helicopter, drones), but supporting ground geophysical methods are used by taking into account the site specific characteristics (e.g. environmental, social). For future innovative technologies, it is vital to know physical properties (density for example) of the subsurface, as these technologies might not be conventional (e.g. Muography). Geological information is in key role on this task.

In addition to technical aspect, INFACT is developing common practices for stakeholder engagement. The dialogue between mining companies, authorities, local administration and people is important when building social acceptance for mining operation. The dialogue focus on developing communication between stakeholders to help building acceptance towards mining. As the exploration stage is one of the first "signs" of a possible mine, we at the University of Oulu are participating in disseminating knowledge of geophysical exploration methods and physics behind them for stakeholders. In social aspect of the project, it is important to have dialogue about possible issues with used geophysical methods, such as magnetic field strength and its change rate in electromagnetic methods.

ACKNOWLEDGEMENTS

This project has received funding from the European Union's Horizon 2020 research and innovation programme under grant agreement No 776487.

REFERENCES

European Commission, 2018. Communication from the Commission to the European Parliament, The European Council, The Council, The European economic and social committee, the committee of the regions and the European investment bank: *A Clean Planet for all A European strategic long-term vision for a prosperous, modern, competitive and climate neutral economy*, Brussels, **COM(2018) 773 Final**, 25 p.

European Commission, 2017. Communication from the commission to the European Parliament, the council, the European economic and social committee and the committee of the regions: *On the 2017 list of Critical Raw Material for the EU*, Brussels, **COM(2017) 490 Final**, 8 p.

European Commission, 2014. REPORT ON CRITICAL RAW MATERIALS FOR THE EU, Brussels, Ref. **Ares(2015)1819503 - 29/04/2015**, 41 p.

European Commission, 2013. Flash Eurobarometer 363: How Companies Influence Our Society: Citizens' View, Ordered survey, European Commission, Brussels, 134 p.

INFACT, 2019. INFACT (Innovative, Non-Invasive and Fully Acceptable Exploration Technologies) homepage, https://www.infactproject.eu/

Litmanen, T, T. Jartti and E. Rantala, 2016. Refining the preconditions of a social license to operate (SLO): reflections on citizens' attitudes towards mining in two Finnish regions. *The Extractive Industries and Society*, **3(3)**, 782-792.

Sairinen. R., H. Tiainen and T. Mononen, 2017. Talvivaara mine and water pollution: An analysis of mining conflict in Finland. *The Extractive Industries and Society*, **4(3)**, 640-651.

High-frequency geomagnetic fluctuations, comparison between northern and southern hemisphere

P. Peitso[1] and E.I. Tanskanen[1]

[1] Aalto University School of Electrical Engineering, Department of Electronics and Nanoengineering, Center of Excellence ReSoLVE, Magnetic unit, pyry.peitso@aalto.fi

Abstract

Rapid geomagnetic fluctuations are linked to several different space weather phenomena. The detailed latitudinal distribution and coverage of these fluctuations is very useful for space weather forecasting purposes. For this purpose we utilize the newly developed Fractional Derivative Rate (FDR) method, recently used to study the latitudinal differences of geomagnetic activity in Greenland. The FDR method calculates a daily percentage value where a given amount of geomagnetic fluctuations is met or exceeded. This allows the efficient usage of high time-resolution magnetometer data as well as clear illustration of geomagnetic fluctuation latitudinal differences. We will compare high-frequency fluctuations between the northern and southern hemisphere. Since the geomagnetic activity comparison between the two hemispheres has several open questions, we start with mapping stations from the south to well-known northern latitude stations. The northern hemisphere standard is provided by DTU operated Greenland magnetometers, covering a wide latitudinal range from the polar cap to the auroral oval latitudes. The southern hemisphere is studied using stations in the southern Indian Ocean, Oceania and Antarctic. Both hemispheres are studied using 1 s measurements of the magnetic field H-component, dH/dt as well as FDR. Seasonal as well as the UT variation of these fluctuations are studied and results presented.

REFERENCES

Peitso, P., E.I. Tanskanen, T.I. Pulkkinen and K. Mursula, 2018. High-Frequency Geomagnetic Fluctuations at Auroral Oval and Polar Cap. *Space Weather*, **16(8)**, 1057-1072.

Geophysical methods in impact crater hunting – Case Summanen

L.J. Pesonen[1], S. Hietala[2]*, J. Plado[3], T. Kreitsmann[3], J. Lerssi[2], and J. Nenonen[2]

[1] Solid Earth Geophysics Laboratory, Physics Department, University of Helsinki, Finland
[2] Geological Survey of Finland, Kuopio, Finland
[3] Department of Geology, University of Tartu, Estonia,
*correspondence: satu.hietala@gtk.fi

Abstract

Impact cratering is a ubiquitous process in our solar system affecting all planetary surfaces throughout geologic time. On Earth, there are currently 190 confirmed impact structures, which are distributed unevenly. The Fennoscandian Shield houses 17 % of them. The large amount of impact structures makes Fennoscandia one of the most densely cratered terrains on Earth. A dozen (12) impact structures have been discovered in Finland. The latest discovery, Lake Summanen is located in Central Finland, about 9 km southeast of city Saarijärvi. An impact generated structure was first hinted by airborne geophysical mapping by the Geological Survey of Finland in the early 2000`s (Lerssi et al., 2007) that revealed a circular ~2.6 km wide striking aeroelectromagnetic resistivity anomaly. Recent studies in 2017-2018 confirmed its impact origin based on the findings of shatter cone-bearing rocks and the identification of planar deformation features in quartz.

1. INTRODUCTION

Summanen impact crater (62°39’00’’N, 25°22’30’’E) is located within the Paleoproterozoic Central Finland Granite Belt and is covered with the Lake Summanen. The lake is somewhat elliptical (8 km x 9 km x 4 km) in shape, whereby the longest axis extends in NW–SE direction due to the erosional influence of the latest (Weichselian) glaciation. The area became deglaciated about 10,700 years ago (Stroeven et al. 2016). At present, the water level of Lake Summanen is at 108.5 m a.s.l. and it is connected to several other surrounding lakes. It also hosts two major islands, Summassaari and Lamposaari.

Lake Summanen was proven to have an impact origin based on diagnostic evidences. Shock-metamorphic features are divided into diagnostic and non-diagnostic features which can be either geological, geochemical, or geophysical. Shock metamorphic features like shatter cones are the only macroscopic evidence of an impact. The most commonly used diagnostic evidence for impact origin are the microscopic planar deformation features (PDFs) in minerals (e.g., quartz and feldspar; French and Koeberl 2010). During the field trip in 2017 a few tens of erratic porphyritic granite boulders, breccias and shatter cone-bearing samples were discovered. Most shatter cone-bearing specimens were found within a distance of 5 km SE from the geophysical anomalies. In two shatter cone-bearing samples PDFs were identified. Measurements of PDF orientations were done at the University of Tartu, with a LOMO FS universal stage mounted on a polarizing microscope using the standard technique (see Langenhorst, 2002) and analyzed using the PDF indexing algorithm ANIE (Huber et al.

2011). These results concluded that Summanen structure represents an old eroded impact structure and were published in Meteoritics & Planetary Science in 2018 (Plado et al. 2018).

2. GEOPHYSICAL CHARACTERISTICS

Geophysical anomaly of Lake Summanen was first identified in the early 2000s by Jouko Vanne, a geologist at the Geological Survey of Finland (Lerssi et al. 2007) who pointed out a regional conductivity anomaly from the geophysical lowaltitude data. In-phase aeroelectromagnetic data (Fig. 1a) over Lake Summanen revealed a strikingly circular c. 2.6 km wide anomaly, which is related to the central part of the lake. The anomaly is distinct as other nearby lakes lack such anomalies. The apparent resistivity map (Fig. 1b) shows an anomaly that is slightly wider and not as circular as the in-phase component anomaly. The anomalies are similar to the apparent resistivity anomaly associated with a nearby (50 km south from Summanen), Lake Karikkoselkä (Pesonen et al. 1999; Lerssi et al. 2007), which impact origin was proven in 1996 (Lehtinen et al. 1996). Noteworthily, lakes in Finland usually do not show such electromagnetic anomalies.

In the winter of 2006 the Lake Summanen was profiled from ice with the electromagnetic multifrequency apparatus (SAMPO) from the Geological Survey of Finland. The transmitter and receiver were located on the profile 500 m apart, and the result was given to the central point of the system. Measurements were performed at every 200 m, but condensed to 50 m in the central parts of two perpendicular SW–NE and NW–SE profiles. For qualitative interpretation, the SAMPO data measured at each frequency were transformed into curves of apparent resistivity as a function of depth using the algorithm of Aittoniemi et al. (1987). The curves were subsequently interpolated into apparent resistivity images (Fig. 2) by Lerssi et al. (2007). Bowl-shaped low resistivity features can be seen on both profiles (Fig. 2). Very low resistivities (<40 Ωm) are associated with Quaternary sediments. The rest of the bowl-shaped depression may be filled with low resistivity (from 40 to about 400 Ωm) sediments, or resistivities are lowered by fracturing of the basement. A report published by GTK (Lerssi et al. 2007) suggested that the possible cause of these features could be old sedimentary rocks or an impact crater structure filled with sedimentary material from the last ice age.

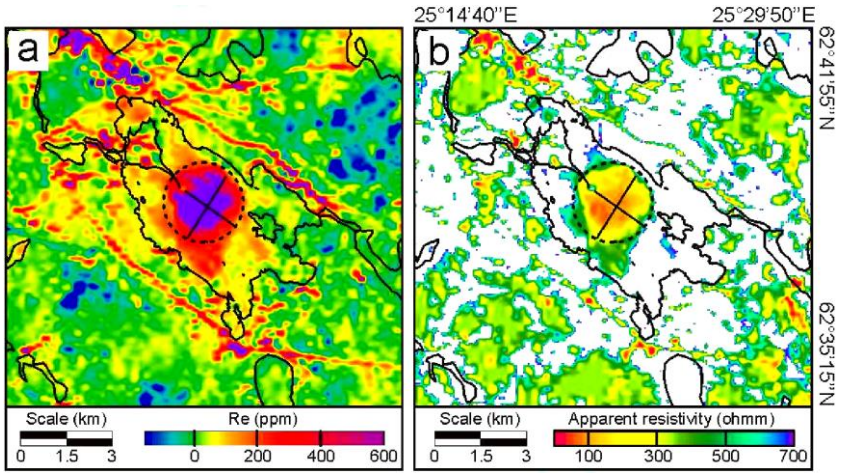

Figure 1: Aeroelectromagnetic (a) in-phase component and (b) apparent resistivity anomaly maps of the Lake Summanen area. Dashed ring with diameter of ~2.6 km indicate interpretational outlines of the anomalies within Lake Summanen. Black lines within the outlines show locations of SAMPO measurements (Fig. 2).

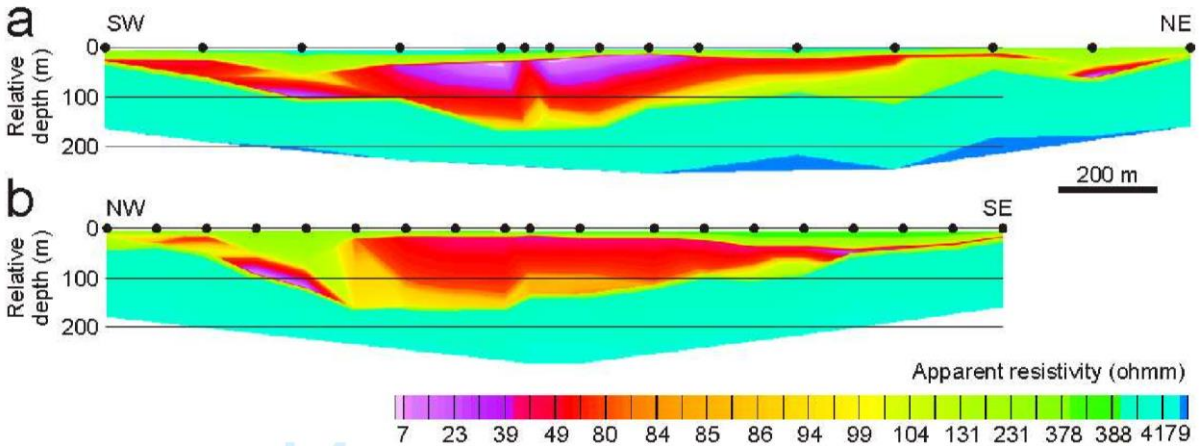

Figure 2: Apparent resistivity models based on the wideband SAMPO electromagnetic measurements from the ice of Lake Summanen (Lerssi et al. 2007). Black dots indicate locations of the original measurements (mid-points of the SAMPO system).

Lake Summanen is also surrounded by strong (up to 1000 nT) regional magnetic anomalies with a general trend from the SW to the NE. The lake area is characterized by weak magnetic relief: lack of prominent anomalies. Such a pattern is not a diagnostic feature for an impact origin, however, it is typical for many impact structures in Fennoscandia that miss highly magnetic impact melt rocks, such as, Jänisjärvi (Elo et al. 2000), Karikkoselkä (Pesonen et al. 1999), Suvasvesi South (Donadini et al. 2006), and Tvären (Ormö & Blomqvist 1996).

3. FUTURE STUDIES

The impact age of Summanen is undefined but must be younger than the age of the target rock 1.88 Ga. Radiometric and paleomagnetic dating techniques will be applied to date the Summanen event. Additionally, there is a need for gravity profiling and modelling. Seismic reflection and wide-band EM surveys may also provide additional information of the structure including the estimate of its erosion level. Drilling is essential to understand geological history of the structure.

4. CONCLUSION

Research of impact structures is constantly developing and receiving increasing international attention. The role of geophysical methods is important how these, mostly ancient, structures can be reliably identified. For example, the electromagnetic anomalies can be the last remaining sign in old, deeply eroded, structures. New developing methods should be used in the study, such as muongraphy. Muons can be used to derive an areal density of bedrock in great depths. In addition, unmanned Aerial Vehicles (UAV) used in magnetic surveys provides more detailed data than traditional airborne electromagnetic measurement. New technologies offer cost-effective, fast, and indestructible research capability. Several meteorite impact structures host economically valuable resources (ores, hydrocarbons, water). Impact sites have also become popular tourist attractions and they will increase tourism in the region and as such strengthen the local economy. Geoscientist must be informed about the potential of impact structures. The Summanen structure is an ideal target for drilling and providing data for multidisciplinary (geology, geophysics, geochemistry and environmental) research.

REFERENCES

Aittoniemi K., J. Rajala and J. Sarvas, 1987. Interactive inversion algorithm and apparent resistivity versus depth (ARD) plot in multifrequency depth soundings. *Acta Polytechnica Scandinavica Applied Physics Series*, **157**, 1-34.

Elo, S., L. Zhdanova, A. Chepik, L.J. Pesonen, N. Philippov and A. Shelemotov, 2000. Comparative geophysical description and modelling of Lappajärvi and Jänisjärvi impact structures, Fennoscandian shield (abstract). In: J. Plado and L.J. Pesonen (Ed.): *Meteorite impacts in Precambrian Shields, programme and abstracts of ESF workshop*, Geological Survey of Finland and University of Helsinki, Espoo, 35p.

Donadini F., J. Plado, S.C. Werner, J. Salminen, L.J. Pesonen and M. Lehtinen, 2006. New evidence for impact from the Suvasvesi South Structure, Central East Finland. In: C. Cockell, C. Koeberl and I. Gilmour (Ed.): *Biological processes associated with impact events*, Springer Verlag, Berlin, p. 287-307.

French, B.M. and C. Koeberl, 2010. The convincing identification of terrestrial meteorite impact structures: What works, what doesn't, and why. *Earth Sci. Rev.*, **98**, 123-170.

Huber, M., L. Ferrière, A. Losiak and C. Koeberl, 2011. ANIE: A mathematical algorithm for automated indexing of planar deformation features in quartz grains. *Meteoritics & Planetary Science*, **46**, 1418-1424.

Langenhorst, F., 2002. Shock metamorphism of some minerals: Basic introduction and microstructural observations. *Bulletin of the Czech Geological Survey*, **77**, 265-282.

Lehtinen, M., L.J. Pesonen, R. Puranen and A. Deutsch, 1996. Karikkoselkä - A new impact structure in Finland (abstract). *27th Lunar and Planetary Science Conference*, p. 739.

Lerssi, J., J. Mursu, M. Niskanen and H. Pajunen, 2007. Summasjärven johtavuusanomalian tutkimukset vuosina 2005 ja 2006. *Geological Survey of Finland, Report Q19/2243*, **2244/2007/1**, 28 p.

Ormö, J. and G. Blomqvist, 1996. Magnetic modelling as a tool in the evaluation of impact structures, with special reference to the Tvären Bay impact crater, SE Sweden. *Tectonophysics*, **262**, 291-300.

Pesonen L.J., S. Elo, M. Lehtinen, T. Jokinen, R. Puranen and L. Kivekäs, 1999. Lake Karikkoselkä impact structure, central Finland: New geophysical and petrographic results. *Geological Society of America Special Paper*, **339**, 131-147.

Plado J., S. Hietala, T. Kreitsmann, J. Lerssi, J. Nenonen and L.J. Pesonen, 2018. Summanen, a new meteorite impact structure in Central Finland. *Meteoritics & Planetary Science*, **53**, 2413-2426.

Stroeven A.P., C. Hättestrand, J. Kleman, J. Heyman, D. Fabel, O. Fredin, B.W. Goodfellow, J.M. Harbor, J.D. Jansen, L. Olsen, M.W. Caffee, D. Fink, J. Lundqvist, G.C. Rosqvist, B. Strömberg and K.N. Jansson, 2016. Deglaciation of Fennoscandia. *Quaternary Science Reviews*, **147**, 91-121.

YLEISÖLUENTO / PUBLIC LECTURE

Piensatelliittien vallankumous

J. Praks[1]

[1] Sähkötekniikan korkeakoulu, Aalto-yliopisto, jaan.praks@aalto.fi

Avaruustekniikan kehittäminen on perinteisesti vaatinut panostusta johon vain isoilla valtioilla on ollut varaa. Kallis rakettiteknologia on liittynyt läheisesti ohjusteknologiaan joten isot sotilasmahdit ovat tyypillisesti olleet avaruusmahteja jotka ovat kiivasti varjelleet omaa asiantuntemusta. Tekniikka on kuitenkin kehittynyt ja maailma muuttumassa. Avaruuden hyödyntäminen on avautumassa pikaista vauhtia pienemmille toimijoille, pääasiassa kaupallistuvan laukaisutoiminnan sekä miniatyrisoituvan satelliittiteknoilogian ansiosta. Molemmat kehitykset ovat merkittävästi alentaneet avaruuteen pääsyn kustannuksia ja lisänneet yhteistyötä. Nykyään rakennetaan pieniä satelliitteja joita voidaan viedä avaruuteen samalla raketilla jopa yli sata kerralla. Tämä satakertainen, paikoitelleen jopa monituhatkertainen hinnan alenemine onkin tuonut avaruuskentälle runsaasti uusia yrityksia ja uusia tutkimushankkeita. Muutos on merkittävä. Satelliitteja laukaistaan avaruuteen nykyään useita satoja, kohta jopa useita tuhansia vuodessa. Edullisista satelliiteista voidaan muodostaa laajoja verkostoja jotka mahdollistavat palveluja, joista ennen voitiin vain unelmoida. Kuvannollista on, että maailman suurimman kuvaussatelliittiverkoston missä on satoja satelliitteja, omistaa start-up yritys joka aloitti alle kymmen vuotta sitten Piilaakson autotallista. Useat uudet maat rakentavat nykyään avaruusohjelmia ja satelliitteja, tieteen, talouden ja puolustuskyvyn tueksi. Satelliittien määrä kasvaa nopeasti ja alemmat kiertoradat täyttyvät sekä kaupallistuvat nopeasti. Nopea kehitys tuo uusien mahdollisuuksien ohessa mukanaan myös uusia haasteita. Radiospektri täyttyy uusilla viesteillä, avaruusromu uhkaa uusia satelliitteja ja kilpailu aiheuttaa poliittisia kiistoja. Tämä kehitys tuo myös tieteelle valtavasti uusia mahdollisuuksia ja samalla uusia haasteita. Uusimman tieteen ja teknologian avulla voidaan taata että avaruus on käytettävissä tulevillakin sukupolvilla.

Lumiolosuhteiden moninaiset vaikutukset petojen aiheuttamiin porovahinkoihin Suomessa

S. Rasmus[1], J. Räihä[2] ja H. Norberg[3]

[1] Lapin yliopisto, Arktinen keskus, sirpa.rasmus@ulapland.fi
[2] Ilmatieteen laitos
[3] Suomen riistakeskus

Abstract
Reindeer management area covers approximately 36% of the Finnish land area. Both reindeer and reindeer management are well adapted to snowy conditions of Northern Finland, but nevertheless deep snow cover, late melt and especially icy snow cause difficulties. Snow conditions affect also the predation efficiency of large carnivores. In this work we discuss the practitioners' knowledge of reindeer herders on effects of snow conditions on predator-caused reindeer losses. We also analyze the local and regional snow conditions during winters when wolverine-caused reindeer damages have been high in the northern part of the reindeer management area of Finland.

1. JOHDANTO

Poronhoitoalue kattaa noin 36% Suomen pinta-alasta (Kuva 1). Ilmatieteen laitoksen 1981-2010 tilastojen mukaan lumipeitepäiviä on alueella vuodessa keskimäärin vähintään 175 eli lumi on oleellinen osa poronhoitoalueen ympäristöä suuren osan vuodesta. Porot ja poronhoito ovatkin hyvin sopeutuneet lumisiin olosuhteisiin. Syvä lumipeite, myöhäinen lumen sulaminen ja jääkerrokset lumessa aiheuttavat kuitenkin ongelmia porojen ravinnonsaannille ja johtavat vasamenetyksiin ja talvikuolleisuuteen (esim. Kumpula ja Colpaert, 2003; Norberg et al. 2005; Turunen et al. 2016). Suurpedot (ahma, ilves, karhu, susi) ovat aina aiheuttaneet poromenetyksiä ja muuta haittaa poronhoidolle (Turunen et al. 2017). Petojen aiheuttama haitta poroelinkeinolle ja porovahingot ovat olleet kasvussa 90-luvun alusta alkaen petokantojen kasvaessa rauhoitusten ja metsästysrajoitusten myötä (Kuva 2.). Myös talven sää- ja lumiolot vaikuttavan porojen riskiin jäädä petoeläinten saaliiksi (Tablado ym. 2014). Erityisesti ahman saalistustehokkuus riippuu paljolti lumiolosuhteista (Kojola et al. 2018). Kokemusperäisesti tiedetään syvän ja pehmeän lumen mahdollistavan ahman tehokkaan saalistuksen, kun poron liikkuminen vaikeutuu. Aiheesta on kuitenkin hyvin vähän tutkittua tietoa.
Tämä työn tavoitteena on

1) kerätä yhteen kokemusperäistä tietoa siitä miten lumiolosuhteet vaikuttavat petojen aiheuttamiin porovahinkoihin ja muuhun petojen aiheuttamaan haittaan poroelinkeinolle,
2) kuvailla petojen, erityisesti ahman aiheuttamien porovahinkojen vuosittaista vaihtelua,
3) tarkastella paikallisia ja alueellisia lumiolosuhteita niinä talvina, kun ahmavahingot ovat olleet suuria.

Tavoitteiden 1) ja 2) osalta keskitytään ajanjaksoon 1990-2015 ja Ylä-Lappiin (Kuva 1), missä petojen tappama poromäärä on ollut suurin muihin suuralueisiin verrattuna, ja missä ahma on ollut eniten vahinkoja aiheuttava peto.

2. MATERIAALI JA MENETELMÄT

Työssä käytettäviä aineistoja ovat:

1. Paliskuntien vuosittaiset toimintakertomukset. Suomen poronhoitoalue on jaettu 54 paliskuntaan (Kuva 1.). Vuodesta 1948 saakka paliskuntien on tullut laatia toimintakertomus poronhoitovuosittain.. Tarkastelemme toimintakertomusten mainintoja, jotka liittyivät petojen aiheuttamiin porovahinkoihin, vaikutuksiin poronhoitotöihin sekä petojen hävittämiseen tai niiden aiheuttamien porovahinkojen vähentämiseen. Toimintakertomusten alueellinen kattavuus on erittäin hyvä, ja vain satunnaisia kertomuksia puuttuu. Toimintakertomusten kirjoittamistyyli on toki vaihdellut paliskunnittain ja eri aikoina. Arkistoituja toimintakertomuksia säilytetään Oulun maakunta-arkistossa (vuoteen 1982 saakka) ja Paliskuntain yhdistyksen arkistossa Rovaniemellä (vuodesta 1982 eteenpäin).
2. Paliskuntien vuosittain raportoimat eri petojen tappamien, löytyneiden ja valtion varoista korvattujen porojen lukumäärät. Tilastojen lähteenä on Paliskuntain yhdistys. Keskitymme tässä kasvavien petokantojen aikaan eli vuosiin 1990-2015.
3. Suuria ahmavahinkoja havaittiin talvina 1999-2000, 2011-2012 sekä 2012-2013. Tutkimuksessa tarkastelemme näiden talvien lumiolosuhteita Ylä-Lapissa käyttäen aineistona Ilmatieteen laitoksen säähavaintoasemien pitkän ajan lumensyvyystietoja (Saariselkä, Nellim, Ivalo, Kilpisjärvi, Alamuonio, Pokka), näiden pohjalta tehtyjä SNOWPACK –mallin simulaatiotuloksia lumen rakenteesta (mallinnuksesta esim. Rasmus et at., 2016) sekä tuoretta hila-aineistoa, joka mahdollistaa lumi- ja sääolojen tarkastelun alueellisesti ja ajallisesti yhteneväisesti koko poronhoitoalueella (Aalto et al., 2016).

Kuva 1: Poronhoitoalueen paliskunnat (ohut viiva) ja poronhoidon suuralueet (paksu viiva; muokattu julkaisusta Danell ja Norberg (2010). Kyrön ja Pohjois-Sallan paliskunnat ovat Ylä-Lapin rajanaapureita. Kyrö on Länsiosan ja Pohjois-Salla Itä-Lapin pohjoisin paliskunta.

3. TULOKSIA

Ylä-Lapissa ahman aiheuttamat vahingot hallitsevat vaihdellen voimakkaasti eri vuosina (Kuva 2). Lisäksi maasuurpedot vaikuttavat moninaisesti poroihin ja poronhoitotöihin. Porojen kokoaminen ja erotustyöt vaikeutuvat, paimennus vaikeutuu porojen hajaantuessa, porojen talvehtiminen ja kaivuu häiriintyy, vasonta häiriintyy ja vaatimet luovat vasoja, tulee tarvetta talvitarhaukseen tai tiettyjen laidunalueitten välttämiseen. Paimennusta ja valvontaa tarvitaan lisää. Suurpetojen tappamien porojen etsimisestä aiheutuu paljon ylimääräistä työtä ja kuluja Välillisiä tappioita syntyy siitosporojen menettämisen ja harkitun kannanjalostuksen vaikeutumisen kautta (Kumpula et al. 2017).

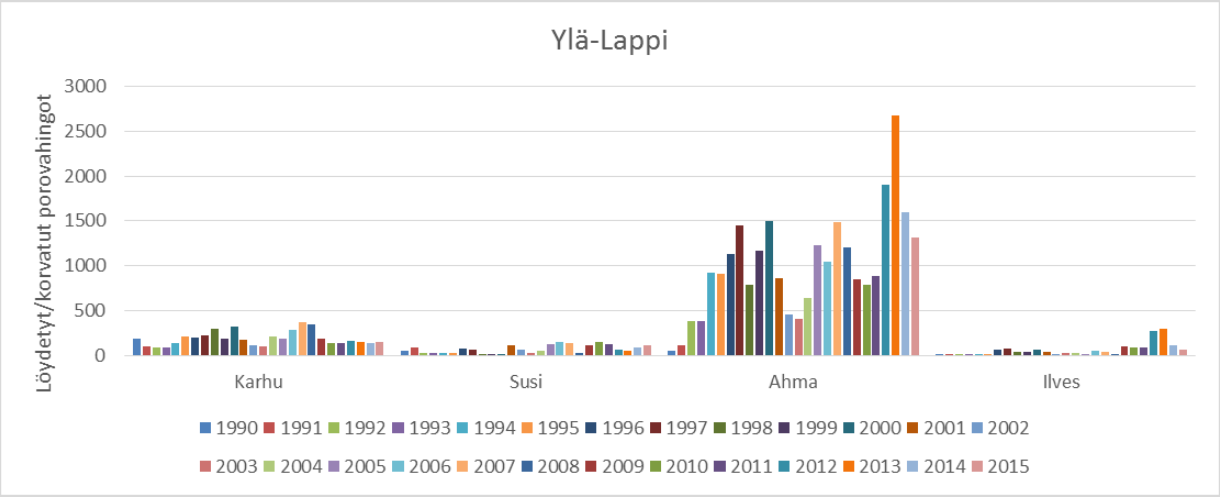

Kuva 2: Ylä-Lapissa löydetyt ja korvatut petojen aiheuttamat porovahingot vuosittain (Lähde: Paliskuntain yhdistys).

Poronhoitajien kokemuksen mukaan tietyt lumiolosuhteet lisäävät petojen saalistustehoa. Syynä voi olla se, että porot ovat jo valmiiksi heikkokuntoisia ja/tai hajallaan esim. maajään vuoksi: *Porojen jouduttua leviämään huonon pohjan takia lupolle, tappoivat ahmat niitä aika paljon* (1962/63, Oraniemi). Syynä voi olla sekin,että syvässä lumessa porojen liikkuminen on esimerkiksi ahman liikkumista hankalampaa tai että lumen pinnassa on ohut ahmaa kantava kerros, joka ei kuitenkaan kanna poroa: *Ahmat saalistivat runsaasti olosuhteiden ollessa suotuisat, poroille revä vaarallinen ja petovahinkoja tuli noin 400 kappaletta* (2015/16, Muotkatunturi). Petovahinkojen minimoimiseksi tehtyä paimennusta tai valvontaa voi myös olla vaikea toteuttaa tietyissä lumioloissa. Paliskuntien kokemuksen mukaan suotuisat lumiolosuhteet ovat olleet välttämättömiä petojen jäljityksessä ja hävittämisessä: *Susien metsästys on onnistunut kohtalaisen hyvin syksyllä lumijäljillä* (1978/79, Salla). Toisaalta lumen puute tai vääränlaiset lumiolosuhteet ovat aiheuttaneet ongelmia, jos tavoitteena on ollut petojen jäljitys ja hävitys: *Susi liikkui syksyllä, mutta kun maa oli sulana ei sitä voitu seurata* (1959/60, Pintamo); *Ahmaa koetetiin pyydystää, mutta kovan hangen vuoksi oli jäljillä pysyminen mahdotonta* (1973/74, Halla). Petovahinkokorvausten saamiseksi on petovahinkojen löytäminen maastosta käynyt entistä tärkeämmäksi. Tätäkin vaikeuttaa lumettomuus, raadot peittävä lumi tai maastossa liikkumista vaikeuttavat lumiolosuhteet.

KIITOKSET

Sirpa Rasmus on tehnyt tutkimusta NordForsk –rahoitetussa Pohjoismaisessa huippututkimusyksikössä ReiGN (”Reindeer husbandry in a Globalizing North”). Arvokkaasta yhteistyöstä kiitämme Paliskuntain yhdistystä ja tutkimuspaliskuntia.

LÄHTEET

Aalto, J., P. Pirinen, ja K. Jylhä, 2016. New gridded daily climatology of Finland: Permutation-based uncertainty estimates and temporal trends in climate. *J. Geophys. Res. Atmos.*, **121**, 3807-3823.

Danell, K. ja H. Norberg, 2010: Petoeläintilanteen ja liikennevahinkojen vaikutukset Suomen porotalouden teurasmääriin vuosina 2005/6-2008/9. *Poromies* **6**, 15-21.

Kojola, I., S. Heikkinen ja S. Kaartinen, 2018. Suurpetojen vaikutus poronhoitoon. *Luonnonvara- ja biotalouden tutkimus* 57. Luonnonvarakeskus, Helsinki.

Kumpula, J. ja A. Colpaert, 2003. Effects of weather and snow conditions on reproduction and survival of semi-domesticated reindeer (R. t. tarandus). *Polar Research*, **22**, 225-233.

Kumpula, J., A.-J. Pekkarinen, O. Tahvonen, J. Siitari ja H. Törmälehto, H, 2017. Petoeläinten vaikutukset porotalouden tuottavuuteen, tuloihin ja taloudelliseen kestävyyteen. *Luonnonvara- ja biotalouden tutkimus* 12. Luonnonvarakeskus, Helsinki.

Norberg, H., Nieminen, M., Kumpula, J., Kojola, I., & Maijala, V. 2005: Yhteenveto vasatutkimuksista Suomen poronhoitoalueella vuosina 1997–2004. Riista- ja kalatalouden tutkimuslaitos. Tutkimusraportti. 65 s.

Rasmus, S., S. Kivinen, M. Bavay ja J. Heiskanen, 2016. Local and regional variability in snow conditions in northern Finland: a reindeer herding perspective. *Ambio*, **45**, 398-414.

Tablado, Z., P. Fauchald, G. Mabille, A. Stien and T. Tveraa, 2014. Environmental variation as a driver of predator-prey interactions. *Ecosphere* **5(12)**, 164.

Turunen, M., S. Rasmus, M. Bavay, K. Ruosteenoja ja J. Heiskanen, 2016. Coping with increasingly difficult weather and snow conditions: Reindeer herders’ views on climate change impacts and coping strategies. *Climate Risk Management*, **11**, 15-36.

Turunen, M., S. Rasmus, H. Norberg, J. Kumpula, I. Kojola ja T. Ollila, 2017. Porot ja pedot – kuinka poronhoidon sopeutuminen petoihin on muuttunut 90 vuodessa? *Suomen Riista*, **63**, 19-42.

Ilmastokasvatus – riittääkö geofysiikan näkökulma?

I. Ratinen[1]

[1] Kasvatustieteiden tiedekunta, Lapin yliopisto, ilkka.ratinen@ulapland.fi

Ilmastonmuutos on yksi aikamme kiharaisimmista ongelmista. Tuoreimman IPCC:n arviointiraportin perusteella meidän tulisi rajoittaa maapallon keskilämpötilan nousu korkeintaan 1,5 asteeseen. Rajoitus merkitsee Suomen ilmastopaneelin laskelmien mukaan Suomen osalta vuoteen 2035 mennessä saavutettavaa hiilineuraalisuutta eli päästöjen ja nielujen samaa kokoa. Edessä on valtavasti haasteita. Päätöksenteon tueksi ja ongelmien ratkaisemiseksi tarvitaan kaikkien kansalaisten ilmastokasvatusta. Pohdin esityksessä, että mitkä ovat ilmastokasvatuksen mahdollisuudet.

Itäisen Suomenlahden GNSS-mittaukset

T. Saari[1], M. Bilker-Koivula[1], H. Koivula[1], S. Lahtinen[1] ja P. Häkli[1]

[1] Geodesian ja Geodynamiikan osasto, Paikkatietokeskus, Maanmittauslaitos,
timo.saari@maanmittauslaitos.fi

Abstract

Traditionally, geoid models have been validated with GNSS-levelling benchmarks (including precise levelling and GNSS measurements) – only on land. In this research, we present a marine-GNSS campaign that studied the possibilities for validating geoid models at sea areas. The campaign was carried out with the marine geology research vessel Geomari (operated by the Geological Survey of Finland), which sailed back and forth the eastern part of the Finnish territorial waters at the Gulf of Finland during the early summer (21–25.5.) of 2018. Based on the promising results of the Geomari campaign, it is possible to recover geoid heights from GNSS observations at sea, with the accuracy of few centimetres. The resulted geoid height differences have revealed differences between geoid models (FIN2005N00 and NKG2015), thus proving the method valuable for validating existing geoid models.

1. JOHDANTO

Perinteisesti korkeudet ilmoitetaan suhteessa keskimerenpintaan, eli ns. nollatasoon. GNSS-havainnoissa korkeudet ilmaisevat korkeuden vertausellipsoidista, joka on matemaattisesti mallinnettu Maan geometrinen muoto, jolla ei ole fysikaalista merkitystä eikä yhteyttä merenpintaan – ts. ei sisällä tietoa mihin suuntaan vesi virtaa. GNSS-korkeudet saadaan sidottua fysikaaliseen Maahan geoidimallin avulla. Geoidilla kuvataan pintaa, johon merenpinnat asettuisivat ilman vaikuttavien voimien (Coriolis- ja vuorovesi-ilmiöt, ilmanpaine, lämpötila, tuulet, aallokot, vedensyvyys sekä painovoima) vaikutuksia (Kuva 1, oikea).

Alkukesästä 2018 (21–25.5.2018) Geologian tutkimuskeskuksen (GTK) merigeologinen tutkimusalus Geomari (Kuva 1, vasen) aloitti mittauskampanjan Itäisellä Suomenlahdella. Geomarin keulahytin katolle oli asennettuina ennalta määritetyille paikoilleen kolme GNSS-antennia: paapuurin ja tyyrpuurin puolelle sekä katamaraanin keskilinjalle. Keskimmäinen antenneista oli kytkettynä inertiamittausyksikköön (Inertial Measurement Unit, IMU), mikä havaitsee laivan akselien (nyökkääminen, kallistuminen, kääntyminen, aaltoilu) liikkeitä, joita aiheuttavat vallitsevat meriolosuhteet.

Kampanjan tavoitteena oli tutkia geoidimallien validointimahdollisuuksia merialueilla, joilla mallien tarkkuuksia ei pystytä tavanomaisin menetelmin (tarkkavaaitus ja GNSS-mittaukset) tutkimaan. Aluksi havainnot siirretään GNSS-antennista IMUn sensoripisteeseen, josta tarkoilla sidosmittauksilla vallitsevaan merenpintaan. Seuraavaksi havainnoista vähennetään

vallitsevan meritopografian vaikutus, jonka jälkeen, ainakin teoriassa, laivan katolta suoritetut GNSS-havainnot ovat geoidin pinnalla ja valmiina vertailuun geoidimallien kanssa.

Kuva 1: GTK:n tutkimusalus Geomari sekä tutkimuksessa käytettävät referenssikorkeudet.

2. GNSS-HAVAINNOISTA MERENPINTAAN – MERENPINNASTA NOLLATASOON

GNSS-havainnot lasketaan jälkilaskennassa haluttuun koordinaatistoon sekä mittaus-epookkiin, IGS14 (2018.39315), pysyvien GNSS-asemien avulla. Laskenta suoritettiin jokaiselle päivälle erikseen Inertial Explorer 8.60 ohjelmalla. Lopuksi havainnot siirretään koordinaattimuunnoksilla koordinaattijärjestelmiin, joihin vertailtavina olevat geoidimallit ovat määritetty (Häkli et al. 2016):

- FIN2005N00, ETRF96 (epookki 1997.0)
- NKG2015, ETRF2000 (epookki 2000.0).

Kun tarkat IMUn sensoripisteeseen koordinaatit ovat laskettuina haluttuun koordinaatti-järjestelmään, havainnot siirretään merenpintaan seuraavien reduktioiden avulla:

- katamaraanin ns. ”aaltoliike”, eli huojuntaliike
- kääntyminen poikkiakselin (nyökkääminen, engl. pitch) tai pituusakselin (kallistuminen, engl. roll) suhteen
- kokonaiskorjaus, eli IMUn sensorikorkeuden ja merenpinnan välinen korkeusero
- katamaraanin syväyksen muutos nopeuden suhteen, eli ns. squat-ilmiö.

Geomari ajoi havaintolinjoja tasaisella 5 solmun nopeudella. Satamiin tulojen sekä lähtöjen yhteyksissä mitattiin syväykset laivan kulmista. Havaintoviikolla merenkäynti oli erittäin vähäistä, minkä johdosta aluksen aaltomainen ylösalainen liike oli enimmäkseen alle 1 cm. Samasta syystä akselien korjaukset olivat alle 1 mm. Kokonaiskorjaus vaihteli viikon aikana 2.46–2.48 m välillä, mikä viittaa siihen, että katamaraanin syväys ei muuttunut massojen muutoksesta (polttoaineen väheneminen yms.) juuri lainkaan kampanjan aikana.

Squat-ilmiöllä tarkoitetaan virtausdynamiikan ilmiötä, missä suhteellisen matalissa vesistöissä tietyllä nopeudella kulkeva alus aiheuttaa allensa heikentyneen hydrostaattisen paineen, minkä johdosta alus painautuu hieman lähemmäksi merenpohjaa. Geomarille kyseistä arvoa ei ollut ennalta määritetty, joten määritimme sen itse laskentamenetelmällä (Barrass, 2004), jonka mukaan Geomarin squat-arvo on viiden solmun nopeudessa 1 cm.

Jotta merenpinnassa olevat havainnot saadaan redusoitua nollatasoon, havaintokorkeuksista poistetaan vallitseva meritopografia, jonka mallinnukseen käytettiin kahta eri menetelmää:

- Suomen ja Viron mareografeista (Kuva 2) interpoloitua pintaa, TG
- TG-pinnalla korjattua Itämeren fysikaalista mallia (CMEMS, 2018), PM.

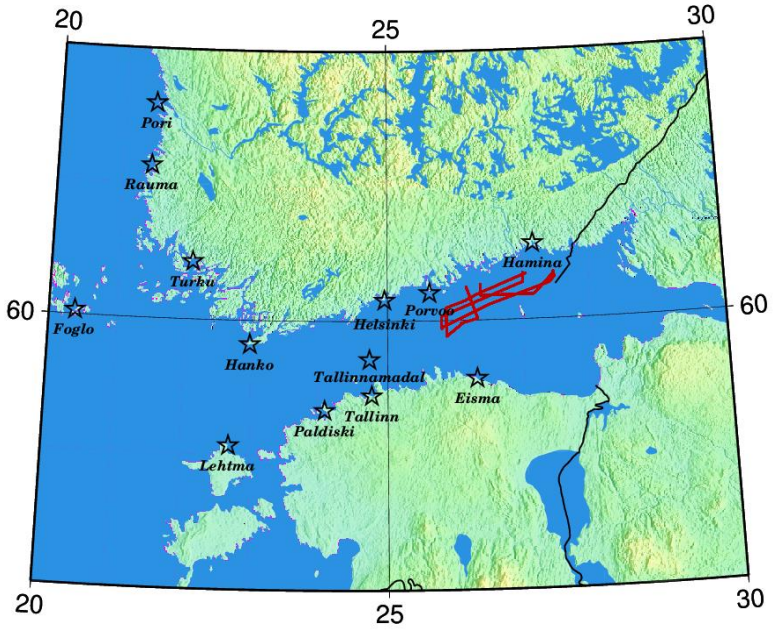

Kuva 2: Meritopografian määritykseen käytetyt Suomen ja Viron mareografit.

3. VERTAILU GEOIDIMALLEIHIN

Meritopografian poistamisen jälkeen havainnot ovat teoriassa lepäävän keskimerenpinnan tasossa – geoidin pinnalla. Seuraavaksi vertailemme tuloksia geoidimalleista saatuihin korkeuksiin, dN:

$$dN = N_{GNSS} - N_{geoidimalli}$$

Vertailussa käytettiin kahta eri mallia: Suomen virallista geoidimallia FIN2005N00 (Bilker-Koivula, 2010) sekä korkearesoluutioista Pohjoismaiden sekä Baltian alueen geoidimallia NKG2015 (Ågren et al., 2016). Yksityiskohtainen vertailu GNSS-kampanjan tuloksista on esitetty Taulukossa 1.

Taulukko 1. GNSS-kampanjan ja geoidimallien väliset korkeuserot.

DOY 141–145	Mareografit, TG (cm)				Fysikaalinen malli, PM (cm)			
	FIN2005N00		NKG2015		FIN2005N00		NKG2015	
	Mean	Std.	Mean	Std.	Mean	Std.	Mean	Std.
Maanantai	5.2	4.1	15.6	4.6	4.6	4.1	15.0	4.6
Tiistai	-3.8	5.7	6.3	6.7	-4.9	5.7	5.2	6.8
Keskiviikko	3.4	3.1	11.6	3.6	2.9	3.1	11.2	3.8
Torstai	7.4	4.3	14.3	4.7	7.5	4.7	14.5	5.2
Perjantai	-5.1	3.7	4.5	4.6	-5.6	3.5	4.1	4.2

Taulukosta 1 nähdään, että GNSS-havainnoilla saatiin määriteltyä geoidikorkeuksia keskimäärin 3–5 cm tarkkuudella geoidimallien suhteen. Geoidimallien välillä huomataan lisäksi yllättäviä eroavaisuuksia, sillä FIN2005N00-malli antaa kampanjan suhteen hieman tarkemmat tulokset, vaikka NKG2015-malli on Suomen alueella todistetusti tarkempi (Saari & Bilker-Koivula, 2017). Todennäköisesti eroavaisuudet johtuvat malleissa käytetyistä painovoima-aineistoista, jotka ovat Venäjän alueelta hieman erilaiset.

6. YHTEENVETO

Geomarin GNSS-kampanjan tavoitteena oli tutkia geoidimallien validoimista merialueilla, joilla mallien tarkkuuksia ei pystytä tavanomaisin menetelmin (tarkkavaaitus ja GNSS-mittaukset) tutkimaan. Vertailut geoidimalleihin suoritettiin keskimäärin 3–5 cm tarkkuudella, mikä on varsin lupaava tulos, sillä ne sisältävät myös geoidimalleissa esiintyvät epävarmuudet. Lupaavien tuloksien pohjalta voidaan todeta, että menetelmä soveltuu geoidimallien validoimiseen sekä niiden eroavaisuuksien ja heikkouksien selvittämiseen.

KIITOKSET

Tekijät esittävät lämpimät kiitoksensa kaikille Geomarilla työskennelleille GTK:n henkilöille, joita ilman kyseistä tutkimusta nykyisessä muodossaan ei olisi ollut mahdollista toteuttaa.

Tutkimus on ollut osana FAMOS (Odin 2016–2018) projektia, mikä on ollut Euroopan Unionin ”Connecting Europe Facility (CEF) for Transport” -rahaston osarahoittama projekti.

LÄHTEET

Barrass, C.B., 2004. Ship Design and Performance for Masters and Mates, *Elsevier Butterworth-Heinemann*, London, 2004.

Bilker-Koivula, M., 2010. Development of the Finnish height conversion surface FIN2005N00, *Nordic Journal of Surveying and Real Estate Research*, 7(1), 76-88.

CMEMS (Copernicus Marine Environment Monitoring Service), 2018. Ocean Products, 29.10.2018, http://marine.copernicus.eu/services-portfolio/access-to-products/.

Häkli, P., M. Lidberg, L. Jivall, T. Nørbech, O. Tangen, M. Weber, P. Pihlak, I. Aleksejenko ja E. Paršeliūnas, 2016. The NKG2008 GPS campaign–final transformation results and a new common Nordic reference frame. *Journal of Geodetic Science*, **6(1)**, 1-33.

Saari, T. ja M. Bilker-Koivula, 2017. Applying the GOCE-based GGMs for the quasi-geoid modelling of Finland. *Journal of Applied Geodesy*, **12(1)**, 15-27, doi:10.1515/jag-2017-0020.

Ågren, J., G. Strykowski, M. Bilker-Koivula, O. Omang, S. Märdla, R. Forsberg, A. Ellmann, T. Oja, I. Liepiņš ja E. Paršeliūnas, 2016. The NKG2015 gravimetric geoid model for the Nordic-Baltic region, *Gravity, Geoid and Height Systems (GGHS) 2016*, September 19–23, Thessaloniki, Greece.

Effects of energetic electron precipitation and quasi-biennial oscillation on the northern polar vortex

A. Salminen[1], **T. Asikainen**[1], **V. Maliniemi**[1,2] **and K. Mursula**[1]

[1] ReSoLVE Centre of Excellence, Space Climate Research Unit, University of Oulu, Finland, antti.salminen@oulu.fi
[2] Birkeland Centre for Space Science, Department of Physics and Technology, University of Bergen, Norway

Abstract

Solar wind accelerates energetic particles in the Earth's magnetosphere that partly precipitate into the atmosphere. Energetic electron precipitation (EEP) maximises in the high-latitude mesosphere and stratosphere. Earlier studies have shown that increased EEP activity in the northern hemisphere is associated with a stronger polar vortex, a westerly wind surrounding the polar stratosphere during the winter. This EEP effect on the polar vortex is found to be modulated by the quasi-biennial oscillation (QBO), an alternating wind system in the equatorial stratosphere. However, mechanisms behind the EEP effect and its modulation by QBO are still partly unresolved. In this study we examine the EEP effect on the northern polar vortex and how the QBO modulates it. We show that the EEP effect on northern polar vortex is stronger and more significant in the easterly QBO phase than in the westerly phase. We also show that the QBO modulates meridional circulation in the northern winter hemisphere, which suggests that the QBO modulation of the EEP effect is mediated via meridional circulation.

1. INTRODUCTION

Electrons from the Earth's magnetosphere are the most common type of particles precipitating into the Earth's atmosphere. These electrons are energised in the interactions between the magnetosphere and solar wind, the plasma escaping from the solar corona. Energetic electron precipitation (EEP) is most intense at high-latitudes, around the auroral oval, and penetrates to the mesosphere and upper stratosphere, corresponding to the altitudes of 40-100 km. There EEP forms odd nitrogen oxide molecules, NOx, which are chemically reactive and deplete ozone catalytically. Although the direct EEP effect is mostly limited to the mesosphere, the EEP-NOx molecules can descend down to the stratosphere in the polar darkness during winter (Funke et al., 2005). This indirect EEP effect can significantly affect the dynamical state of the stratosphere by depleting ozone in the main ozone layer.

Polar stratosphere cools in the absence of solar UV radiation during the winter. The temperature difference between the high- and mid-latitudes induces a strong westerly wind jet, the

so-called polar vortex. Earlier studies (e.g., Rozanov et al., 2005; Seppälä et al., 2013) have shown that high EEP activity is associated with decreased ozone, modified temperatures and a strengthening of polar vortex in the northern wintertime stratosphere. This EEP effect propagates to the troposphere and surface, where it affects, e.g., the Northern Annular Mode (NAM) weather pattern (Maliniemi et al., 2013). However, the mechanism behind the EEP effect and its development in the atmosphere are not well-known. Furthermore, the EEP effect on polar vortex is found to be modulated by internal atmospheric variability. The quasi-biennial oscillation (QBO), a wind mode in the equatorial stratosphere, has been found to modulate the strength of the EEP effect on the polar vortex (Maliniemi et al., 2013; Seppälä et al., 2013), but the mechanism behind this modulation has not been resolved.

2. DATA AND METHODS

We used measurements of precipitating electrons by the MEPED instrument onboard POES satellites to quantify the EEP fluxes. These satellites have been operated since 1979 and they orbit the Earth at 800-900 km altitude. We used electron fluxes corrected by Asikainen and Mursula (2013). As atmospheric variables, we used ERA-Interim reanalysis data of ozone mass mixing ratio, temperature and zonal wind. The ERA-Interim provides global coverage of these variables at 37 pressure levels from the surface to the upper stratosphere (at 1 hPa altitude). We used zonally averaged values of the atmospheric variables.

We calculated linear regressions in which EEP is the explaining variable and one of the atmospheric variables is the response variable at a turn. We studied the four northern winter months (December-March) of years 1979-2016. Data are firstly monthly averaged and detrended by a 31-year running mean filter. To calculate linear regressions, we used the Cochrane-Orcutt method (Cochrane and Orcutt, 1949), which models the residual term as an autoregressive AR(1) process. In this way the significance of the results can be estimated reliably. Regressions were calculated separately for each latitude-pressure level grid box. Slopes of regression were multiplied with one standard deviation of the EEP time-series to estimate the response in the corresponding atmospheric variable. We excluded two winters after large volcanic eruptions (winters 1982/1983 and 1991/1992) and two winters with exceptionally early and strong stratospheric sudden warming (winters 1984/1985 and 2003/2004).

3. RESULTS

Figure 1 shows the calculated EEP responses on zonal wind, temperature and ozone mass mixing ratio separately in the four months (December-March). Increased EEP activity strengthens the polar vortex (positive zonal wind at the high-latitudes), cools the lower stratosphere and decreases ozone in the lower stratosphere in every winter month. Additionally, increased EEP leads to a warming and ozone decrease in the upper stratosphere in February and March. During polar winter, in the absence of solar UV radiation, the ozone acts as a radiative cooler in the upper stratosphere and mesosphere. Thus, its depletion by EEP-NOx warms the upper strato-

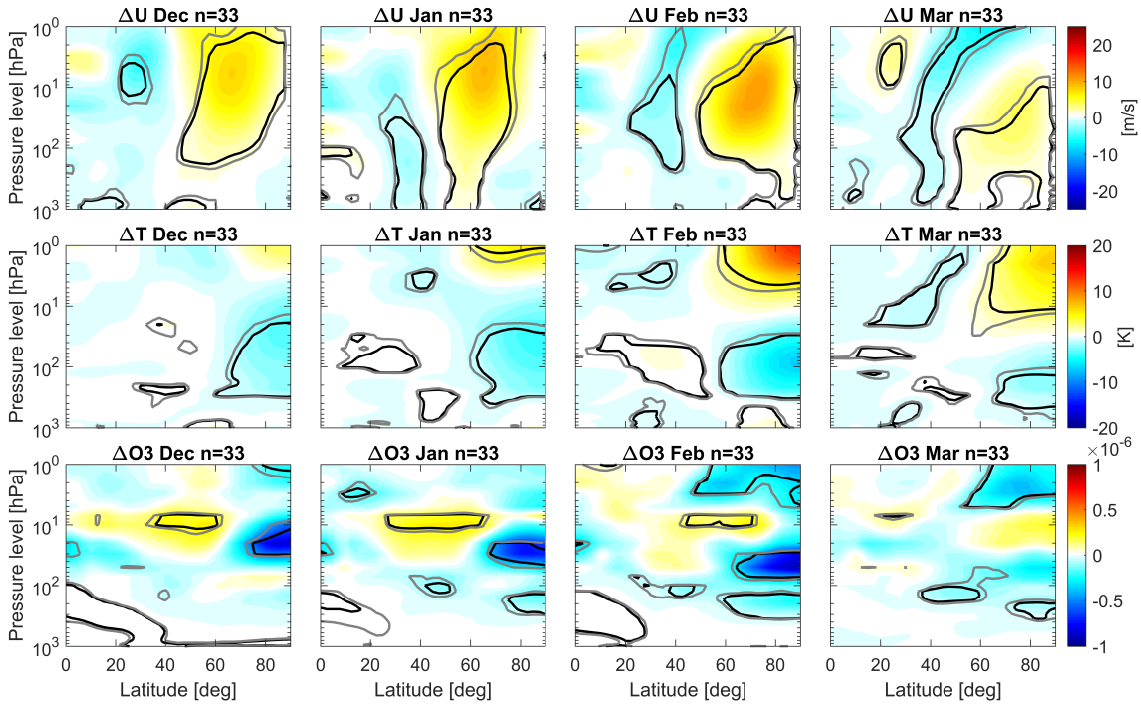

Figure 1: EEP responses on zonal wind (1. row), temperature (2. row) and ozone mass mixing ratio (3. row) in December-March (1.-4. columns). Black contours correspond to 95% significance level and grey contours to 90% level.

sphere and mesosphere, as is seen in February and March. (We note that this ozone-depletion related warming takes place even in early winter but slightly higher, and is therefore not visible in the ERA-Interim data that are limited to below 1hPa). This warming affects the dynamics of the stratosphere so that the polar vortex is increased below the warming region. Moreover, the meridional circulation toward the pole, the so-called Brewer-Dobson circulation (BDC), is weakened by the stronger vortex. Since the BDC transports ozone from the equator poleward and adiabatically warms the polar stratosphere, its weakening decreases the ozone and lowers the temperature in the lower stratosphere, as seen in Figure 1.

Figure 2 shows the EEP effect to the zonal wind in the four months, but now calculated separately in the two QBO phases. The effect is stronger and more significant in the easterly phase of QBO than in the westerly phase, especially in February and March. We found that this difference in the EEP effect to polar vortex between the two QBO phases is largest, if the QBO phase is indeed determined about 6 months earlier, i.e., using its summertime values. Therefore the QBO was determined in Figure 2 with a 6-month lag. We have also found that the ozone mass mixing ratio in the polar lower stratosphere is significantly higher in winter months in the easterly phase than in the westerly phase if the QBO is lagged by roughly 6 months (not shown here). Since the amount of ozone in the wintertime polar stratosphere is mostly controlled by the BDC, this difference indicates that the BDC is stronger in the 6-month lagged QBO easterly phase than in the westerly phase. This is in agreement with the equatorial branch of the northernly BDC being strongest in northern summertime. Since the EEP effect in the lower stratosphere is a dynamical response to the initial ozone loss and warming in the upper

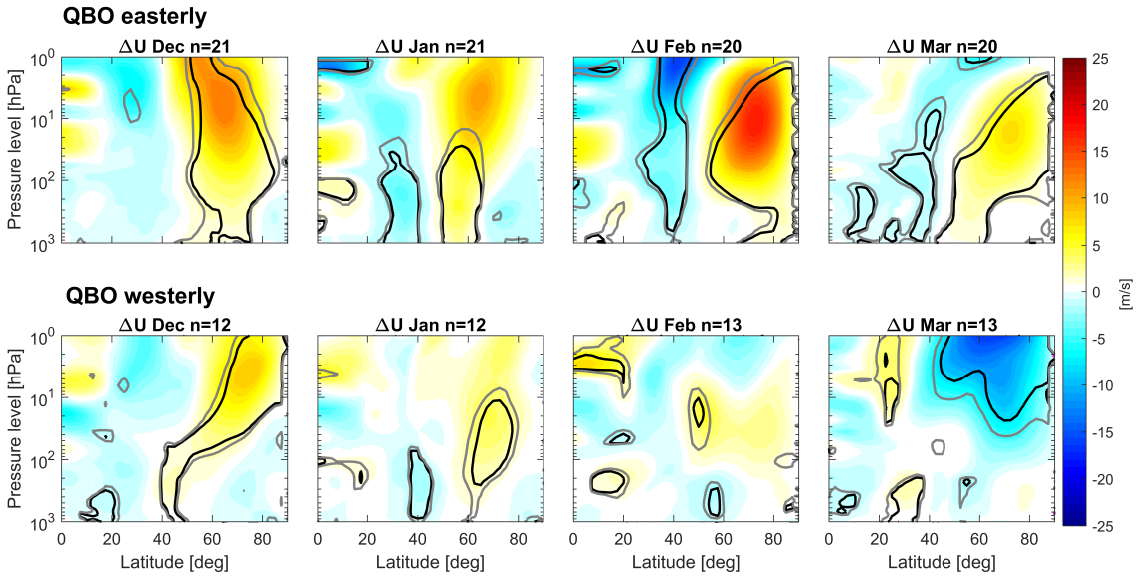

Figure 2: EEP responses on zonal wind in December-March separately in the QBO easterly (top row) and westerly (bottom row) phase. QBO is determined with a 6-month lag. Black contours correspond to 95% significance level and grey contours to 90% level.

stratosphere and mesosphere, it seems that a stronger meridional circulation (in the lagged QBO easterly phase) establishes a stronger EEP effect.

LÄHTEET

Asikainen, T., and K. Mursula (2013), Correcting the NOAA/MEPED energetic electron fluxes for detector efficiency and proton contamination, *J. Geophys. Res. Space*, *118*(10), 6500–6510.

Cochrane, D., and G. H. Orcutt (1949), Application of least squares regression to relationships containing auto-correlated error terms, *J. Am. Stat. Assoc.*, *44*(245), 32–61.

Funke, B., M. López-Puertas, S. Gil-López, T. Von Clarmann, G. Stiller, H. Fischer, and S. Kellmann (2005), Downward transport of upper atmospheric NOx into the polar stratosphere and lower mesosphere during the Antarctic 2003 and Arctic 2002/2003 winters, *J. Geophys. Res.: Atmos.*, *110*(D24).

Maliniemi, V., T. Asikainen, K. Mursula, and A. Seppälä (2013), QBO-dependent relation between electron precipitation and wintertime surface temperature, *J. Geophys. Res.: Atmos.*, *118*(12), 6302–6310.

Rozanov, E., L. Callis, M. Schlesinger, F. Yang, N. Andronova, and V. Zubov (2005), Atmospheric response to NOy source due to energetic electron precipitation, *Geophys. Res. Lett.*, *32*(14).

Seppälä, A., H. Lu, M. Clilverd, and C. Rodger (2013), Geomagnetic activity signatures in wintertime stratosphere wind, temperature, and wave response, *J. Geophys. Res.: Atmos.*, *118*(5), 2169–2183.

Data-driven Modelling for Wind Fields Over Lakes

T. Shuku[1], J. Ropponen[2], J. Juntunen[2], H. Suito[3], and T. Huttula[2]

[1] Graduate School of Environmental and Life Science, Okayama University,
shuku@cc.okayama-u.ac.jp
[2] Freshwater Centre, Finnish Environment Institute
[3] Advanced Institute for Materials Research, Tohoku University

Abstract

This study presents data-driven modelling for local wind fields over two small lakes in Jyväskylä, Finland. We built simple statistical regression models for wind speed and direction based on the spatially sparse data. We compared the model predictions of local wind speed and directions with the corresponding observation data, and the predictions agree well with the observation data.

1. INTRODUCTION

Dynamics of lake ecosystem are dependent on the circulation and diffusion processes, and these processes are dominantly influenced by wind shear stress particularly in shallow lakes. Spatial distribution of wind shear stress over lakes need to be estimated accurately to evaluate lake environment. In many applications, however, the local wind fields over lakes are usually considered to be spatially homogeneous for simplicity though the importance of spatial wind distribution is widely recognized. Although the computational fluid dynamics (CFD) models can be used in order to consider the spatial variation of the wind shear stress, there still remain some problems in practical application. The problems include computational cost, how to determine the input parameters, and how to define initial/boundary conditions. Recently data-driven modelling has had much attention because of developing the methodologies of machine learning and how to handle large amount of data. There have been many studies on data-driven modeling for wind fields (Robert et al. 2013; Bessac et al. 2015; Torma and Kramer 2017). This study presents a simplified data-drive modelling for estimating local wind fields over lakes. The target lakes in this study are Palokkajärvi and Tuomiojärvi which are located in the northern part of Jyväskylä, Finland (Figure 1). Five transient monitoring stations observing wind speed/direction were installed around two lakes during summer time in 2015 and 2016. In addition to the local station data, Tikkakoski official station is also available for the modelling. We attempted to build a data-driven model for estimating local wind fields over two lakes using only official station data.

2. TARGET LAKES AND OBSERVATION DATA

Figure 2 shows the wind speed and direction observed in 16th July – 11th October 2015. This study used observation data in 2015 for the modelling and 2016 only for the model validation.

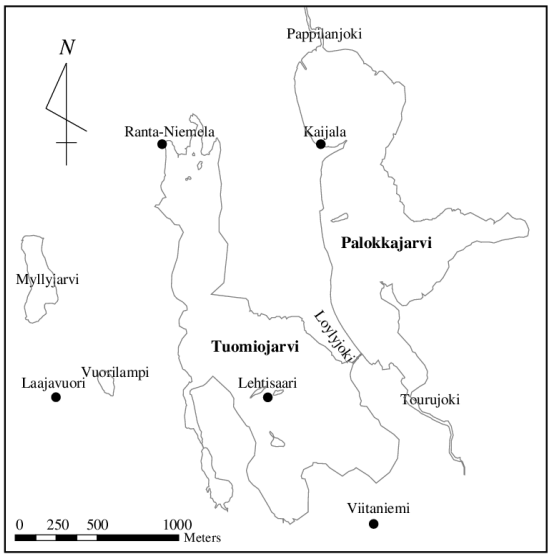

Figure 1: Target lakes and local observation.

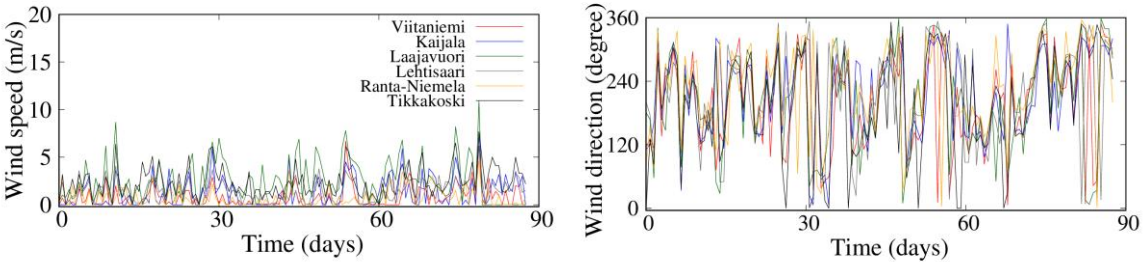

Figure 2: Observed wind speed and direction in 2015.

First, we examined the correlations between wind speed and direction by using the correlation coefficient defined by Johnson and Wherly (1977). Let Y' = (Y_1, Y_2, Y_3) = (cosθ, sinθ, *v*), and let s_{ij} be the sample covariance between Y_i and Y_j. Then the required canonical correlation coefficient between (cosθ, sinθ) and *v* is shown to be the positive square root of

$$r_{AL}^2 = \frac{s_{11}s_{23}^2 + s_{22}s_{13}^2 - 2s_{12}s_{23}s_{31}}{s_{33}(s_{11}s_{22} - s_{12}^2)} \quad (1)$$

The calculated correlation coefficients for all the data are less than 0.1, and these results indicate that there is no strong correlation between wind speed and direction in the data, and two variables can be independently modeled.

3. DATA DRIVEN MODELING

On the wind speed, we found that two characteristics in the data, which are 1) identical periodical cycles can be observed, 2) wind speed is proportional to the elevation of the monitoring stations. Based on these two facts, we attempted to make a simple regression model for estimating local wind speed using only official station data. Since the periodical characteristic of local wind data is identical to that of official Tikkakoski station, we assume that the wind speed in local wind fields can be simply expressed by

$$v_t^{(i)} = \alpha_t^{(i)} v_t^{o} \tag{2}$$

where, $\alpha_t^{(i)}$ is the adjusting parameter for local station (i) at time t. We calculated the adjusting parameters for all the time step of all the data and built a regression model for the elevation of the monitoring stations z(m) (Figure 3).

$$\log_{10} \alpha(z) = 0.0044z - 1.2439 + \varepsilon_\alpha \tag{3}$$

where ε_α is model error following normal distribution.

On the wind directions, we found that the wind directions at local stations strongly correlates that of official stations, and simple models can be applied to the data. Downs and Mardia (2002) proposed the following regression model for circular variables, and we simply used this for the direction modeling.

$$\mu = \beta + 2\text{atan}\left\{\omega \tan(\theta - \alpha)/2\right\} + \varepsilon_{\text{cir}} \tag{4}$$

where, μ and u are angular variables, α and β are angular location parameters, ω is a slope parameter, and ε_{dir} is the error term. We assumed that ε_{dir} follows the von Mises distribution with mean μ and nonnegative concentration parameter κ. The four unknown parameters, α, β, ω, and κ are identified by using particle swarm optimization (PSO) method (Kennedy and Eberhart 1995) to estimate the statistical circular regression model. The estimated regression model with the identified parameters for wind direction is shown in Figure 3.

4. MODEL VALIDATION

Model validation was made by comparing the estimated wind speed/direction and the corresponding data observed in 2016. Since the proposed model is based on the data observed

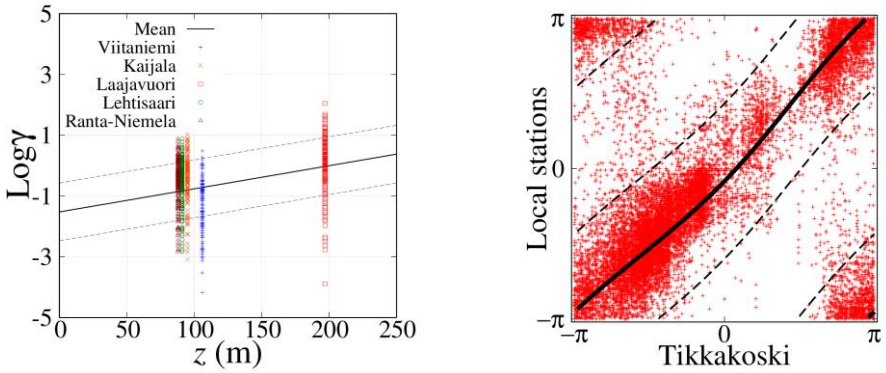

Figure 3: Observed wind speed and direction in 2015.

in 2015, the applicability can be evaluated evidently. Figure 4 show comparisons between the estimation of the wind speed and directions by the proposed model and the corresponding observation. In the figure, "prediction" indicates the mean value computed by the wind speed/direction models. Although the proposed model is very simple, the predictions agree

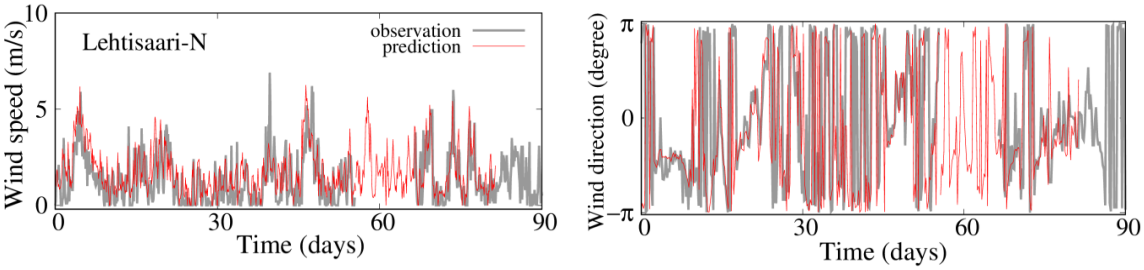

Figure 4: Comparison between the model predictions and the corresponding data.

well with the data. In addition, the main advantage of the proposed models is to stochastically estimate the local wind fields. The model provides not only the most probable estimation but the accuracy as standard deviation.

4. CONCLUSIONS

This study newly proposed the data-driven model for estimating local wind field over two small lakes in Jyvaskyla Finland. We found that the wind speed and direction can be estimated by the simple regression models. We compared the model predictions with the corresponding observation data and found that the proposed model can accurately predict the local wind speed and directions using only the official station data. The proposed model is simple and can be useful to evaluate aquatic environment of lakes.

ACKNOWLEDGEMENTS

This work was supported by JSPS KAKENHI Grant Number 18K03408.

REFERENCES

Bessac, J., P. Ailliot and V. Monbet, 2015. Gaussian linear state-space model for wind fields in the north-east Atlantic, *Environmetrics*, **26**, 29-38.

Downs, T.D. and K.V. Mardia, 2002. Circular regression, *Biometrika*, **89(3)**, 683-69.

Johnson, R.A. and T.E. Wehrly, 1977. Measures and models for angular correlation and angular-linear correlation. *Journal of the Royal Statistical Society*, **39**, 222-229.

Kennedy, J. and R. Eberhart, 1995. Particle Swarm Optimization, *Proceedings of IEEE International Conference on Neural Networks*, 1942-1948.

Robert, S., L. Foresti and M. Kanevski, 2013. Spatial prediction of monthly wind speeds in complex terrain with adaptive general regression neural networks, *Int. J. Climatol.*, **33**, 1793-1804.

Torma, P. and T. Kramer, 2017. Wind shear stress interpolation over lake surface from routine weather data considering the IBL development, *Period. Polytech. Civil Eng.*, **61(1)**, 14-26.

Hyönteiset ilmakehämallien vieminä

P. Siljamo[1], K. Ashbrook[2], R. Comont[2], E. Huusela-Veistola[3], M. Leskinen[4] ja S. Neuvonen[5]

[1] Ilmatieteen laitos, pilvi.siljamo@fmi.fi
[2] Worcesterin yliopisto, Iso-Britannia
[3] Luonnonvarakeskus (Luke)
[4] Helsingin yliopisto
[5] Turun yliopisto

Abstract

Atmospheric dispersion models have been used to calculate atmospheric dispersion and concentrations of air pollution like primary particles or chemical compounds, but they are also suitable for calculating the atmospheric transport of biological organisms. This article explains how the atmospheric dispersion model SILAM calculates migrations of the bird cherry-oat aphid (Rhopalosiphum padi) to Finland. The SILAM model calculations for the bird cherry-oat aphid migrations are realistic. It also maps out the potential route of an invasive species harlequin ladybird (Harmonia axyridis) to disperse from continental Europe to the UK. The model suggests that the most likely route for the harlequin ladybirds from the continental Europe to the UK was not anthropogenic introductions, but wind-assisted dispersal over the English Channel.

1. JOHDANTO

Ilmakehän leviämismalleilla (jatkossa vain leviämismalli) lasketaan tyypillisesti ilman epäpuhtauksien leviämistä ja pitoisuuksia, mutta niitä voidaan käyttää myös biologisten organismien kuten siitepölyjen ja pienten hyönteisten ilmakehässä tapahtuvan kulkeuman ja leviämisen arviointiin.

Tuhohyönteiset voivat aiheuttaa merkittävää haittaa viljelyksille. Erityisesti Suomessa ja muilla pohjoisilla alueille lämpimämmiltä seuduilta tulevat tuholaiset ovat hankalasti ennakoitavissa. Torjuntatoimien oikea-aikaiseksi ajoittamiseksi olisi kuitenkin hyödyllistä saada ennakkotietoa mahdollisista hyönteisvaelluksista. Ilmatieteen laitoksen SILAM-leviämismallia (Sofiev et al. 2015, http://silam.fmi.fi) onkin kehitetty ennustamaan tuomikirvan (*Rhopalosiphum padi*) migraatioita.

Sen lisäksi että leviämismallia voidaan käyttää varoituspalvelun tukena, SILAMilla on laskettu, miten haitallinen vieraslaji harlekiinileppäkerttu (*Harmonia axyridis*) valloitti Britannian. Harlekiinileppäkerttu on alun perin aasialainen laji, jota on tuotu biologiseen

tuholaistorjuntaan myös Euroopaan, esim. Belgiaan. Valitettavasti harlekiinileppäkerttu syö kirvojen lisäksi myös muiden leppäkerttujen toukkia. Iso-Britanniassa ensimmäinen harlekiinihavainto tehtiin 2004, jonka jälkeen se on runsastunut voimakkaasti ja onkin todennäköisesti pääsyyllinen kotoperäisten leppäkerttukantojen romahtamiseen Iso-Britanniassa (Roy et al. 2012). Harlekiinejä tiedetään tulleen laivojen ja matkalaukkujen mukana, mutta olisiko pääasiallinen reitti kuitenkin Englannin kanaalin ylitys lentäen?

2. MENETELMÄT

SILAM on Ilmatieteen laitoksella kehitetty sekä Lagrange- että Euler-tyyppinen ilmakehän leviämismalli. Leviämismallilla lasketaan kuinka aine vapautuu ilmakehään, miten tuuli kuljettaa ja turbulenttiset pyörteet sekoittavat sitä ja miten se poistuu märkä- ja kuivalaskumana. SILAMilla voi laskea sekä aineen kulkeumaa päästöpisteestä että jäljittää havaitun aineen lähdealueita. Tässä esitetyt tulokset on laskettu käyttäen Euler-tyyppistä SILAM-mallia.

Kuvassa 1 on esitetty SILAM-kirvamallin toimintaperiaate. Kirvamalli muistuttaa paljon SILAM-siitepölymallin toimintaa (Sofiev et al 2013). Säätiedot malli saa numeerisesta säänennustemallista (laskuissa käytetty ECMWF:n säämallia http://www.ecmwf.int). Kirvojen kehitystä munista lentokykyisiksi yksilöiksi säätelee lämpösumma. Myös lämpösumman laskentaan tarvittava 2 m:n lämpötila otetaan säänennustusmallista.

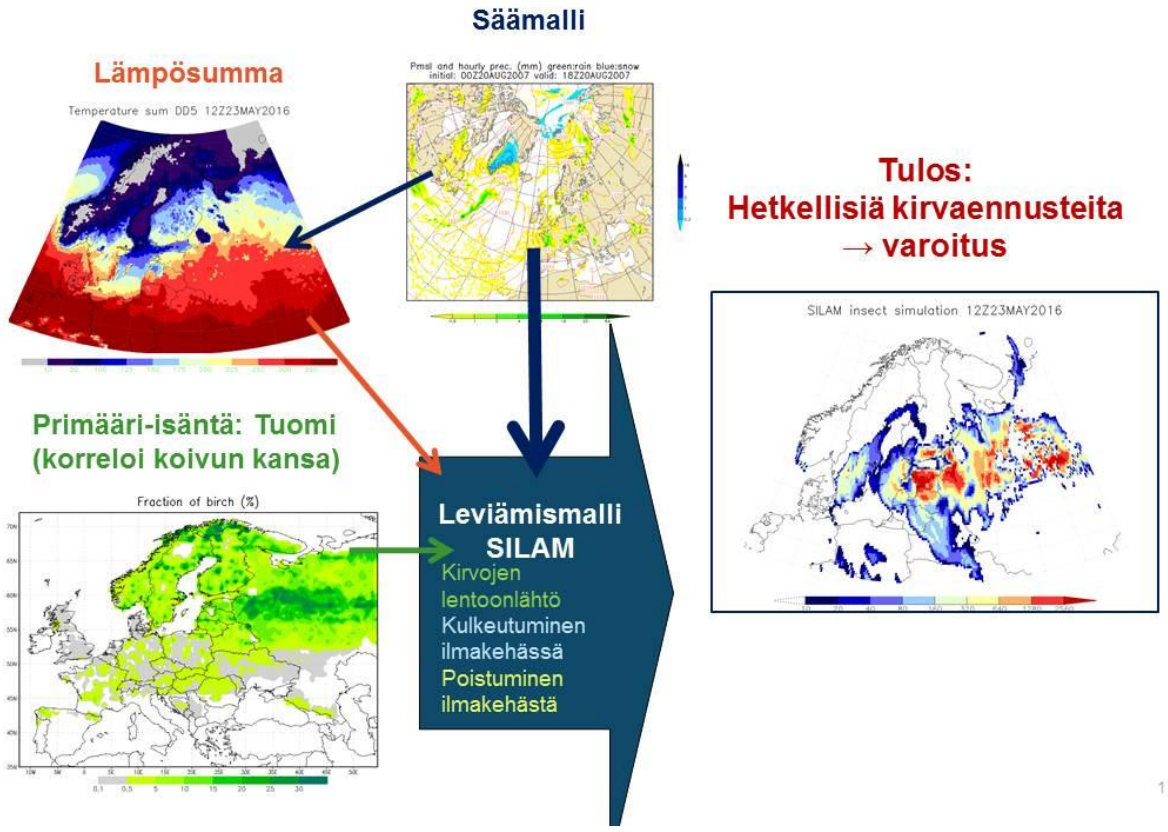

Kuva 1. SILAM-kirvamallin toiminta

Tuomikirvan ensisijainen isäntäkasvi on tuomi. Laji talvehtii tuomella, jolla kehittyy keväällä ensimmäinen sukupolvi, minkä jälkeen kirvat siirtyvät viljakasveille ja voivat myös levittää viljojen virustauteja. Mallissa on yksinkertaistaen oletettu, että mitä enemmän tuomia on lähdealueella, sitä enemmän on myös lentoon lähteviä kirvoja. Kun tiedetään lähdealueet, lämpösumma, joka vaaditaan lentokykyisen kirvan kehittymiseen sekä sopivat sääolosuhteet, voidaan laskea kirvojen liikkeet ilmakehässä. Pieninä hyönteisinä kirvat ovat ilmakehässä melko tahdottomia ja joutuvat seuraamaan ilmavirtauksia (Wainwright et al. 2017).

Harlekiinileppäkerttujen mahdollisten lentoreittien laskenta on kirvamallia yksinkertaisempaa, sillä laskuissa on oletettu, että leppäkertut voivat lähteä liikkeelle milloin vain päiväaikaan Alankomaiden, Belgian ja Ranskan rannikkokaupungeista. Leppäkerttuja mahdollisia lähtöalueita on hahmoteltu myös käänteismallinnuksella.

3. TULOKSET

Vaikka SILAMin kirvamalli on yksinkertaistettu kuvaus kirvojen kehityksestä ja lennosta ilmakehässä, mallin tulokset antavat melko realistisen kuvan kirvamigraatioista Suomeen. Havaittujen kirvojen (pyydykset, pellot, tutkahavainnot) ajoitus sopii SILAMilla laskettuihin muutaman päivän tarkkuudella useimmissa tutkituissa tapauksissa. Koska tiedot lähtöalueen kirvamääristä ovat hyvin suppeat, varsinaista tarkkaa kirvamäärää SILAM ei kykene ennustamaan. Sen sijaan mallin ennustaessa hyönteismigraatiota maanviljelijät voivat valmistautua tarkkailemaan viljelyksiään tavallista huolellisemmin.

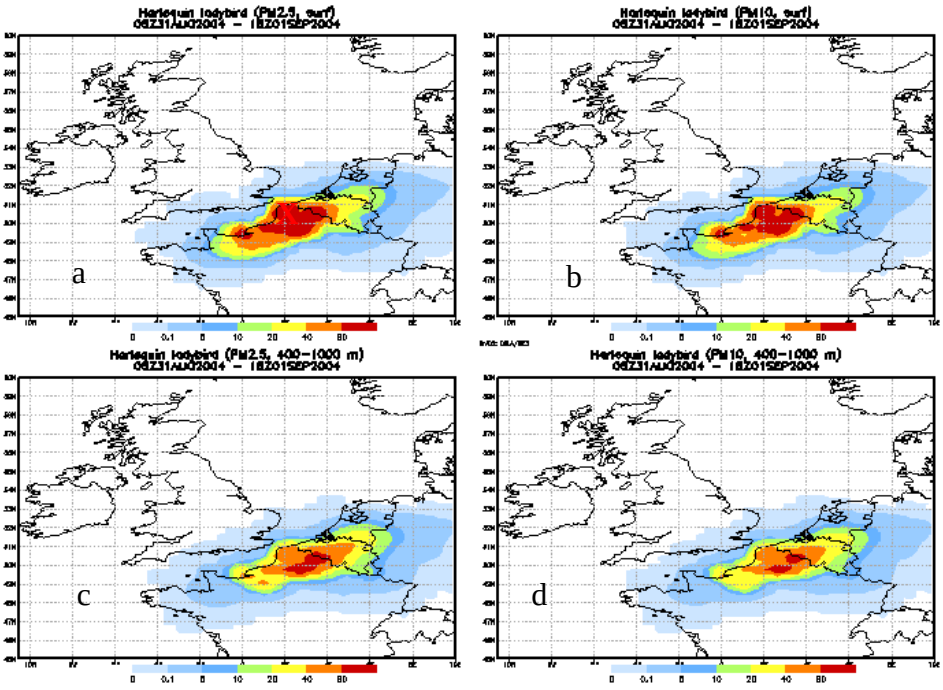

Kuva 2. Esimerkki SILAMilla lasketusta harlekiinileppäkerttujen kulkeumaennusteesta. Harlekiinit on oletettu joko PM2.5- tai PM10-hiukkasiksi. Lähtöalueena Ranskan rannikkoa. Leppäkerttujen oletetaan lähteneen liikkeelle aikaisintaan 31.8.2004 6 UTC, kuvan ennustepituus +37 tuntia. Leppäkerttuja havaittiin Essexissä, Englannissa (X) 1.9.2004. a) PM2.5 pitoisuus maanpintatasolla b) PM10 pitoisuus maanpintatasolla c) PM2.5 pitoisuus 400-1000 m korkeudella d) PM10 pitoisuus 400-1000 m korkeudella.

Harlekiinileppäkertun tiedetään kulkeutuneen Iso-Britanniaan ihmisen mukana, mutta on kuitenkin hyvin todennäköistä, että tärkein reitti Manner-Euroopasta Britanniaan kulki Englannin kanaalin yli lentäen. Tähän viittaavat harlekiinileppäkerttuhavaintojen ajoitus pian suotuisten lento-olosuhteiden jälkeen (esimerkkinä kuva 2). Harlekiinihavainnot eivät myöskään mitenkään erityisesti keskity lentokenttien ja satamien läheisyyteen.

KIITOKSET

Suomen Akatemian SAPID (a novel approach to predict Source areas and Atmospheric transport of plant Pathogens and pest Insects migration using atmospheric Dispersion models) -projekti on rahoittanut tätä tutkimusta.

LÄHTEET

Roy, H.E, T. Adriaens, N.J.B. Isaac, M. Kenis, T. Onkelinx, *et al.*, 2012. Invasive alien predator causes rapid declines of native European ladybirds, *Diversity and Distributions*, **18**, 717-725.

Sofiev, M., P. Siljamo, H. Ranta, T. Linkosalo, S. Jäger, A. Rasmussen *et al.*, 2013. A numerical model of birch pollen emission and dispersion in the atmosphere. Description of the emission module. *Int J Biometeorol*, **57**, 45-58.

Sofiev, M., J. Vira, R. Kouznetsov, M. Prank, J. Soares ja E. Genichovich, 2015. Construction of the SILAM Eulerian atmospheric dispersion model based on the advection algorithm of Michael Galperin, *Geosci. Model Dev.*, **8**, 3497-522 .

Wainwright C.E, P.M. Stepanian, D.R. Reynolds ja A.M. Reynolds, 2017. The movement of small insects in the convective boundary layer: linking patterns to processes. *Sci Rep.*, **7**, 5438.

Northern Finland seismological network: status in early 2019

H. Silvennoinen[1] and J. Narkilahti[1]

[1] Sodankylä geophysical observatory, University of Oulu, hanna.silvennoinen@oulu.fi

Abstract

Northern Finland seismological network is a network of permanent seismic broadband stations operated by Sodankylä geophysical observatory. The current network consists of 4 fully operational stations connected to the international data centres offering open access real-time data and 5 stations currently working on test regime.

1. INTRODUCTION

The early part of the development of Northern Finland seismological network happened in two different organizations. The first permanent seismic station in Sodankylä geophysical observatory started in 1956 on the initiative of the Institute of Seismology of University of Helsinki (Kozlovskaya et al., 2016). There has been an operational seismic station in Sodankylä fairly continuously since though the exact site has been moved a few times. The station has been located in the current coordinates since 2001 with the station code SGF. Institute of Seismology also collaborated with the newly established University of Oulu and the Department of Physics by starting seismic measurements in Oulu 1959. In 1963, the seismic station was established in its current location about 18 km from downtown Oulu (station code OUL). In 1970, the University of Oulu established its second seismic station in Kuusamo region (MSF). In 1998, Sodankylä geophysical observatory merged into University of Oulu also merging the two separate seismic measurements under the umbrella of Sodankylä geophysical observatory (Kozlovskaya et al. 2016).

The modernization of the permanent seismic network started 2005-2007 with replacing the old short-period instruments with state of the art very broadband seismometers and modern data acquisition system. As a part of the modernization project, the fourth station was established in Rovaniemi (station code RNF). These four stations form the Northern Finland seismological network operating under the network code FN in the Federation of Digital Seismograph Networks. The continuous and real-time data from the stations is freely distributed and archived by GeoForschungsZentrum Potsdam (GFZ) in addition to the archive held at the observatory. Via GFZ the data is used for the monitoring of the seismic activity in Northern Europe as well as internationally (Kozlovskaya et al, 2016).

The seismic stations of Sodankylä geophysical observatory are a part of the EPOS infrastructure. EPOS is an integrated open-access research infrastructure for solid earth sciences with a long-term plan to integrate the existing national research infrastructures.

2. CURRENT ACTIVITIES

Between 2014-2017 5 new stations were installed in Oulanka (OLKF), Kolari (KLF), Ranua (RANF), Raja-Jooseppi (RAJF) and Kaamanen (KMNF). These stations are currently working on a test regime and will be added to the network after the testing period is done. Of these stations, RNF, RAJF, and KMNF were found during an Academy of Finland funded co-project with Institute of Seismology as a part of the EPOS effort of these institutes.

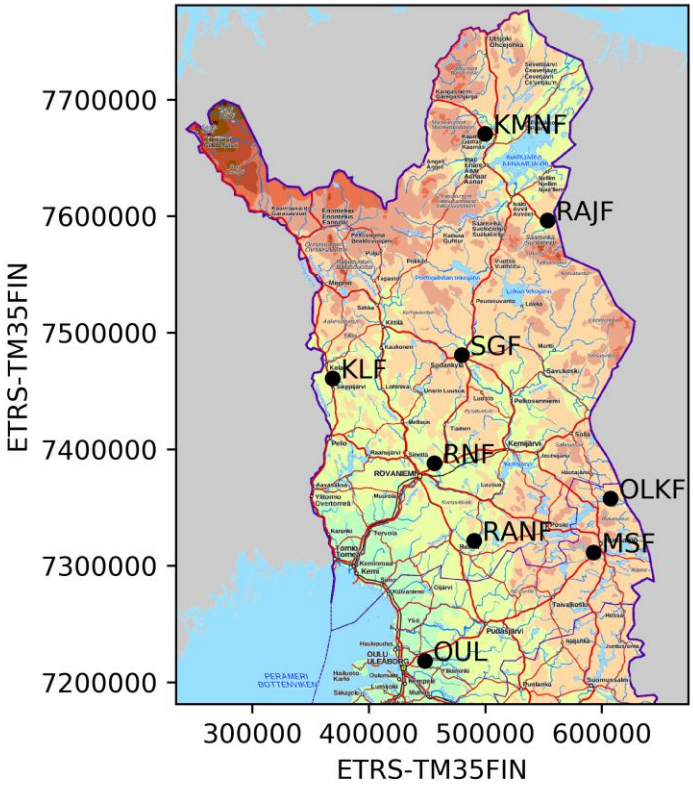

Figure 1: The map of the permanent seismic stations operated by Sodankylä geophysical observatory.

The new stations at OLKF, RAJF, and KMNF have been installed in boreholes equipped with so-called posthole seismometers standing freely at the bottom of the borehole while KLF and RANF are more "traditional" setups. The installation in a borehole offers several benefits, for example, the stable temperature throughout the year and attenuation of certain types of seismic noise. On the other hand, this type of installation offers new challenges and SGO staff has been testing new solutions and materials for the installation, as well as insulation, power supply, and other practical details on all the five new sites.

REFERENCES

Kozlovskaya, E., J. Narkilahti, J. Nevalainen, R. Hurskainen ja H. Silvennoinen, 2016. Seismic observations at the Sodankylä Geophysical Observatory: history, present and future, *Geosci. Instrum. Mathod. Data Syst.*, **5**, 365-382.

Comparing sea ice thickness in the Arctic from reanalysis and satellite altimetry

Joula Siponen[1,2]

[1] University of Helsinki, joula.siponen@helsinki.fi
[2] Finnish Meteorological Institute

Abstract

Changes in sea ice cover are one of the most visible signs of climate change. Long time series of thickness observations are needed to study climatological changes. The knowledge of sea ice thickness is also important for human activities in the Arctic. Need for better predictions of sea ice conditions is increasing due to opening of the Arctic sea routes for longer operational season among other things. Improving predictions requires high-quality observations.

However, measuring sea ice thickness with adequate resolution, accuracy and coverage over the Arctic is a major challenge. Here a new product of sea ice thickness, ESA-CCI (Climate Change Initiative), based on satellite radar altimetry is used for assessment of sea ice thickness from ocean reanalysis ORAS5. The CCI product combines two satellite missions, CryoSat-2 and ENVISAT, which leads to 15-year time series, 2002-2017, of winter sea ice thickness over the Arctic. Radar altimetry is based on measuring distance to the surface of ice and water, and the assumption that the sea ice is in hydrostatic equilibrium. The method has major uncertainty sources but it has been shown to produce generally good overview of sea ice thickness over the whole Arctic monthly.

This work shows that the new CCI product performs well in validation of the reanalysis. Overall average difference (RMSE) between sea ice thickness in the CCI product and reanalysis is below 1 m but seasonal and interannual variation during the time series is from 0.5 m to 1.3 m. There are strong regional differences. The results of this work support previous research. Differences are a sum of model biases as well as uncertainties in satellite altimetry, such as the snow product used in thickness retrieval.

Monthly separated time series of sea ice volume for the CCI coverage reveal years of extremely low volume and recovery during the season. The trends in sea ice volume are clearly negative. Monthly CCI trends are statistically significant. ORAS5 trends have larger interannual variability and therefore show no significance. The observed negative trends are connected to changes in both, atmospheric and oceanic forcing.

Influence of climate change on water resource availability in a watershed

H. Somura[1], S. Saboory[2], E. Rabanizada[3], and T.M. Mosier[4]
[1] Graduate school of Environmental and Life Sciences, Okayama University, Japan
somura@okayama-u.ac.jp
[2] National Statistics and Information Authority, Afghanistan
[3] Administrative Office of the President, Afghanistan
[4] Energy and Environment Science and Technology, Idaho National Laboratory, USA

Abstract

Afghanistan is essentially semi-arid to desert and most crop production is limited to pockets of irrigable land, with some rain-fed areas in the north and at high-altitudes (FAO, 2017). To consider water resources management for stabilizing crop production, Soil and Water Assessment Tool (SWAT) was applied to Khulm watershed from 2012 to 2015. The runoff rate at the outlet of the target watershed was about 5.0 % and water resources were limited for irrigation, from the obtained information. At this moment the reproducibility of stream flow achieved slightly lower than satisfactory level in daily bases, because of input data quality. Then sensitivity analysis of stream flow was conducted by using future predictions of precipitation and temperature from ERA-Interim information to understand water resources availability and crop production variation. It was understood that water resources will slightly decrease in average in the watershed, but uncertainty of future predictions are large and it is difficult to conclude specifically. Also it was estimated that crop yield will increase or decrease depending on the scenarios.

1. INTRODUCTION

Afghanistan is located in the Middle East and Central Asia, and is an inland country surrounded by Pakistan, Iran, Tajikistan, Turkmenistan, Uzbekistan, China. The climate is classified as dry to semi-arid zone, and the most agricultural production is limited to irrigable areas (FAO, 2017). The annual rainfall is small nationwide, divided into dry season from April to November and rainy season from December to March. Also, since precipitation hardly occurs from May to August, securing irrigation water and proper water management are important issues. For considering it, basin-scale hydrological analysis was conducted by applying a hydrological model, Soil and Water Assessment Tool (SWAT), to estimate water resources availability in the Khulm watershed. Then climate change scenarios, especially focusing on precipitation and temperature changes, was input to the model for predicting monthly future water availability for irrigation.

2. STUDY AREA

Khulm watershed is located in the northern region with about 8300km^2. There are three stations for river discharge and four stations for weather information. Precipitation,

temperature, and humidity are observed at every stations and wind speed is at a station. Solar radiation was started to measure from December 2015, and no information is existed about it before. Instead, the solar radiation data were developed using the Angstrom formula (FAO, 1998) based on data collected by the Ministry of Agriculture, Irrigation, and Livestock (MAIL) and actual sunshine hours collected by the Ministry of Energy and Water in the watershed. From the land use GIS data, 69.1% were pasture lands, 21.1% were rainwater farmlands, 5.7% were barren and 1.6% were irrigated farmland. From the FAO world soil map, Haplic Yermosols was 45.3%, Cambic Arenosols 39.6% and Lithosols 15.1%. Major crops in the watershed are irrigated and rain-fed wheats, melons, pistachios, grapes and others.

3. RESULTS AND CONCLUSION

A sensitivity analysis was conducted by using the ERA-Interim output for future climate change. In this project, RCP 4.5 and RCP 8.5 scenarios were employed. In precipitation, annual amount did not change drastically in average among scenarios. In addition, the amount of precipitation showed increase trends in high ensemble member and decrease trends in low ensemble member, and the magnitude of variations became gradually larger from RCP4.5 through RCP8.5. Thus, the amount of water input to the watershed is likely to decrease for the future but it is difficult to determine the situation because of the different trends. In ET, actual ET (ETa) showed decrease trend slightly in average. As well as precipitation, the trend changed with low and high ensemble members, and the magnitude of variations changed larger from RCP4.5 through RCP8.5 scenarios.

From the analysis of monthly discharge at the watershed outlet, it was considered that the flows with mean ensemble member were likely to be decreased for the future, but the variations among scenarios were large and the amount could increase / decrease more than the base simulation. In monthly basis with the multi-models ensemble mean member, especially from July through October, discharge amount showed larger decrease trends in a year in every scenarios. In the agricultural profile of the target province, Khulm district had 28,800 ha of irrigated agricultural land. Thus, irrigation water to their agricultural area could be influenced by the future climate conditions, especially in decreasing cases, and it should be considered how to deliver irrigation water efficiently to the area without any conflict. In addition, it will be necessary to be considered cropping schedule and crop type to avoid too much water scarcity (conflict among crop varieties) in necessary timing. However strong conclusion would be difficult to state because of great variations of precipitation in each scenario (high and low ensemble member).

ACKNOWLEDGEMENTS

This study was supported by the World Bank, the Ministry of Energy and Water, Afghanistan, and the Ministry of Agriculture Irrigation and Livestock, Afghanistan, for providing local data.

REFERENCES

FAO, 1998. In Irrigation and Drainage Paper No.56 Crop Evapotranspiration (guidelines for computing crop water requirements): In: R.G. Allen, L.S. Pereira, D., Raes and M. Smith (Ed.). FAO: Rome, Italy; 290, ISBN 92-5-104219-5.

FAO, 2017. Country Pasture/ Forage Resource Profiles - Afghanistan -, http://www.fao.org/ag/agp/agpc/doc/counprof/afgan/afgan.htm (2017.4.21).

Observations of MeV electron precipitation to the upper atmosphere and differences in the electron energy spectrum between satellite and ground based measurements.

J. Sorri[1] on behalf of B-TRUE research community

[1] Sodankylä Geophysical Observatory, juha.sorri@oulu.fi

Existence of a high energy electron population in the radiation belts is very well established fact. The energy distribution and flux of these electrons have been measured and is relatively well known. Due to various processes these electrons may precipitate to the upper atmosphere. In contrast with the electron population in the radiation belts the energy distribution of the precipitation is not well known. This article gives an overview of the electron energy measurements, both in atmosphere and orbit, and gives a description of a proposed system for direct relativistic electron measurements in the upper atmosphere.

1. INTRODUCTION

Earths radiation belts, or Van Allen radiation belts, were discovered during late 1950's by Explorer 1 and 3. Radiation belts consists mainly of energetic electrons and protons and are trapped by a magnetic bottle formed by the Earth's magnetic field. These charged particles are thought to be originating from solar wind and cosmic ray interactions. Consequently these trapped particles protect the Earth's atmosphere from the destructive effects of ths solar wind.

Direct measurements of the electron distribution of the particles began shortly after the discovery of the radiation belts. A more recent dedicated study of the energetic properties of the radiation belt particles was made by NASA by means of Van Allen probes (Radiation Belt Storm Probes) that were launched 2012 and are now becoming close to ending their operations. In parallel with Van Allen Probes atmospheric precipitation was studied with high altitude balloons named Balloon Array for Radiation-belt Relativistic Electron Losses (BARREL) in four separate campaigns between 2013-2016 with launch locations being in Antarctica and Sweden.

2. ELECTRON OBSERVATIONS WITH THE PROBES AND OBSERVATION BALLOONS

There are two main particle detectors on board Van Allen Probes, The Magnetic Electron Ion Spectrometer (MagEIS) [Blake (2013)] and The Relativistic Electron-Proton Telescope (REPT)

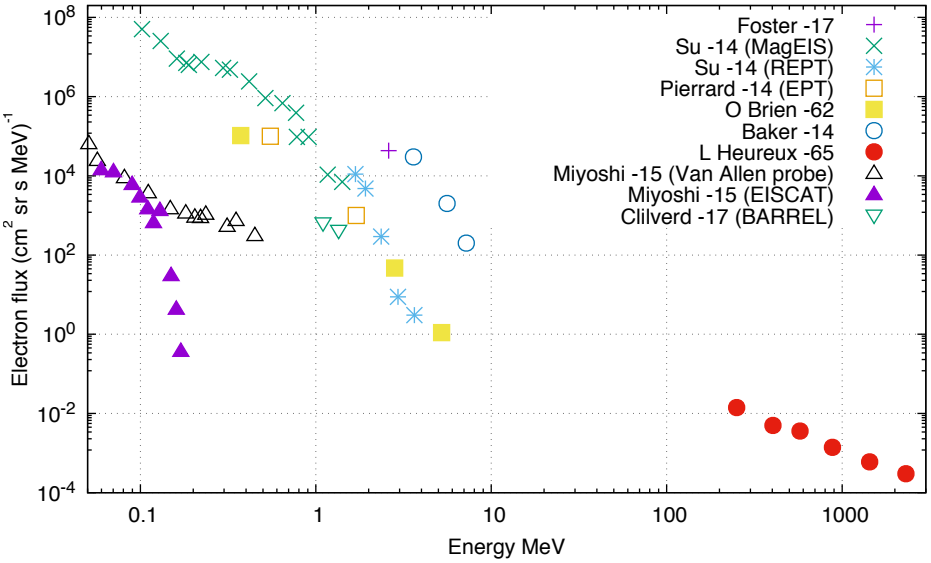

Figure 1: A compostion of measured electron fluxes from satellite measurements, balloon borne measurements and during EISCAT campaign. The high energy points above 500 MeV are cosmic primary electrons and presented as an example.

[Baker (2013)]. To summarize the working principles of these devises: MagEIS is a magnetic electron spectrometer with energy observation range between 20 - 4800 keV divided in low, medium and high energy ranges. REPT is a stacked silicon telescope with a maximum electron energy range of approximately 20 MeV. In BARREL NaI scintillation detectors were used to detect the secondary X-ray and gamma-radiation and acquired photon spectrum was subsequently converted to electron flux. An overview of the results obtained with these devices is shown in figure 1. Electron flux data is obtained from refs. [Foster (2017), Su (2014), Pierrard (2014), O'Brien (1962), Baker (2014), L'Heureux (1965), Miyoshi (2015)] and [Cliverd (2017)]. Note that electron flux values from ref. [Cliverd (2017)], labeled Cliverd -17 in the figure 1, are for mono-energetic flux and scaled to correct unit by assuming 2π field-of-view for the BARREL NaI detector.

There are two distinctive features in the figure 1. First, there is a very wide gap in the data between 10 to 500 MeV energies and second EISCAT measurements do not reproduce the overall energy spectrum very well. The simple experimental challenges explain the gap in the energy spectrum but difference between EISCAT data and other sources is significant as the EISCAT data is used as an input to the Sodankylä Ion Chemistry (SIC) model (see for example [Turunen (2016)]).

3. OBSERVATION OF THE RELATIVISTIC ELECTRONS IN THE UPPER ATMOSPHERE

To help the science community to better understand the relativistic electron precipitation we have proposed an electron detector to be flown into the upper atmosphere. Experiment of this

type, using a measurement system described here, has been approved on flight in zero-pressure sounding balloon under HEMERA H2020 project [HEMERA]. Device, named Balloon-borne Telescope for Relativistic and Ultra-relativistic Electrons (B-TRUE), includes a silicon telescope for electron detection, plastic scintillators to detect secondary particle showers from cosmic rays and supporting electronics. Optionally or additionally device can carry a software radio to detect cosmic ray induced RF-echoes [Falcke (2003)]. A schematic view of the Si-telescope designed for the B-TRUE is shown in the figure 2. Main components of the silicon telescope

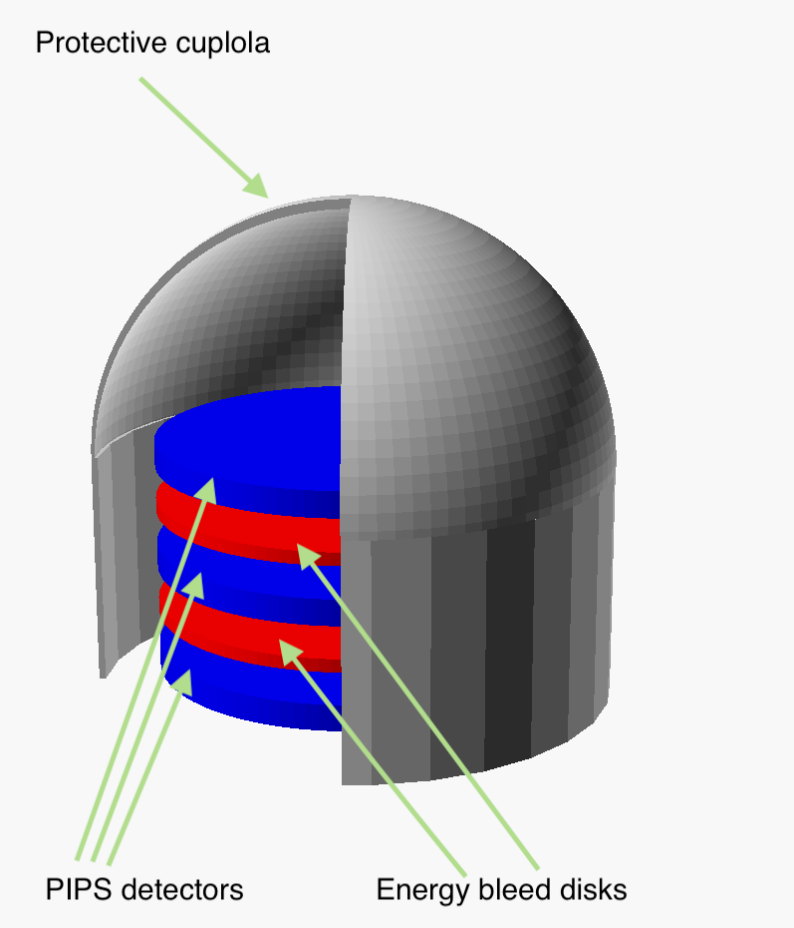

Figure 2: A schematic view of the proposed Si-telescope naming the main parts. The cupola above the silicon detectors can be build using 3D printed frame and aluminized mylar. The energy bleed disks are optional depending of the energy range chosen to be observed. The cables, supporting structures and connectors are omitted for clarity. Drawing is not to scale.

are PIPS-silicon detectors that are mechanically robust to withstand stresses occurring during HEMERA payload decent and have good energy resolution for distinguishing between cosmic ray induced muons and electrons. Discrimination will be done by comparing energy losses in

the silicon detectors. Muons, with energies up to several GeV, leave approximately the same amount of energy in the silicon detectors as for electrons subsequent energy losses per detector deviate [Groom (2001), ESTAR]. The secondary electrons produced by cosmic rays will be vetoed by demanding anti-coincidence with plastic scintillators and/or RF-echoes. The zero-pressure observation balloons have the maximum flight altitude of 35 km. At that altitude the atmospheric depth is approximately 8 g/cm^2 and consequently the minimum energy that a precipitating electron must have before entering atmosphere is approximately 15 MeV [ESTAR]. A rough directional information for the detected particles can be deduced if a detection coincidence is demanded between PIPS detectors. The Upper limit of the observed energy range is limited by the energy after which electrons have enough energy to punch-trough the whole telescope. An upper energy limit can be adjusted with the thicknesses of the detectors and bleed disks, however, using thick bleed disks will reduce the energy resolution and the detection efficiency. HEMERA zero-pressure balloons are equipped with an auxiliary balloon 30 m above the payload [ZPB]. Auxiliary balloon will limit the telescopes field-of-view near the lower energy limit but for muons and primary cosmic electrons the balloons are nearly transparent.

HEMERA 2020 flight is provisionally scheduled to fall 2020. Main goal of the flight is to test the proposed detection system and to serve as proof of concept for more dedicated experiments.

LÄHTEET

[Blake (2013)] Blake, J. et al. *Space Sci Rev* (2013) **179**:383

[Baker (2013)] Baker, D.N. et al. *Space Sci Rev* (2013) **179**:337

[Foster (2017)] Foster, J. C. et al. *J. Geophys. Res. Space Physics* (2017) **122** 324–339

[Su (2014)] Su, Z. et al. *Geophys. Res. Lett.* (2014) **41**, 229–235

[Pierrard (2014)] Pierrard, V. et al. *Space Sci Rev* (2014) **184**:87

[O'Brien (1962)] O'Brien, B. J. et al. *J. Geophys. Res.* (1962) **67(1)**:397–403

[Baker (2014)] D. N. Baker et al. *Nature* (2014) **515**:531–534

[L'Heureux (1965)] L'Heureux et al. *Phys. Rev. Lett.* (1965) **15**:93

[Miyoshi (2015)] Miyoshi, Y., et al. *J. Geophys. Res. Space Physics* (2015) **120**:2754–2766

[Cliverd (2017)] Clilverd, M. A. et al. *J. Geophys. Res. Space Physics* (2017) **122**534–546

[Turunen (2016)] Turunen, E. et al. *J. Geophys. Res. Atmos.* (2016) **121**:11852–11861

[HEMERA] https://www.hemera-h2020.eu (cited March 13, 2019)

[Falcke (2003)] Falcke H. et al. *Astroparticle Physics Volume 19* (2003) **4**:477-494

[Groom (2001)] Groom D. E. et al. *Atomic Data and Nuclear Data Tables Vol. 76* (2001) **No. 2**

[ESTAR] https://physics.nist.gov/PhysRefData/Star/Text/ESTAR.html (cited March 13, 2019)

[ZPB] *User Manual for ZPB Infrastructure Access* **issue 1 revision 0** dated 03/19/2018

Historical overview of wind gust measurement techniques – from traditional anemometry to new possibilities

I. Suomi[1] **and T. Vihma**[1]

[1]Finnish Meteorological Institute, irene.suomi@fmi.fi

Abstract

The short-duration (seconds) wind speed maxima, the wind gusts, represent the maximum load that wind can pose on structures. The first mentions of the measured maximum wind force are already from the middle of the 18th century, but the first real wind gust records were possible only in the end of 19th century when an anemograph was invented. At weather stations, anemographs were applied from 1950s onwards, and the gusts were manually read from the graph. From about 1990s onwards, after the digitalization of wind measurements, it was possible to calculate wind gusts in terms of running means. Today, anemometer systems based on cup and sonic anemometers can provide accurate measurements of wind gusts, but the measurements are point-wise and thus represent the heights and regions where the supporting structures can reach. Therefore, the data are mainly concentrated to the densely populated land areas. New developments, based on research aircraft and Doppler lidar measurements can potentially fill this spatial gap of information in the future and provide new information also on the spatial structure of wind gust events. This presentation will provide an overview of the development of anemometry from the perspective of wind gust measurements.

1. INTRODUCTION

The impact of extreme winds on our environment at sea, over land, and in the air has been in our interests already for centuries. The wind gusts, the short-duration (seconds) wind speed maxima, have been, however, one of the most challenging meteorological parameters to measure, because of the required fast response of the anemometer system. That comprises not only the anemometer itself, but also the signal processing and recording systems, and the (international) data exchange and archiving. Moreover, the overall accuracy of the measurement depends on the environmental conditions at the measurement site. This presentation will provide an overview of wind gust measurement methods including a short historical review, the current status and a discussion on future directions. The presentation is based on the work by Suomi and Vihma (2018).

2. HISTORY

The first known anemometer was introduced by Leone Battista Alberti in Italy already in 1450 (e.g. Jacobson, 1999). This anemometer was a swinging-plate anemometer similar to the famous Hooke's anemometer from 1667 (Figure 1). This type of an anemometer also provided

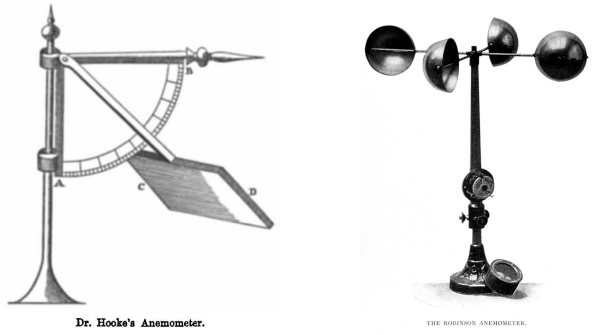

Figure 1: On the left: Hooke's anemometer from 1667 (source: Laughton, 1882) and on the right: Robinson's cup anemometer (source: wikipedia, *https://en.wikipedia.org/wiki/Anemometer*, accessed: 28.2.2019).

perhaps the first wind gust measurement ever, as Roger Pickering developed a similar device in 1744 (without knowing these previous versions), but his anemometer consisted in addition of a spring catch that showed the maximum force caused by the wind (Laughton, 1882).

The 18th century was time for exploring different techniques to measure wind. These were based on pressure, rotation, temperature change, evaporation, and even on the sound of the wind. Some of the inventions were also groundbreaking. In 1732, Pitot introduced a pressure tube to measure flow velocity in water. A few years later, in 1738, Bernoulli presented the theory to relate the flow velocity to the difference between the total and static pressure in the tube. Thereby, it was possible to measure velocities using the Pitot tube both in liquid and gas (Sheppard, 1941). However, it took almost four decades until in 1775, Lind introduced the first pressure tube anemometer. Today, pressure tube anemometers are widely used in meteorological research, especially on board aircraft (five-hole tubes) and in wind tunnels.

In the 19th century, the focus of research was mostly on developing the recording techniques for wind measurements, but also the anemometry developed. For example, in 1846, Robinson took a major step forward in the development of the class of rotating anemometers by developing his well-known cup anemometer, which closely resembles the instruments still used today (Figure 1). In the end of the century, in 1892, Dines proposed the first self-recording anemometer. It was a pressure tube anemometer, which included pens that recorded both the wind speed and direction. For the first time, it was possible to have also records of wind gusts and lulls (Sheppard, 1941). This kind of recorders, later called anemographs, were used at weather stations from the 1950s onwards from where the wind gusts were read manually (Sloan and Clark, 2012).

The third class of anemometers widely used today are the sonic anemometers. The history of using sound waves to measure wind also dates back to the end of the 18th century. However, the first instruments were not based on the propagation velocity of sound waves but instead they were composed of an organ that produced different tones with varying wind speed and direction (Laughton, 1882). The interpretation of such measurements was not trivial, and still, in 1941, Sheppard commented that the class of acoustic anemometers is "of no practical importance". However, already in 1955, Schotland introduced the theory to measure wind by sonic means, and in the 1960s the first sonic anemometers measuring both wind and temperature were introduced (e.g., Kaimal and Businger, 1963). Today, sonic anemometers are widely used in measurement of atmospheric turbulence, and they can also be considered as reference instruments for measuring wind gusts because of their fast response to wind speed fluctuations and

because they allow high sampling rates.

Towards the end of the 20th century, the advances in Radio Frequency (RF) communications and microprocessor technology made it possible to establish automatic networks for mesoscale measurement systems (Serafin et al., 1987). Automatization allowed also the calculation of gust speeds using running means (Sloan and Clark, 2012). Today, wind gust observations are no longer limited by data processing, recording or reporting techniques because of powerful computers, efficient means of RF communications and inexpensive data storage resources.

3. CURRENT CHALLENGES AND FUTURE POSSIBILITIES

Until the digitalization of wind measurements in the 1990s, the wind gust measurements suffered from the limited recording and data processing resources. Therefore, the majority of continuous wind gust records date back by about 30 years at most. Although the response characteristics of anemometer systems based on cup and sonic anemometers are good enough today, these in-situ wind measurements applied at weather stations are limited to heights and regions where the supporting structures can reach. In other words, existing measurements are mainly available from densely populated land areas, whereas from remote locations, such as the marine Arctic, wind gust information is available only from sparse coastal locations. Moreover, the overall accuracy of the measurement comprises not only the instrumentation but also the effects of the environmental conditions at the weather station. Methods have been proposed to correct the mean wind speed for the non-optimal site exposure, but not wind gusts.

Recent developments of wind gust measurement techniques based on turbulence measurements from research aircraft (Suomi et al., 2016) and from Doppler lidar (Suomi et al., 2017) can provide information from heights and locations unreachable by traditional measurement techniques (Figure 2). Moreover, rapidly developing measurement methods based on Unmanned Aircraft Systems (UASs) may add to better coverage of wind gust measurements in the future.

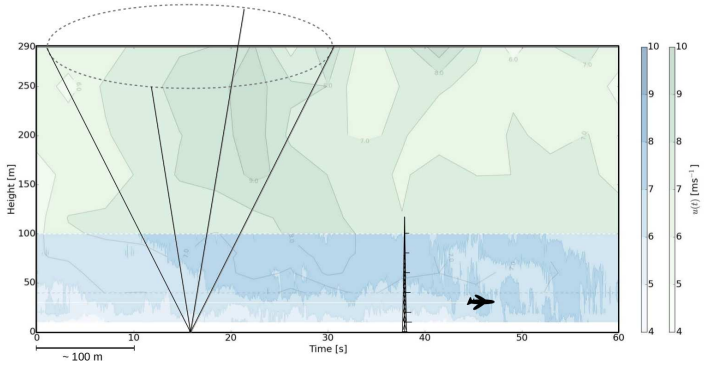

Figure 2: Illustration of simultaneous measurements from Doppler lidar (green) and a meteorological mast (blue). Furthermore, wind gusts can be measured from a research aircraft. Reproduced with permission from Suomi (2017).

4. SUMMARY

The first attempts to measure wind gusts are from the middle of the 18th century. However, the true records of gusts, and lulls, have been possible only since the end of the 19th century

when the anemograph was invented. At weather stations anemographs were applied from 1950s onwards, and the wind gusts were manually read from the graph. Continuous recording of wind gusts in terms of running means became possible only in the end of 1980s after the digitalization of wind measurements. Therefore the longest continuous wind gust records are available only from the last couple of decades. However, still today, there exist challenges in wind gust measurements due to the sparse network of in-situ measurements. The new developments based on research and unmanned aircraft and Doppler lidar techniques are expected to provide new information on wind gusts and contribute to the better understanding of the processes leading to extreme gust events.

ACKNOWLEDGEMENTS

This work has received funding from the Academy of Finland project Towards Better Tailored Weather and Marine Forecasts in the Arctic to Serve Sustainable Economic Activities and Infrastructure (TWASE; Contract 283101).

REFERENCES

Jacobson, M.Z., 1999. Fundamentals of Atmospheric Modeling; Cambridge university Press: Cambridge, UK.

Kaimal, J. and J. Businger, 1963. A continuous wave sonic anemometer-thermometer. *J. Appl. Meteorol.*, **2**, 156–164.

Laughton, J.K., 1882. Historical sketch of anemometry and anemometers. *Q. J. R. Meteorol. Soc.*, , **8**, 161–189.

Schotland, R., 1955. The measurement of wind velocity by sonic means. *J. Meteorol.*, **12**, 386–390.

Serafin, R. J., Dabberdt, W. F. and W. A. Cooper, 1987. Advances in meteorological instrumentation. *Rev. Geophys.* 1987, 25, 393–402.

Sheppard, P., 1941. Anemometry: A critical and historical survey. *Proc. Phys. Soc.*, **53**, 361.

Sloan, C. and M. Clark, 2012. A comparison of three Met Office wind observing systems. *Atmos. Sci. Lett.*, **13**, 283–288.

Suomi, I., 2017. Wind Gusts in the Atmospheric Boundary Layer. Ph.D. Thesis, University of Helsinki, Helsinki, Finland.

Suomi, I., Gryning, S.-E., O'Connor, E. and T. Vihma, 2017. Methodology for obtaining wind gusts using Doppler lidar. *Q. J. R. Meteorol. Soc.*, **143**, 2061–2072.

Suomi, I., Lüpkes, C., Hartmann, J., Vihma, T., Gryning, S.-E. and C. Fortelius, 2016. Gust factor based on research aircraft measurements: A new methodology applied to the Arctic marine boundary layer. *Q. J. R. Meteorol. Soc.*, 142, 2985–3000.

Suomi, I. and T. Vihma, 2018. Wind gust measurement techniques – from traditional anemometry to new possibilities. *Sensors*, **18(4)**, 1300.

Magnetic environment in polar and equatorial regions during space era

E. Tanskanen[1,2], I. Björklund[1] and T. Jha[1]

[1] Aalto University, eija.tanskanen@aalto.fi
[2] University of Helsinki

Abstract

Changes in the magnetic environment are continuously recorded by several hundred magnetometers on ground, atmosphere and space. Magnetometers are used to detect signals on geomagnetic storms, auroral substorms, pulsations covering wide frequency range and other highly variable phenomena. Magnetic recordings are continuously registered both at auroral and equatorial regions since the beginning of space era at 1957. We have identified auroral substorms from the auroral region recordings and geomagnetic storms from the magnetometers close to the magnetic equator. We found out that by far the largest number of stormy hours is seen in 1989, 1991 and 1960 while the least stormy hours is found in 1964 and between 2007-2009. The last interval match well with the time span when the least magnetic disturbances are seen in the auroral region. The strength of the largest storm in each year varies almost an order of magnitude being the largest in 1989 and the smallest in 2007. With this study we seek an answer to the question that "how common the classical seasonal pattern is in polar and equatorial latitudes".

A new spectral riometer for ionosphere research

T. Teppo[1,2], A. Kero[1], M. Orispää[1] and E. Turunen[1]

[1] Sodankylä Geophysical Observatory, University of Oulu, tomi.teppo@sgo.fi
[2] Arctic Centre, University of Lapland

Abstract

Measurement of the cosmic radio noise flux can be used for remote sensing of the ionisation taking place in the collisional plasma of the D-region ionosphere. The measurement device based on this method is called riometer (relative ionosphere opaque meter) and it is essentially just a passive radio receiver. The cosmic radio noise absorption (CNA) is estimated by comparing the quiet day level and the instant measurement level of the received radio noise. Traditionally riometers monitor a single narrow frequency band in the range of 25 to 50MHz. These kind of riometers have been used from 1960's and they are based on Dicke type of switch in which the collected noise power by antenna is compared to the known noise diode reference.

Here we present a new type of riometer, called spectriometer, sampling a wide frequency band to monitor the cosmic noise. The main advantage of the wide bandwidth is robustness against narrow man-made radio frequency interferences. Moreover, we also expect to detect a change in the spectral shape of the cosmic radio noise absorption during energetic particle precipitation, such as solar proton events, providing more information on the energy spectrum of the ionisation source.

The new spectriometer prototype has been initiated at Sodankylä geophysical observatory and has been purchased commercially during the ERDF-project. The device is based on a software defined radio concept and a new broad band antenna design. A log periodic antenna with the flat frequency response is designed to collect the cosmic radio noise over the band of 20 to 55MHz. The noise power information is transformed to the voltage information in an analog part of the receiver where the amplification and a band limiting filtering is performed. The voltage information is converted to a digital form and directed to the digital signal processing unit based on field programmable gate array logic (FPGA) and a normal micro processor (CPU). The spectral analysis of the received signal is carried out in an FPGA and further analysis is done in a CPU or a parallel minicomputer.

The software defined radio approach enables a flexible modification of the signal processing inside operational station. This approach also gives an opportunity to save low-level data products to be used in data analysis off-line.

Ilmaston vaihtelut puulustojen valossa

M. Timonen[1]

[1] Luonnonvarakeskus (Luke), mauri.timonen@luke.fi

Abstract

The growth of Scots pine (Pinus sylvestris L.) at the Finnish pine timberline is highly sensitive to June-July temperatures. Exceptional preservation of wood and its accumulation in non-oxygen muddy bottoms of ice-cold lakes have made it possible to build an over 7650 years long continuous tree-ring chronology. The characteristics of this chronology, the distribution of the samples (on both sides of the present timberline) and a strong June-July temperature connection have made it possible to rebuild past climate and forest history based on dendro-climatic analysis. Some cyclic patterns and climatic fingerprints,for example, can be identified afterward in well-preservedtree rings, which opens a fascinating approach to explore the past even on monthly level.

1. MITÄ ON PUULUSTOTUTKIMUS?

Dendrokronologia (puiden vuosilustotutkimus) on tieteenala, jossa puiden vuotuista kasvua tutkimalla on mahdollista tarkastella taannehtivasti luonnossa ja ihmiskulttuureissa tapahtuneita muutoksia. Tämä perustuu siihen, että esimerkiksi ilmaston vaihtelut jättävät jälkensä kronologisesti tallentuviin luonnonilmiöihin kuten puiden vuosilustoihin. Erityisesti ajoitusten vuodentarkkuus on asia, joka antaa eri alojen tutkijoille mahdollisuuden kerääntyä saman pyöreän pöydän ääreen poikkitieteelliseen yhteistyöhön.

Viimeisten parinkymmenen vuoden suursaavutus on tutkimuksen aikaperspektiivin laajentuminen päivistä ja kuukausista tuhansiin vuosiin, mikä on vahvistanut tieteenalan asemaa erityisesti ilmasto- ja ympäristönmuutostutkimuksessa.

Lapin metsänrajamännyn kasvu ja puuaineen tiheys (kuva 1) riippuvat pääosin kesän lämpöoloista. Vaganovin ym. (2006) mukaan voimakkaimmat ilmastosignaalit löytyvät vuosilustojen leveydestä ja puuaineen maksimitiheydestä, joista ensimmäinen kertoo pääasiassa kesäheinäkuun ja jälkimmäinen huhti-syyskuun lämpöoloista.

Puulustot voivat selittää parhaimmillaan jopa 70 % tutkittavan ilmastomuuttujan vaihtelusta (Briffa ym. 2001). Kasvuprosessissa lustojen solurakenteisiin tallentuu myös hiilen, hapen ja vedyn isotooppeja, jotka yhdessä merten pohjasedimenteistä mitattavan proksitiedon kanssa laajentavat ilmastotutkimusta kasvukausien lämpötiloista ja sademääristä meri- ja ilmavirtojen sekä aurinkoisuuden ja pilvisyyden ilmastovaikutusten arviointiin (Mielikäinen ym. 2012).

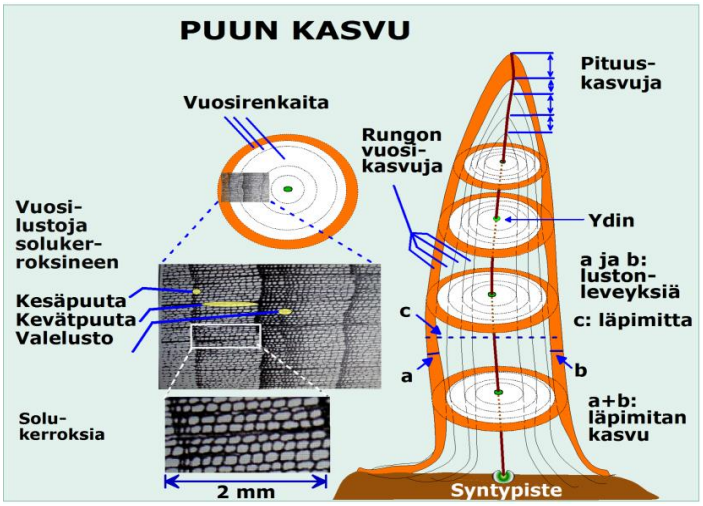

Kuva 1: Puun runko kasvaa vuosittain pituus- ja paksuussuuntaan. Vuotuinen paksuuskasvu koostuu soluista ja solukerroksista ja on havupuilla nähtävissä rungon poikkileikkauksessa vuosirenkaana eli vuosilustona.

Kotimaisella lustotutkimuksellamme on myös globaalista ulottuvuutta, sillä erityisesti ilmastoherkkä Lapin metsänrajamänty taltioi Aurinko- ja avaruusperäisiä ilmastosignaaleja ja Maapallon sisäiseen ilmastodynamiikkaan liittyviä tapahtumia.

2. METSÄNRAJAMÄNNYN PITKÄN LUSTOKALENTERIN TARKASTELUA

Lapin järvien pohjamudista on löydetty suuri määrä tuhansia vuosia sitten kasvaneiden muinaismäntyjen jäänteitä (*megafossiileja*). Puut ovat aikoinaan kasvaneet järvien rantavyöhykkeillä ja suistuneet lopulta vanhuuttaan tai myrskyjen, metsäpalojen ja muiden syiden seurauksena veteen. Jos kylmävetisen järven ranta on syvä ja pehmeäpohjainen, mutaan uponneet rungot voivat säilyä lahoamattomina jopa vuosituhansien ajan (Kuva 2).

Lapin metsänrajamännyn yli 7650 vuoden pituinen vuodentarkka lustokronologia on maailman toiseksi pisin yhdestä havupuulajista laadittu aikasarja. Professori Matti Eronen aloitti sen kokoamisen 1970-luvun alussa ajoittamalla radiohiilimenetelmällä järvistä löytämiään männyn megafossiileja. Vuodentarkan lustokalenterin valmistumista vuosikymmenen hidastanut näytteetön ajanjakso välillä 350–170 eaa. saatiin umpeen vasta 25 vuotta myöhemmin eli vuonna 1999 yhdeksän maan yhteisessä EU-projektissa. (Eronen ym. 2002).

Mäntymegafossiilien löytöpaikat osoittavat männyn metsänrajan sijainneen vuosituhansia sitten 80 km nykyistä pohjoisempana ja tuntureilla noin 100 metriä ylempänä. Kultin ym. (2006) tutkimuksen mukaan Lapin kesät olivat tuolloin 2,6 ^{o}C nykyistä lämpimämpiä. Noin 4000 vuotta sitten alkoi parin tuhannen vuoden viileä ja kostea ajanjakso. Ilmasto oli ankarimmillaan jaksolla 500 eaa. – 150 jaa., jolloin metsänraja perääntyi nykyistä etelämmäksi ja tuntureilla alemmaksi. Tähän viittaa vaikeus löytää senaikaisia männyn megafossiileita nykyiseltä metsänrajalta tai sen pohjoispuolelta.

Ilmasto lämpeni kylmän jakson jälkeen asteittain. Seuraava lämpöhuippu saavutettiin keskiajan lämpökaudeksi kutsutulla jaksolla 900–1300, jolloin mänty levisi takaisin pohjoisen puuttomille alueille. Lämmin kausi päättyi pienenä jääkautena tunnettuun viileään jaksoon, joka kesti meillä 1800-luvun puoliväliin tai 1900-luvun alkuun. Ilmasto ei tuolloinkaan ollut

Kuva 2: Männyn nykyisen metsänrajan yläpuolisista pikku järvistä voi löytyä muinaisia mäntyrunkoja. Pääkuvassa Inarin Iijärven seudun Selkäjärvet ja pienessä kuvassa Näkkälä–Pöyrisjärvi-tien vieressä sijaitsevan lammen pohjamudasta pilkistävät männyn megafossiilit elivät vajaat 7000 vuotta sitten.

kaiken aikaa kylmä. Lämpimistä vaiheista kertovat nykyisellä metsänrajalla 1700-luvun puolivälin jälkeen syntyneet mäntysukupolvet. Sirén (1961) osoitti metsänrajametsien uudistumisen keskittyvän syklisesti tapahtuviin lämpimiin ilmastojaksoihin. Ilmaston viileneminen,

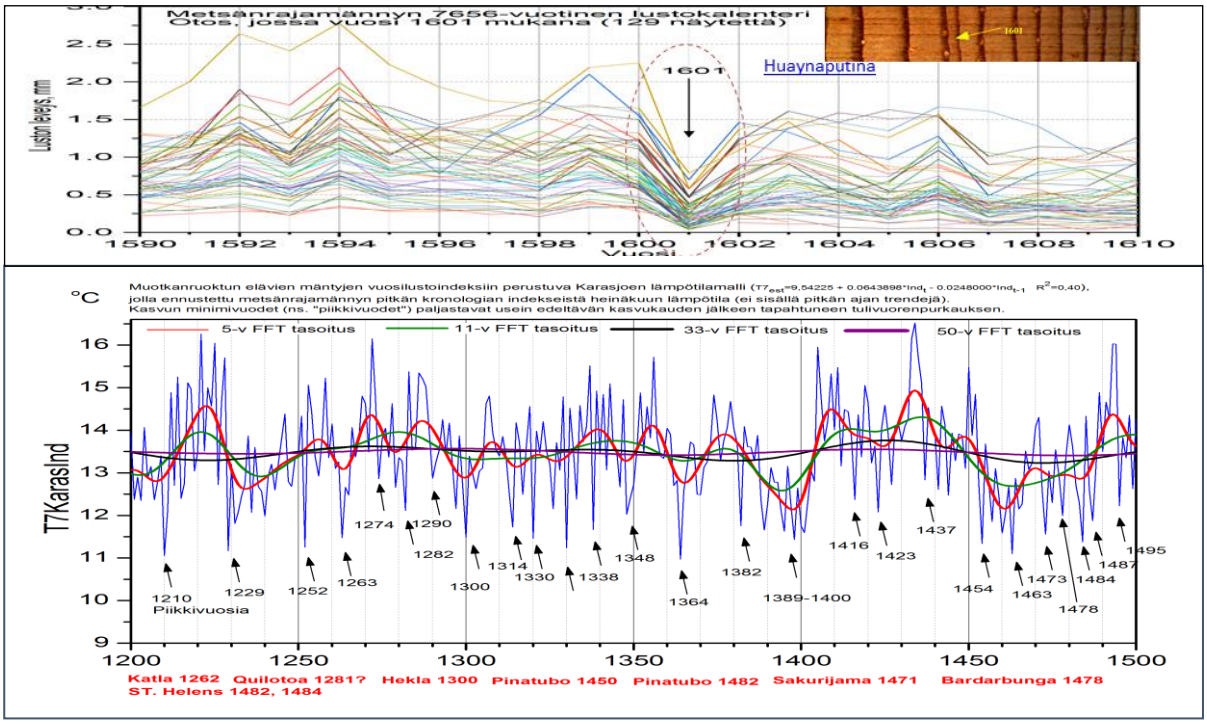

Kuva 3: Huaynaputinan purkaus Perussa vuonna 1600 pimensi Lapinkin taivaan niin, että seuraavana kesänä ilmasto viileni, männyn kasvu puolittui ja suureksi olkivuodeksi kutsuttu nälänhätä iski. Vuosilustominimit antavat vinkkejä mahdollisista purkausvuosista.

ja vuotuisen vaihtelun äärevöityminen johtavat pitkään jatkuessaan metsien harvenemiseen ja metsänrajan alenemiseen. Ilmaston viiletessä metsänrajametsät aluksi vain harvenevat metsänrajan pysyessä paikallaan. Vasta kun uutta puusukupolvea ei metsänrajalle enää synny ja vanha puusukupolvi väistyy, seuraava metsänraja siirtyy kohtaan, jossa puusto on vakiintunut. Uuden ja vanhan metsänrajan väliselle vyöhykkeelle muodostuu keloista ja kantojuurakoista muodostuva puujäämistö, joka vähitellen lahoaa pois tai varastoituu soihin ja järvien pohjamutaan. Metsänrajan muutokset molempiin suuntiin ovat hitaita.

Pari sanaa metsän kasvuun vaikuttavista tulivuorista. Salzerin ja Hughesin (2006) mukaan jopa 86 % suurista tulivuorten purkauksista näkyy puiden vuosilustoissa tai jäätikkökerrostumissa. Kreikan saaristossa vallinnut minolainen kulttuuri tuhoutui Santorinin rajussa purkauksessa 1600-luvulla eaa. Purkauksen aiheuttama pölypilvi vaikutti dramaattisesti myös Lapin männyn kasvuun kuten myös vuonna 1601 (Kuva 3).

LOPUKSI

Ehkä tästäkin kirjoituksesta käy ilmi lustotutkimuksen monet mahdollisuudet. Laajempi tarkastelu kalvosarjassani linkissä http://lustiag.pp.fi/data/pdf/geofysroi2019.pdf.

LÄHTEET

Briffa, K.R., T.J. Osborn, F.H. Schweingruber, I.C. Harris, P.D. Jones, S.G. Shiyatov ja E.A. Vaganov, 2001. Low-frequency temperature variations from a northern tree ring density network. *Journal of Geophysical Research* **106**, 2929-2941.

Eronen, M., P. Zetterberg, K. Briffa, M. Lindholm, J. Meriläinen ja M. Timonen, 2002. Part 1: The supra-long Scots pine tree-ring record for northern Finnish Lapland; Chronology construction and initial inferences. *The Holocene* **12(6)**, 673-680.

Kultti, S., Mikkola, K., Virtanen, T., Timonen, M. & Eronen, M. 2006. Past changes in the Scots pine forest line and climate in Finnish Lapland: a study based on megafossils, lake sediments, and GIS-based vegetation and climate data. *The Holocene* **16(3)**, 381-391.

Mielikäinen, K., M. Timonen ja S. Helama, 2012. Ilmastonmuutokset ja niiden syyt puulustojen ja muiden proksitietojen pohjalta. *Metlan verkkojulkaisussa: Bioenergia, ilmastonmuutos ja Suomen metsät*, **Luku 2.1**, s. 32-52.

Salzer, M.W. ja M.K. Hughes, 2007. Bristlecone pine tree rings and volcanic eruptions over the last 5000 yr. *Quaternary Research*, **67**, 57-68.

Siren, G., 1961. Skogsgränstallen som indikator för klimatfluktuationerna i norra Fennoskandien under historisk tid. *Commun. Inst. For. Fenn.*, **54(2)**, 66 p.

Vaganov, E.A., Hughes, M.K. & Shaskin, A.V. 2006. Growth Dynamics of Conifer Tree Rings. *Ecological Studies, 183. Springer Berlin – Heidelberg - New York*, ISBN-10 3-540-26086-2.

The Scientific Payload of the Lappi satellite (LAPPISAT) and Data Visualisation in the Service Concept of the Satellite

E. Turunen[1], T. Teppo, P. Koskimaa[2], A. Kestilä[3], E. Kallio[3], S. Nyman[3], J. Norberg[2] and A-M. Harri[2]

[1] Sodankylä Geophysical Observatory, University of Oulu, esa.turunen@oulu.fi
[2]Finnish Meteorological Institute
[3]Department of Electronics and Nanotechnology, Aalto University

Abstract

The Lappi satellite project builds a new service concept for aurora tourism in Lapland, based on open data produced by an own Finnish satellite. The service combines the real-time scientific data from ground instruments and the data from satellite instruments as the starting point from where the service concept is further developed. We describe the satellite instruments, its construction and operation and the contents of the service concept. The basic service idea is to produce new open data as a public service, which could then be used commercially by anyone to improve the service products offered in the tourism sector. The instruments of the satellite are an auroral camera, communication receiver/transmitter, a beacon transmitter and passive retroreflectors for satellite laser ranging. The beacon transmitter acts as an instrumental precursor in preparation to improve ionospheric satellite tomography, where 3-dimensional distribution of ionospheric free electron concentration above Finland is determined by a distributed network of ground-based receivers. We propose improvement of the current Finnish satellite tomography system operated by SGO and FMI, achieved by an own nanosatellite fleet, a dedicated fleet of satellites, whose sole instrument is the radio beacon. Such improvement not only enhances scientific output of satellite tomography, but will allow visualizations of aurora as public service, which adds to the Lappi satellite concept.

1. SHORT DESCRIPTION OF THE LAPPI SATELLITE PROJECT

In Finland, we have annually 70-80 million overnight stays by foreign visitors. Of these people, 3-6% want to see Nature's most beautiful color show, Northern Lights, the Aurora. However, the current tourism services are not at the same level as our technology would allow today. Forecasts are rare, mostly difficult to interpret - and moreover, often the skies are cloudy. Scientific real-time data exists, but it is difficult to use, advanced data products which would serve the Aurora tourism in practice are not developed. There is not even a live video stream of Aurora as now. Specifically, there is no live video stream of Aurora from space when it is overcast.

The feasibility study of the technology solutions for the Lappi satellite was finished in 2018. Currently we work out how to build a new service concept for aurora tourism in whole

Lapland, based on open data produced by the proposed own Finnish satellite. The service would combine the real-time scientific data from ground instruments and the data from satellite instruments as the starting point from where the service concept could further be developed. Here we provide short descriptions of the satellite instruments and contents of the service concept, with a sample visualization of the data produced. Naturally, only final financing of the satellite, which then would make it possible to build the satellite itself, launch and operate the satellite, would make it possible to produce the new services. The basic service idea is to produce new open data as a public service, which could then be used commercially by anyone to improve the service products offered in the tourism sector.

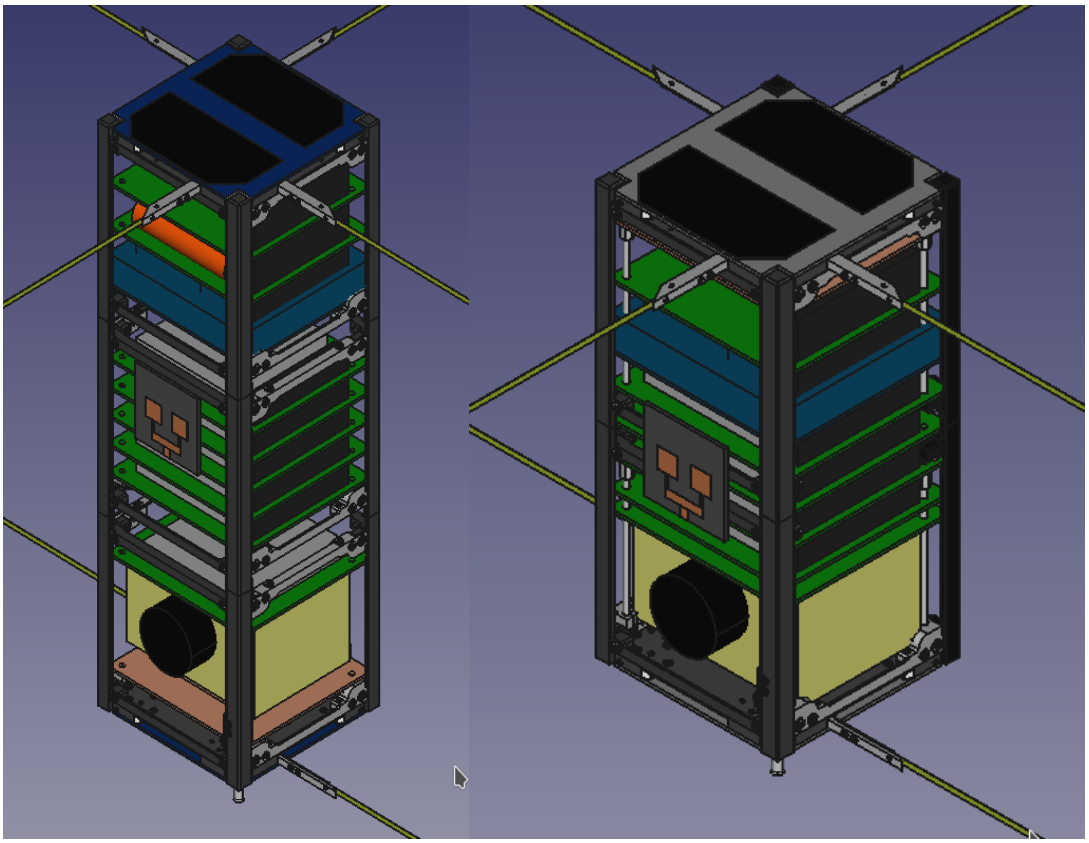

Figure 1: The Lappi satellite concept in a 3-unit configuration and in the minimum configuration, as a 2-unit cubesat. In reality the technological feasibility study concludes that a realistic Lappi satellite would be a 3-unit cubesat, such as Aalto-1 for example.

The instruments of the satellite are an auroral camera, communication receiver/transmitter, a beacon transmitter and passive retroreflectors for satellite laser ranging.

The beacon transmitter acts as an instrumental precursor in preparation to improve ionospheric satellite tomography, where 3-dimensional distribution of ionospheric free electron concentration above Finland is determined by a distributed network of ground-based receivers. We also propose future improvement of the current Finnish satellite tomography system operated by SGO and FMI, achieved by an own nanosatellite fleet, a dedicated fleet of satellites, whose sole instrument is the radio beacon. Such improvement not only enhances scientific output of satellite tomography, but will allow visualizations of aurora as public

service, which adds to the Lappi satellite concept, since the resolution of inversion in the satellite tomography will dramatically increase, both in time and space.

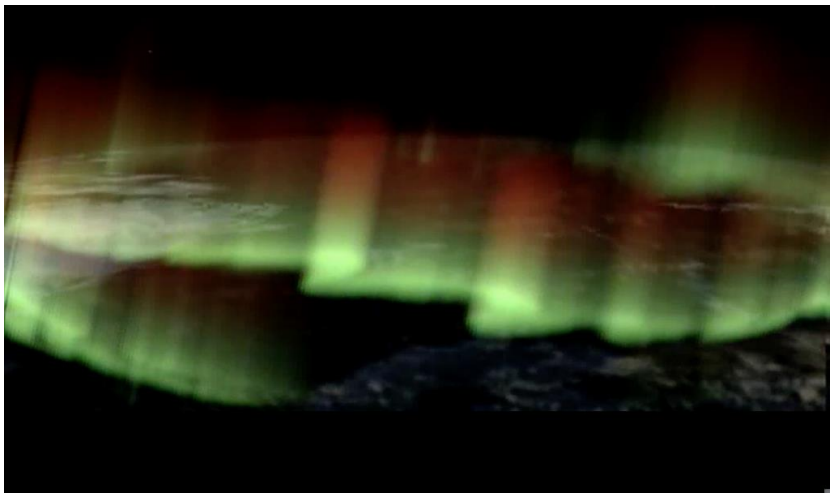

Figure 2: Sample basic visualisation data product by the Lappi satellite, Northern Lights above Finland. Note that this data could be drawn on a more accurate map, and tailored to viewing angle from whichever location, since emission data is given in 3-dimensional geographical coordinates as function of time. The image above is in the expected resolution of the live video stream.

The video stream from the satellite would be very limited both in resolution and coverage in time. This however would be complemented by the processed available ground-based geophysical data, which makes it possible to give two basic open datasets, which can be further processed and applied by anyone interested. These would be:

1) short-lasting video streams, near real-time or accumulated from space in case of non-existing suitable orbits. The video streams would be produced form individual images in as high resolution as the communication link would allow.

2) real-time location of auroral emissions above Finland in 3-dimensional geographic coordinates, combined from various ground-based instruments.

The time resolution of data product 2 would be determined by the availability of real-time or near real-time data. In general, this is the weak point of anything currently offered as tourism service. Often despite of whatever alarm or camera system is being used locally, the tourists will be too late for watching the most active phases of the shows in the sky. By combining data from products 1) and 2) one would be are able to push this now-casting failure to a more successful short-term reliable forecasting.

2. SOCIETAL IMPACT AND AND SIGNIFICANCE OF THE LAPPI SATELLITE

The Lappi satellite project will enable construction of a totally new service concept in Lapland, as a result of modern smart specialization in sparsely populated regions. The physical realization of this becomes possible in the current era of New Space economy.

The service is based on a regional competence centre, which is currently being formed in Lapland. The core of this already exists at Sodankylä in the activities of the Sodankylä Space Campus, which was established in 2018. The Space Campus consists of Sodankylä Geophysical Observatory run by University of Oulu and the Arcic Space Research Centre of Finnish Meteorological Institute. In the future this can be complemented by the competence of Lapland University in service design, tourism development and space law, as well as by the technology know-how by University of Oulu, Lapland University of Applied Sciences and Digipolis. Currently competence by all these institutions is applied towards regional development of Lapland. This regional competence centre is supported by the activities targeted to nanosatellites and space weather issues by the knowledge cluster from Helsinki, the Department of Electronics and Nanotechnology in the Aalto University, Finnish Geodetic Institute of National Land Survey, and the Arctic Research at Finnish Meteorological Institute.

The vision is to create an entity which serves the tourism industry in the whole northern region. This would be based on further processing of the data produced by the own Finnish satellite into service products, where the know-how resulting from scientific basic research enables application of high technology in practical service solutions. The satellite produces auroral imaging data from several polar orbits near and above Northern Finland during a day. The satellite is operated from the Sodankylä Satellite Station of the Arctic Space Research Centre, the satellite data is combined with ground-based auroral imaging, magnetic field measurements, cosmic radio noise measurements and satellite tomography measurements.

The Lappi satellite project is part of Finland's fast moving to the next phase of Space activities, where the vision of European Union is that applications of space technology are directly utilized by EU citizens by the year 2020. The cube satellites by Aalto University, Aalto-1 and Aalto-2 were launched in 2017, the third one in this series is the already flying Suomi-100 satellite and the fourth (Aalto-3), as well as the first cubesat by the Finnish CoE of Sustainable Space Research (FORESAIL-1) are being constructed. The satellite series of Aalto University has created innovation activity and commercial spinoffs, where already 3 satellites were successfully launched, and more is being constructed. The Lappi satellite would take one year to construct and could be launched to serve two auroral tourism seasons in 2019-2020 an 2020-2021.

The tourism services based on the first Lappi satellite would make it possible to construct a series of specialized Lappi satellite in 2020-2030. Their operation could in the end be totally commercial. Because the construction and launch of small satellites is getting economically more and more feasible all the time, the final vision is to have a fleet of satellites, where several simultaneous satellites enable continuous imaging of aurora from orbits passing over Northern Finland. The service concept is easily enlarged to produce also other services required in the arctic region, such as for example services related to safety in the arctic region.

ACKNOWLEDGEMENTS

The feasibility study of the Lappi satellite is financed by the regional Council of Lapland, through its AIKO program, complemented by self-financing share of Sodankylä Geophysical Observatory, University of Oulu.

Suomen ja Ruotsin kallioperän lämmöntuoton vertailua

T. Veikkolainen[1], **I.T. Kukkonen**[1] **ja J.-O. Näslund**[2]

[1] Geotieteiden ja maantieteen osasto, Helsingin yliopisto, toni.veikkolainen@helsinki.fi
[2] Svensk kärnbränslehantering AB

Abstract

Radiogenic heat production in Finland and Sweden has been largely studied using airborne gamma-ray surveys and glacial till measurements alike. For the first time, we have applied geological maps and national lithogeochemical databases to determine heat production from all important rock units of both countries. In Finland, heat production data covers the entire country, and has yielded an average of 1.3 ± 1.2 $\mu W m^{-3}$ as calculated directly from point data, and 1.4 ± 1.2 $\mu W m^{-3}$ as averaged by geological units. Corresponding values for Sweden are 2.5 ± 4.1 $\mu W m^{-3}$ from point data, and 2.3 ± 4.1 $\mu W m^{-3}$. The larger heat production in Sweden is in agreement with higher heat flow.

1. JOHDANTO

Kallioperän lämmöntuotto aiheutuu nykyisin pääosin neljän isotoopin (^{238}U, ^{235}U, ^{232}Th ja ^{40}K hajoamisesta (Rybach, 1973). Pintalämpövuon ja pintanäytteistä kootun lämmöntuottodatan havaittu lineaarinen riippuvuus rajatuilla alueilla johti lämpövuoprovinssien käsitteeseen, joka kuitenkaan ei ota huomioon lämmönsiirtoa kolmiulotteisena ilmiönä. Kiinnostus kuoren ja vaipan termisiä ominaisuuksia kohtaan on kasvanut myös energiateollisuuden tarpeiden myötä ja Fennoskandiassa tunnetuimpia osoituksia tästä on kaukolämpötuotannon tarpeisiin kairattu Espoon syväreikä (Leary et al. 2017).

2. MENETELMÄT

Geotermisissä tutkimuksissa kallioperän lämmöntuotto (A) lasketaan yleisimmin Rybachin (1973) empiirisen kaavan $A = \rho(9.52C_U + 2.56C_{Th} + 3.48C_K) \times 10^{-5}$ avulla. Tässä on määritelty kiviaineksen tiheys ρ [kg/m^3] sekä uraanin, toriumin ja kaliumin pitoisuudet C_U [ppm], C_{Th} [ppm] ja C_K [%]. Tiheydet määritetään punnitsemalla kalliopaljastumista otettuja kairasydännäytteitä ilmassa ja vedessä, ja pitoisuusmittaukset tehdään massaspektrometreilla laboratoriossa. Suomessa kivinäytteiden geokemiallista aineistoa on koottu Geologian tutkimuskeskuksen (GTK) kalliogeokemialliseen tietokantaan (Rasilainen et al. 2007), kun taas Ruotsin data on julkaisematonta ja saatavilla SGU:lta (Ruotsin geologinen tutkimuslaitos) erillistä lisenssiä vastaan. Suomen osalta lämmöntuotosta on juuri julkaistu kattava tutkimus (Veikkolainen ja Kukkonen, 2019), kun taas Ruotsin lämmöntuottoanalyysi perustuu vielä vertaisarvioimattomaan

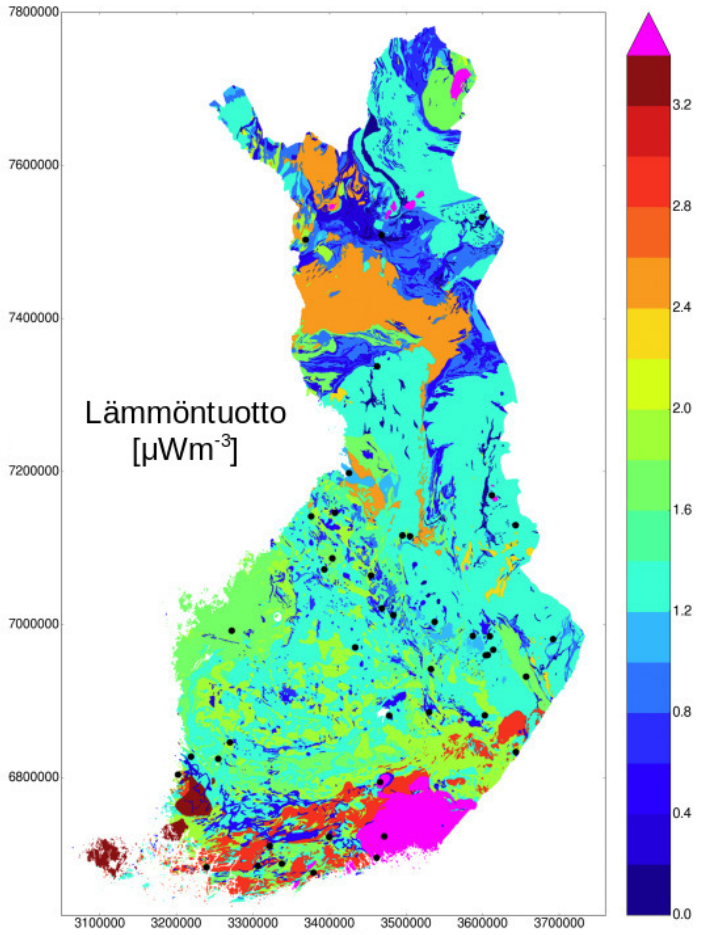

Kuva 1: Suomen kallioperän lämmöntuotto geologisten yksiköiden mukaan keskiarvoistettuna (Veikkolainen ja Kukkonen, 2019). Lämpövuomääritykset on merkitty mustilla symboleilla. Paikkakoordinaatit EUREF-FIN-järjestelmässä.

tutkimukseen, jonka tuloksia esitellään tässä kokouksessa. Sekä Suomen että Ruotsin datan analysointiin on käytetty ArcGIS-ohjelmistoa ja Python-ohjelmointikieltä.

3. LÄMMÖNTUOTTODATAN TULKINTAA

Lämmöntuoton ja myös lämpövuon tulkinnassa geologisen ympäristön tuntemus on erittäin tärkeää. Sekä Suomessa että Ruotsissa irtomaapeite on jääkausien seurauksena hyvin ohut, ja kalliopaljastumien runsauden sekä toimivan infrastruktuurin vuoksi molemmat maat ovat ihanteellisia lämmöntuottotutkimuksille. Suomen kallioperän lämmöntuotto on 6465 pistehavainnon perusteella 1.3 $\pm$ 1.2 μWm^{-3} ja geologisten yksikköjen perusteella keskiarvoistettuna 1.4 $\pm$ 1.2 μWm^{-3}. Kaakkois- ja Lounais-Suomen 1.65-1.47 vuosimiljardin ikäiset rapakivialueet (yli 3.4 μWm^{-3} ja 3.2-3.4 μWm^{-3}) ovat laajimpia suuren lämmöntuoton esiintymiä koko maan kartalla. Näiden välissä on 1.85-1.75 vuosimiljardin ikäisiä graniitti- ja migmatiittialueita, joilla 2.8-3.2 μWm^{3} on tyypillinen lämmöntuoton jakauma. Pohjois-Suomen mafisilla alueilla lämmöntuotto on lähellä nollaa, mutta hyvin pienissä 1.85-1.66 vuosimiljardin ikäisissä pohjoisen granitoidiesiintymässä tavataan yli 3.4 μWm^{-3}:n arvoja. Arkeeisella alueella lämmöntuotto on pääosin alle 1.4 μWm^{-3} (Veikkolainen et al. 2017).

Ruotsin lämmöntuottoaineiston alueellinen jakauma on hyvin epäyhtenäinen, mutta data silti

kattaa Ruotsin useimmat merkittävät geologiset yksiköt. Peräti 39915 havainnon pistedatasta laskettu lämmöntuotto on 2.5 $\pm$ 4.1 μWm^{-3} ja geologisten yksikköjen avulla keskiarvoistettu 2.3 $\pm$ 4.1 μWm^{-3}. Ruotsissa rapakiviesiintymät ovat erittäin pieniä, ja suurimmat lämmöntuottoarvot tavataan maan pohjoisosan 1.85-1.75 vuosimiljardin ikäisissä granitoideissa. Toisaalta Etelä-Ruotsin länsiosassa 1.10-0.92 vuosimiljardin ikäinen svekonorjalainen alue erottuu matalalla lämmöntuotollaan (alle 2.0 μWm^{-3}) idemmistä 1.96-1.66 vuosimiljardin ikäisistä kivistä, joiden lämmöntuotto Ruotsissa on suurempaa kuin samanikäisten kivien lämmöntuotto Suomessa. Pienimmillään lämmöntuotto on Ruotsin sedimenttipeitteisillä alueilla kuten Skånessa ja Gotlannissa, joskin sedimenttien alla olevan kiteisen kallioperän lämmöntuotto voi olla suurempi.

4. TULOKSET JA JOHTOPÄÄTÖKSET

Tutkimuksen perusteella Ruotsin lämmöntuotto on keskimäärin suurempi kuin Suomen ja vastaava ero on karkeasti näkyvissä myös pohjoismaisella lämpövuokartalla (Veikkolainen et al. 2017), joskin lämpövuodatan hajanaisuus ei oikeuta yksinkertaisten matemaattisten mallien sovittamista dataan. Ruotsissa kallioperän ikäjakauma on myös monipuolisempi eikä Suomen tapaan rajoitu lähes yksinomaan prekambrisiin kiviin. Koska kalliopaljastumista tehdyt lämmöntuottomääritykset ja tyypillisesti myös lämpövuomäärityksiin tarkoitetut kairareiät rajoittuvat kallion pintaosiin, tarvitaan epäsuoria menetelmiä kuten kivilajien seismisten ominaisuuksien tutkimista ja ksenoliiteista tehtävää termobarometriaa, jotta voidaan ymmärtää lämmöntuoton ja muiden termisten ominaisuuksien käyttäytymistä syvemmällä litosfäärissä.

KIITOKSET

Tekijät kiittävät GTK:ta ja SGU:ta oikeuksista käyttää kalliopaljastumadataa tutkimustarkoituksiin. Jenny ja Antti Wihurin rahasto on tukenut työn valmistumista.

LÄHTEET

Leary, P., P. Malin, T. Saarno ja I. Kukkonen, 2017. Prospects for assessing Enhanced Geothermal System (EGS) basement rock flow simulation by Wellbore Temperature data. *Energies*, **10**, 12.

Rasilainen, K., R. Lahtinen ja T.J. Bornhorst, 2008. Chemical Characteristics of Finnish Bedrock - 1 : 1 000 000 Scale Bedrock Map Units. *Geol. Surv. Fin. Rep. Inv.*, **171**, 94pp.

Rybach, L., 2002. Wärmeproduktionsbestimmungen an Gesteinen der Schweizer Alpen. *Beiträge zur Geologie der Schweiz: Geotechnische Serie*, **51**, 43pp.

Veikkolainen, T., I.T. Kukkonen ja T. Tiira, 2017. Heat flow, seismic cut-off depth and thermal modeling of the Fennoscandian Shield. *Geophys. J. Int.*, **211**, 1414-1427.

Veikkolainen, T. ja I.T. Kukkonen, 2019. Highly varying radiogenic heat production in Finland, Fennoscandian Shield. *Tectonophys.*, **750**, 93-116.

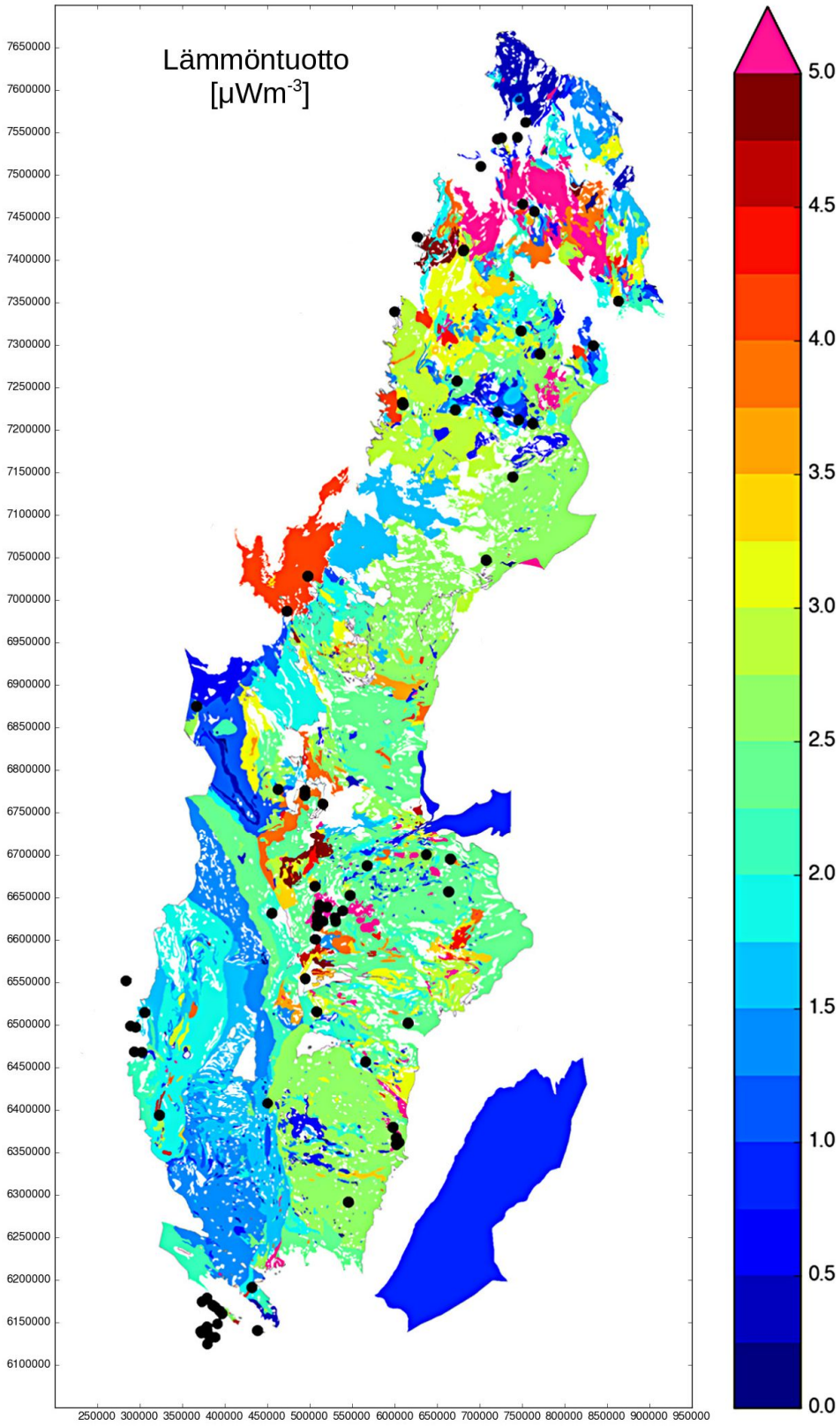

Kuva 2: Ruotsin kallioperän lämmöntuotto geologisten yksiköiden mukaan keskiarvoistettuna. Lämpövuomääritykset on merkitty mustilla symboleilla. Paikkakoordinaatit SWEREF99-järjestelmässä.

Suhteellisen tarkka vaaitus – aika-avaruuden geometria maanmittareille

Martin Vermeer[1]

[1] Rakennetun ympäristön laitos, Insinööritieteiden korkeakoulu, Aalto-yliopisto, Espoo
martin.vermeer@aalto.fi

Abstract

Thanks to general relativity we know that the deeper we are inside the gravitational well of a celestial body, the slower time ticks. Already in the 1920s it was attempted to measure the unusually large gravitational redshift of a white dwarf star, Sirius B, spectroscopically. Later, Pound and Rebka (1959) measured the gravitational redshift over a vertical distance of 22.5 m using gamma radiation exploiting the Mössbauer effect.

In the 1970s and 1980s, atomic clocks started to become already so precise, that geodesists, such as Arne Bjerhammar, started thinking about the possibility to use them to measure geopotential differences, i.e., to carry out 'levelling'. But only the new generation of atomic clocks invented some years ago, so called optical lattice clocks, are sufficiently precise to finally realize this dream.

The presentation explains the geometric backgrounds of both the method and of the theory of relativity, which are surprisingly simple.

Arctic climate change and its mid-latitude linkages

T. Vihma[1]

[1] Finnish Meteorological Institute, timo.vihma@fmi.fi

Abstract

A review on the Arctic climate change and its linkages with mid-latitudes is presented. During recent decades Arctic has warmed 2-3 times faster than the global mean, which is called the Arctic Amplification (AA) of climate warming. The AA is due to (a) several positive feedback mechanisms acting in the Arctic and (b) changes in the transports of heat and moisture from mid-latitudes to the Arctic. The positive feedbacks include those related to Earth surface albedo, cloud radiative forcing, insulation effect of sea ice and snow, and the vertical profile of air temperature. In addition to atmospheric transport of dry static energy, the transport of moisture from mid-latitudes to the Arctic is a particularly important factor for AA, because it does not only transport latent heat but also results in stronger cloud radiative forcing in the Arctic. Due to AA, the meridional temperature gradient between the Arctic and mid-latitudes has decreased, in particular in autumn and winter. This impacts mid-latitude weather via various physical mechanisms, including (1) increased temperatures of air-masses advected from the Arctic to mid-latitudes, (2) reduction of upper-tropospheric zonal winds in the Polar front jet stream, which allows more meridional circulation patterns, (3) changes in the occurrence of high-latitude blockings, (4) planetary wave trains and their resonance with surface forcing, and (5) stratosphere-troposphere interactions. However, multiple forcing factors acting simultaneously in a chaotic dynamical system makes the Arctic effects on mid-latitudes inconsistent, episodic, non-linear and hard to distinguish from other effects. Usually there is no one-to-one cause and effect, but the effects of a certain Arctic forcing depend on the region, season, and the state of the atmosphere and ocean.

Suprajohtavat gravimetrit Metsähovissa 1994 - 2019

H. Virtanen[1] ja A. Raja-Halli[1]

[1] Finnish Geospatial Research Institute, FGI, heikki.virtanen@nls.fi

Abstract

The superconducting or cryogenic gravimeter (SG) is based on the levitation of a superconducting sphere in a stable magnetic field created by current in superconducting coils. Depending on frequency, it is capable of detecting gravity variations as small as $10^{-11} ms^{-2}$. Due to its high sensitivity and low drift rate it has been over three decades eminently suitable for the study of geodynamical phenomena through their gravity signatures. The first superconducting gravimeter (SG) at Metsähovi (ME) Geodetic Research Station T020, operated continuously from Aug 1994 till Sep 2016. Installation of the new instruments was started in February 2014. We have continuous SG timeseries at ME for over 24 years. The final setup was carried out in November 2017, when iGrav-013 was moved to the pier of the old T020, and the new iOSG-022 on its own pier. There are now two operating SGs at ME with a horizontal distance of 3 m.

We have found that about 2/3 of the gravity variations due to local hydrology is produced within 100 m distance of SG. Seasonal variation can be up to µGal (80 nms^{-2}). Within a distance of 100 m from the gravity laboratory there are multiple automated hydrological sensors for hydrological studies such as deep boreholes in the bedrock, groundwater observation tubes in the sediments, and arrays of soil moisture-sensors and pluviometer. The gravity residual correlates clearly with the level of the local groundwater. By subtracting hydrological gravity effects we strive to enhance other studies e.g. loading effect of Baltic Sea and, after major earthquakes, investigations of lowest modes of Earth's free oscillations.

The SG is a relative instrument, hence the scale factors of the SGs were determined using simultaneous observations with the absolute gravimeter (AG) FG5X-221 at ME. Comparison of the SG and AG support the AG observations by detecting gravity variations due to environmental effects. SG can improve the precision of determination of the gravity trend due to postglacial rebound. Data is uploaded monthly to IGETS (International Geodynamics and Earth Tide Service) and is freely available among the data from over 40 other similar stations.

1. JOHDANTO

Suprajohtavan gravimetrin toiminta perustuu suprajohtavan testimassan leijumiseen suprajohtavilla magneeteilla aikaansaaduilla magneettikentässä. Testimassa on ontto Niobium pallo, jonka paikalla pysymiseen tarvittava virta antaa mittaussignaalin Suprajohtava gravimetri (SG) on ollut yli kolme vuosikymmentä erinomaisesti soveltuva kaikkien sellaisten geofysikaalisten ilmiöitten tutkimiseen, jotka tuottavat painovoiman vaihtelua. Tämä johtuu

laitteen pienestä käynnistä ja huomattavasta herkkyydestä. Riippuen taajuudesta, erotuskyky on parempi kuin $10^{-11}ms^{-2}$ ($\approx 10^{-12}g$). Ajallisesti voidaan tutkia ilmiöitä joiden periodi on sekunneista (mikroseismi) vuosiin (Chandlerin periodi). Laitteita on globaalisesti käytössä (2019) yli 40 asemalla. GWR yhtiö San Diegossa on laitteiden ainoa valmistaja. Globaali painovoimadata on yhteisessä tietopankissa Potsdamissa: *International Geodynamics and Earth Tide Service* (IGETS) (https://isdc.gfz-potsdam.de/igets-data-base). Aineistot ovat vapaasti tutkijoitten käytössä.

2. SUPRAJOHTAVAT GRAVIMETRIT SUOMESSA

Ensimmäinen suprajohtava gravimetri T020 aloitti toimintansa Metsähovissa elokuussa 1994 ja lopetti syyskuussa 2016. Uusi kaksi-ilmaisimen gravimetri asennettiin helmikuussa 2014. Marraskuusta 2017 on ollut käytössä 2 suprajohtavaa ravimetriä iGrav-013 ja iOSG-022 kolmen metrin etäisyydellä toisistaan (kuva 1.). iGrav on samalla pilarilla kuin vanha T020 ja iOSG on uudella pilarilla. Uusien SG:n testimassat ovat 5g (iGrav) ja 20g (iOSG). Edellinen massa on tyypillinen arvo. iOSG-022 on osoittautunut erityisen vähäkohinaiseksi instrumentiksi kaikkien SG:n joukossa. Globaalisesti asema ME on todettu taustakohinaltaan matalaksi. Havainnot tehdään sekunnin välein 7.5 numeron (24 bittiä) tarkkuudella. Laitteet vaativat toimiakseen nestemäisen heliumin lämpötilan (-269 C). Uusimmassa laitteissa on suljettu jäähdytyskoneisto. Helium nesteytyy laitteessa itsessään ja eikä haihtumista juurikaan tapahdu. SG on relatiivinen mittauslaite ja se täytyy kalibroida AGn avulla, (Virtanen et.al, 2014)

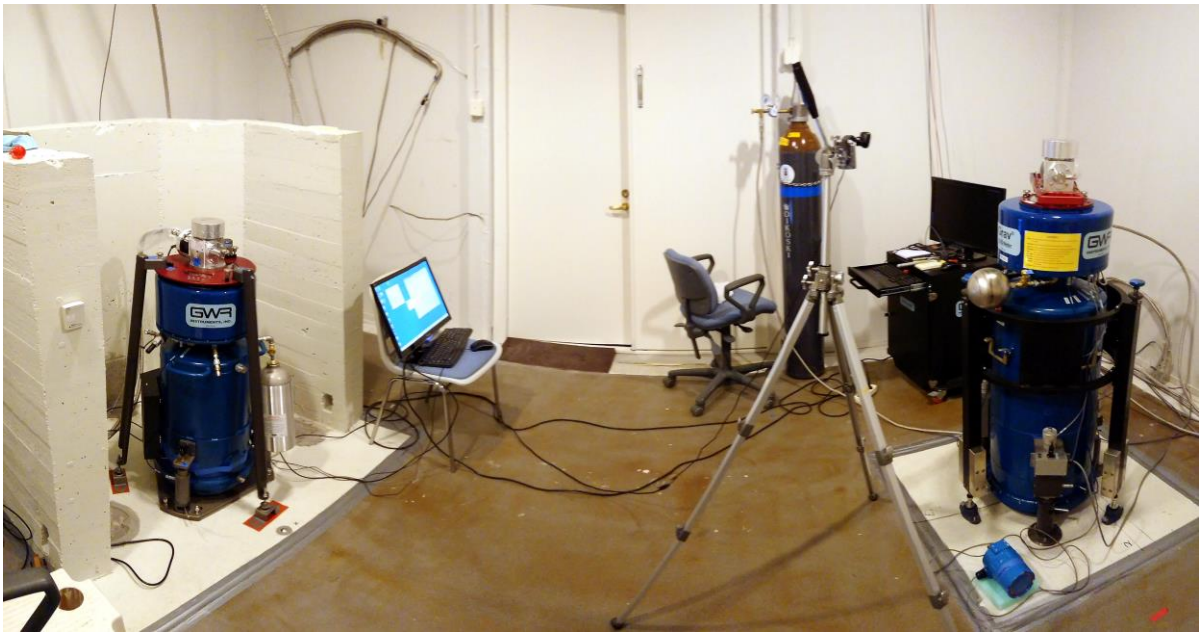

Kuva 1: Suprajohtavat gravimetrit painovoimalaboratoriossa Metsähovissa marraskuussa 2017. Vasemmalla on iGrav-013, joka on vanhalla T020:n pilarilla. Oikealla on iOSG-022. Laitteiden sensorit ovat 3 metrin etäisyydellä ja noin 10 cm korkeudella pilarista.

3. TUTKIMUSTÖITÄ

Metsähovin havaintoja on käytetty maan ominaisvärähtelyiden havaitsemiseen suurten maanjäristysten jälkeen, Itämeren pinnan vaihtelun ja ilmakehän aiheuttamien kuormitusten tutkimiseen. Vuoksi- ja ilmakehäkorjauksen jälkeen 2/3 painovoiman vaihtelusta tulee noin sadan metrin säteeltä SG laitteista (Virtanen et al. 2006). Paikallisen hydrologian vaikutusten tutkiminen on suuressa roolissa tällä hetkellä. SG T020 on tuottanut tehty kaksi väitöskirjaa: Virtanen (2006) ja Hokkanen (2016). Uudempia tutkimuksia perustuen useisiin sensoreihin on esitetty julkaisussa: Virtanen ja Raja-Halli (2017). Kuvassa 2. on esitetty SG:n painovoimahavaintoja Metsähovissa 1994-2018. Havainnoista on poistettu vuoksi ja ilmakehän vaikutusta ja navanliike. Jäljellä on Itämeren vaikutus ja hydrologia. Vertailuna on painovoimalaboratorion vieressä olevan porareiän pohjaveden syvyyden vaihtelu (5m -7 m). Vaikutus on noin 1.5 µGal/m).

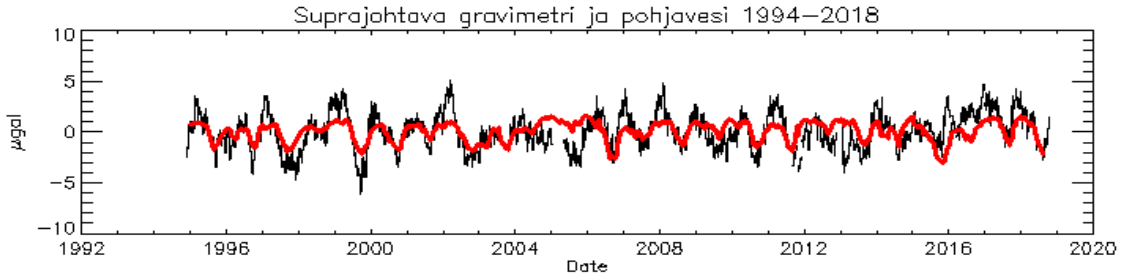

Kuva 2: Musta: painovoiman vaihtelu 1994 – 2018 [πGal]. Punainen on pohjaveden syvyys.

4. LOPUKSI

SG aikasarjaa on Metsähovissa 24 vuotta. SG T020 toimi yhtäjaksoisesti 22 vuotta, ollen aikoinaan vanhin käytössä oleva laite. On odotettavissa pitkää käyttöikää uusimmille laitteille. Paikallisen hydrologian vaikutuksia tutkitaan ja mallinnetaan myös teoreettisesti hyödyntäen horisontaalista gradienttia.

iOSG-022 kuuluu maailmanluokassa pienikohinaisempiin instrumentteihin. Metsähovissa pyritään hyödyntämään tätä ominaisuutta esimerkiksi maapallon sisäytimen poikittaisliikkeen tutkimisessa (Slichterin tripletti). iGrav-013 on myös tarvittaessa helposti siirrettävissä toiseen paikkaan. Riippuen tutkimustuloksista muutaman vuoden kuluttua se voidaan asentaa mahdollisesti toiseen paikkaan Suomessa.

LÄHTEET

Hokkanen, T., 2016. Gravity effect of local soil moisture and groundwater fluctuations the superconducting gravimeter at Metsähovi, Finland, Aalto University publication series DOCTORAL DISSERTATIONS, 253/2016, ISBN: 978-952-60-7169-5.

Virtanen, H., M. Tervo ja M. Bilker-Koivula, 2006. Comparison of superconducting gravimeter observations with hydrological models of various spatial extents. *Inf. Marées Terrestres*, **142**, 11361-11368

Virtanen, H., 2006. Studies of Earth Dynamics with The Superconducting Gravimeter, *Academic dissertation in Geophysics, Helsinki*. Also published as No 133 in the

series of *Publications of the Finnish Geodetic Institute*. http://urn.fi/URN:ISBN:952-10-3057-7.

Virtanen, H., M. Bilker-Koivula, J. Mäkinen, J. Näränen ja H. Ruotsalainen, 2014. Comparison between measurements with the superconducting gravimeter T020 and the absolute gravimeter FG5-221 at Metsähovi, Finland in 2003-2012. *Bull. Inf. Marées Terrestres*, **148**, 11923-11928.

Virtanen, H. ja A. Raja-Halli, 2017. Parallel Observations with Three Superconducting Gravity Sensors During 2014-2015 at Metsähovi Geodetic Research Station, Finland. *Pure and Applied Geophysics*, https://doi.org/10.1007/s00024-017-1719-3.

New geophysics study programs at the University of Helsinki

D. Whipp[1], P. Uotila[2], I. Kukkonen[1], E. Koivisto[1] and T. Luhta[1]

[1] University of Helsinki, Department of Geosciences and Geography,
david.whipp@helsinki.fi
[2] University of Helsinki, Institute for Atmospheric and Earth System Research,
petteri.uotila@helsinki.fi

Abstract

In 2017 the University of Helsinki launched new Bachelor's and Master's degree programmes, including programmes that offer specialisations in solid Earth and hydrosphere geophysics. Here we provide an overview of the new degree programmes.

Solid Earth Geophysics courses at the University of Helsinki are mainly available at the Master's level, but we also offer some Geophysics opportunities in the Bachelor's degree programme in Geosciences. Solid Earth Geophysics is one study track (specialisation) in the Master's Programme in Geology in Geophysics. Courses in the study track feature a compulsory set of general geophysics courses and a variety of elective course groupings including lithospheric properties, applied and environmental geophysics, Earth dynamics, geodesy, planetary geophysics, and seismology. We also offer the option to include courses in scientific computing in addition to a set of required courses common for all students in the Master's Programme. We aim to provide broad basic training in Solid Earth Geophysics to our students while also offering opportunities to dive deeper and gain expertise in select topics (i.e., the elective course groupings). We welcome students with Bachelor`s degrees in Geosciences including at least 25 credit points of studies in Physics, as well as students with Bachelor's degrees in Physics with at least 25 credit points of studies in Geosciences. As the only program in Finland offering specialisation in Solid Earth Geophysics at the Master's level, we see our role as vital in providing the necessary training to the next generation of Earth and planetary geophysicists. At the Bachelor's level we offer an introductory course in Solid Earth Geophysics as a part of the Bachelor`s degree programmes in Geosciences and Physics, and have integrated geophysical concepts into several other courses in the Bachelor`s degree programme in Geosciences.

Geophysics of the Hydrosphere is divided to three disciplines: physical oceanography, hydrology and cryology. The University of Helsinki is the only place in Finland where these three disciplines are taught at Bachelor's and Master's levels. At Bachelor's level basics in oceanography, hydrology, the geophysics of snow and ice and the oceanography of the Baltic Sea can be studied as optional courses as a part of the Bachelor`s degree programme in Physics. At Master's level Geophysics of the Hydrosphere is a study track of the Master's Programme in Atmospheric Sciences at the University of Helsinki. The Geophysics of the Hydrosphere study track is consisted of compulsory courses providing necessary skills for advanced studies and elective course packages of physical oceanography, hydrology, cryology and data science.

Ionospheric currents in the two hemispheres during low and high magnetic activity by the Swarm satellite

A. Workayehu, H. Vanhamäki and A. Aikio

University of Oulu, Ionospheric Research Unit, abiyot.workayehu@oulu.fi

Abstract

We present statistical investigation of the high-latitude ionospheric current systems in the Northern and Southern hemispheres during low ($Kp < 2$) and high ($Kp \geq 2$) geomagnetic activity levels. We analyse nearly four years of vector magnetic field measurements from the two parallel flying Swarm satellites using the spherical elementary current system (SECS) method (Amm et al. 2015), and determine the ionospheric horizontal and field-aligned currents (FAC) for each auroral oval crossing separately. We bin the FAC as well as the horizontal curl-free (CF) and divergence-free (DF) currents in magnetic latitude and local time grid for each hemisphere and activity level separately. Bootstrap resampling is used to estimate the statistical significance, and to remove seasonal bias in the data distribution.

We find that overall the currents are stronger in the Northern hemisphere than in the Southern hemisphere, but the difference depends on the geomagnetic activity level. Large hemispheric asymmetry is observed during low magnetic activity, with larger magnitudes of FACs and horizontal currents in the Northern hemisphere. In contrast, the interhemispheric difference is very small during high magnetic activity, which suggests that the local ionospheric conditions may be important, playing a larger role during quiet than disturbed periods. The local conditions may be related to factors such as variations in solar illumination or magnetic field strength due to different offsets between the geographical and magnetic poles, and dynamics of neutral atmosphere. We plan to study these factors in the future.

REFERENCES

Amm, O., H. Vanhamäki, K. and Kauristie, C. Stolle, F. Christiansen, R. Haagmans, A. Masson, M.G.G.T. Taylor, R. Floberghagen and C.P. Escoubet, 2015. A method to derive maps of ionospheric conductances, currents, and convection from the Swarm multisatellite mission. *Journal of Geophysical Research: Space Physics*, **120**, 3263-3282.

Towards revision of current theory of turbulence in stratified sheared flows

S. Zilitinkevich[1,2]

[1] Finnish Meteorological Institute, sergej.zilitinkevich@fmi.fi
[2] Institute of Atmospheric and Earth System Research (INAR), University of Helsinki

Abstract

The conventional vision of stratified turbulence, underlying modern theory of turbulence closure and turbulent diffusion, and the Monin-Obukhov (1954) Similarity Theory (MOST) of turbulence in the surface-layer flows, is based on the paradigm attributed to Kolmogorov (1941a,b, 1942). However, Kolmogorov has declared his vision, namely the only forward cascade of turbulent kinetic energy (TKE) and other statistical moments of turbulence from large to small scales – towards molecular dissipation, and the only down-gradient turbulent fluxes, bearing in mind the non-stratified shear-generated turbulence. Then the paradigm was extended to stratified flows by his followers, factually without proof.

The paradigm yields a good approximation of weakly and moderately stably stratified turbulent flows (e.g., in atmospheric boundary layers), and also of the low Reynolds number (low-Re) flows (e.g., in lab experiments). However, it fails to explain the well-documented universal maintenance of turbulence in supercritically stable high-Re flows (e.g., in the free atmosphere). In atmospheric modelling, this intolerable drawback was attributed to an "unknown mechanism" of turbulence generation, whereas the turbulent exchange coefficients were defined without physical reasoning by the trail-and-error method. The Energy- and Flux-Budget (EFB) turbulence closure theory (Zilitinkevich et al, 2007, 2008, 2009, 2013, 2019) defines the "unknown mechanism" as the non-gradient (oriented along the buoyancy force, that is positive) heat transfer performed by the fluctuations of temperature causing fluctuations of buoyancy, hence, positive accelerations and, hence, positive buoyancy and heat fluxes. This mechanism essentially mitigates the background negative buoyancy flux and, thus, assures maintaining of turbulence in the supercritically stable stratifications typical of the free atmosphere. The EFB theory explains and quantifies tis phenomenon, and provides physically and empirically grounded tool for calculating the high-Re turbulence in any stable stratification.

In unstable stratification, conventional theories do not distinguish the shear-generated eddies, which indeed break down to perform the forward cascade of TKE, from the buoyancy-generated (convective) chaotic plumes, which merge to perform the inverse cascade of TKE towards larger plumes and, eventually, towards conversion of TKE into kinetic energy of self-organised convective structures: cells or rolls in atmospheric convective boundary layers. In spite of wrong vision of convective turbulence, MOST happened to be in many respects successful. Deducing characteristic of turbulence versus governing parameters via the scaling and dimensional analysis, MOST by lucky chance yielded correct formulation of the

most practically important characteristic of turbulence, namely, the TKE of vertical velocity fluctuations and the coefficients of vertical turbulent exchange of momentum and scalars. At the same time, MOST offers fully erroneous formulation of many other characteristics, including TKE of horizontal velocity fluctuations, horizontal turbulent heat flux and, the rates of molecular dissipation of TKE and all other second moments (Zilitinkevich 1973, 2006, 2010, 2013).

This paper demonstrates deadlocks of conventional vision and theories of stratified turbulence and sketches revised theory.

REFERENCES

Kolmogorov, A., 1941a. The local structure of turbulence in incompressible viscous fluid for very large Reynolds number (in Russian). *Dokl. Akad. Nauk SSSR*, **30**, 301 (English translation: S. Friedlander, S. and L. Topper., Turbulence, Interscience, New York, 1961).

Kolmogorov, A., 1941b. Dissipation of energy in locally isotropic turbulence. *Dokl. Akad. Nauk SSSR*, **31**, 538.

Kolmogorov, A., 1942. Equations of turbulent motion of an incompressible turbulent fluid. *Izv. Akad. Nauk SSSR Ser. Phys. VI*, **No. 1-2**, p. 56.

Monin, A., and A. Obukhov, 1954. Basic laws of turbulence mixing in the surface layer of the atmosphere. *Trudy Geofiz. Inst. AN SSSR*, **24(151)**, 163-187.

Zilitinkevich, S.S. 1973. Shear convection. *Boundary-Layer Meteorol.*, **3**, 416-423.

Zilitinkevich, S.S., J.C.R. Hunt, A.A. Grachev, I.N. Esau, D.P. Lalas, E. Akylas, M. Tombrou, C.W. Fairall, H.J.S. Fernando, A. Baklanov and S.M. Joffre, 2006. The influence of large convective eddies on the surface layer turbulence. *Quart. J. Roy. Met. Soc.*, **132**, 1423-1456.

Zilitinkevich, S.S., T. Elperin, N. Kleeorin and I. Rogachevskii, 2007. Energy- and flux-budget (EFB) turbulence closure model for the stably stratified flows. Part I: Steady-state, homogeneous regimes. *Boundary-Layer Meteorol.*, **125**, 167-192.

Zilitinkevich, S.S., T. Elperin, N. Kleeorin, I. Rogachevskii, I. Esau, T. Mauritsen and M.W. Miles, 2008. Turbulence energetics in stably stratified geophysical flows: strong and weak mixing regimes, *Quart. J. Roy. Met. Soc.*, **134**, 793-799.

Zilitinkevich, S.S., 2010. Self-organisation and non-local nature of geophysical turbulence and planetary boundary layers. *Geophysical J.*, **6**, 168-174.

Zilitinkevich, S.S., 2013. Atmospheric turbulence and planetary boundary layers. Fizmatlit, Moscow, 248 p.

Zilitinkevich, S., T. Elperin, N. Kleeorin, I. Rogachevskii and I. Esau, 2013. A hierarchy of energy- and flux-budget turbulence closure models for stably stratified geophysical flows. *Boundary-Layer Meteorol.*, **146**, 341-373.

Zilitinkevich, S., O. Druzhinin, A. Glazunov, E. Kadantsev, E. Mortikov, I. Repina and Yu. Troitskaya, 2019. Dissipation rate of turbulent kinetic energy in stably stratified sheared flows. *Atmos. Chem. Phys.*, **19**, 1-7.

Geofysiikan Seura r.y. (perustettu 1926) edistää geofysiikan tutkimusta ja on sitä harjoittavien henkilöiden yhdyssiteenä. Geofysiikan aihepiirejä ovat maa, vesi, ilma ja lähiavaruus. Seuran toimintaan kuuluvat kaikille avoimet esitelmätilaisuudet ja Geophysica-lehden julkaiseminen. Seura järjestää joka toinen vuosi Geofysiikan Päivät -kokouksen.

The Geophysical Society of Finland (founded in 1926) advances geophysical research and serves as a link between those involved in it. Geophysics focuses on the solid earth, water, atmosphere and near space. The Society arranges public lectures on different geophysical topics and publishes the journal Geophysica. Every second year it arranges a meeting titled Geophysics Days.